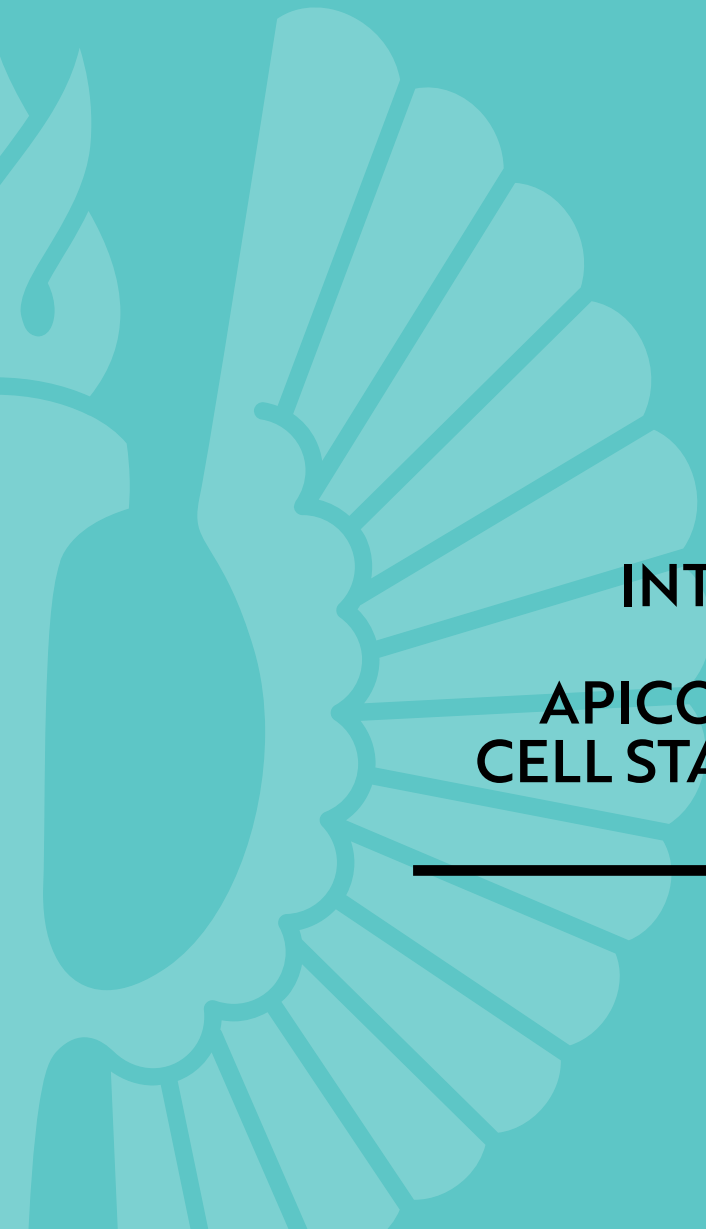




**TURUN
YLIOPISTO**
UNIVERSITY
OF TURKU

université
PARIS-SACLAY



INTEGRIN-MEDIATED REGULATION OF APICOBASAL POLARITY, CELL STATES AND CANCER PROGRESSION

Nicolas Pasquier



TURUN
YLIOPISTO
UNIVERSITY
OF TURKU

université
PARIS-SACLAY

INTEGRIN-MEDIATED REGULATION OF APICOBASAL POLARITY, CELL STATES AND CANCER PROGRESSION

Nicolas Pasquier

University of Turku

Faculty of Technology
Department of Life Technologies
Biochemistry
Doctoral programme in Technology

Université Paris-Saclay

Faculté de Médecine
Sciences de la Vie et Santé
Aspects moléculaires et cellulaires de la biologie
Ecole doctorale 582, Cancérologie : biologie – médecine – santé

Supervised by

Professor Johanna Ivaska, PhD
Turku Bioscience Center
University of Turku and Åbo Akademi
Turku, Finland

Fanny Jaulin, PhD
INSERM U1279
Institut Gustave Roussy
Villejuif, France

Reviewed by

Jean-Léon Maître, PhD
Institut Curie
Paris, France

Julie Pannequin, PhD
Institut de Génétique Fonctionnelle
Montpellier, France

Opponent

Professor Patrick Caswell, PhD
Wellcome Trust Centre for Cell-Matrix
Research, University of Manchester, UK

Other jury members

Professor David Bryant, PhD
CRUK Beatson Institute
Glasgow, UK

Emilia Peuhu, PhD
University of Turku
Turku, Finland

Guillaume Montagnac, PhD
Institut Gustave Roussy
Villejuif, France

The originality of this publication has been checked in accordance with the University of Turku quality assurance system using the Turnitin OriginalityCheck service.

ISBN 978-951-29-9869-2 (PRINT)
ISBN 978-951-29-9870-8 (PDF)
ISSN 2736-9390 (Print)
ISSN 2736-9684 (Online)

UNIVERSITY OF TURKU
Faculty of Technology
Department of Life Technologies
Biochemistry

UNIVERSITE PARIS-SACLAY
Faculty of Medicine
Life and Health Science
Molecular and Cellular Biology

NICOLAS PASQUIER: Integrin-mediated regulation of apicobasal polarity, cell states and cancer progression
Doctoral Dissertation, 270 pp.

Doctoral Programme in
Technology

Doctoral School 582 Cancer:
Biology – medicine – health

September 2024

ABSTRACT

Integrins regulate cell adhesion, migration and architecture which play a role both in development of healthy tissues and disease. While integrins have been widely studied amongst models, the way their availability acts on polarity, spreading and cell capacitation is not fully understood.

Here we investigate the role of integrins, and mainly integrin- β 1, on polarity establishment as well as cell spreading in cancer models. We also decipher their action on cell states by studying their role in human induced pluripotent stem cells (hiPSCs) capacitation.

This thesis reveals a newly described SorLA, HER2 and HER3-dependent Integrin- β 1 recycling loop, allowing colon cancer cells to sense the matrix and orient their polarity accordingly. We also go deeper in cancer cell spreading on matrix, by identifying two matrix compositions (collagen + laminin and laminin + tenascin C) allowing osteosarcoma cancer cells and fibroblasts to spread in a stiffness-independent fashion through an increased amount of integrin- β 1-positive molecular clutches. We also investigate the role of Integrin- β 1 on the capacitation process of stem cells and show that inhibition of integrin- β 1 maintains a naïve-like phenotype in hiPSCs.

Taken together, these data highlight the importance of integrins, and mainly integrin- β 1, in many cell processes amongst models, thus explaining its key role in cell adhesion, cancer cell architecture and cell state establishment.

KEYWORDS: Integrin- β 1, Apicobasal polarity, Spreading, Colorectal Cancer, hiPSC, Capacitation, Matrix, Stiffness

TURUN YLIOPISTO
Teknillinen tiedekunta
Bioteknologian laitos
Biokemia

PARIS-SACLAY YLIOPISTO
Lääketieteellinen tiedekunta
Bio- ja terveystieteet
Molekyyl- ja solubiologia

NICOLAS PASQUIER: Integriinien säätelmä apikobasaalinen polariteetti, solutilat ja syövän kehitys
Väitöskirja, 270 s.

Teknologian tohtoriohjelma

Tohtorikoulu 582 Syöpä: Biologia
– lääketiede – terveys

Syyskuu 2024

TIIVISTELMÄ

Integriinit säätävät solujen tarttumista, migraatiota ja arkkitehtuuria. Näillä on rooli sekä terveiden kudosten että sairauksien kehittymisessä. Vaikka integriinejä on tutkittu laajasti eri malleissa, niiden saatavuuden vaikutusta polariteettiin, leviämiseen ja solukapasitaatioon, ei täysin ymmärretä.

Tässä työssä tutkimme integriinien, pääasiassa integriini- β 1:n, roolia polariteetin muodostumisessa sekä solujen leviämässä syöpämalleissa. Selvitämme myös niiden vaikutusta solutiloihin tutkimalla niiden roolia ihmisen soluista indusoimien pluripotenttien kantasolujen (hiPSC) kapasitaatioissa.

Tämä opinnäytetyö paljastaa äskettäin kuvatun SorLA-, HER2- ja HER3-riippuvaisen Integrin- β 1-kierrätysilmukan, jonka avulla paksusuolen syöpäsolut voivat aistia matriisin ja suunnata polariteettinsa sen mukaisesti. Syvennymme myös syöpäsolujen leviämiseen matriisissa, tunnistamalla kaksi matriisikoostumusta (kollageeni + laminiini ja laminiini + tenaskiini C), jotka mahdollistavat osteosarkooma syöpäsolujen ja fibroblastien leviämisen jäykkyydestä riippumattomalla tavalla, lisääntyneen integriini- β 1-positiivisten molekyylikytkimien määrän ansiosta. Tutkimme myös Integriini- β 1:n roolia kantasolujen kapasitaatioprosessissa ja osoitamme, että integriini- β 1:n estäminen säilyttää naiivin kaltaisen fenotyypin hiPSC:issä.

Yhdessä nämä tulokset korostavat integriinien, pääasiassa integriini- β 1:n, merkittävyyden monissa soluprosesseissa, mikä selittää niiden keskeisen roolin solujen tartumisessa, syöpäsolujen arkkitehtuurissa ja solutilojenmuodostumisessa.

AVAINSANAT: Integriini- β 1, apiko-basaalinen polariteetti, leviäminen, paksusuolen syöpä, hiPSC, kapasitaatio, matriisi, jäykkyys

Table of Contents

1	Abbreviations	12
2	List of Publications	18
3	Introduction	19
4	Review of the literature	21
	4.1 Integrins: Adhesion and Trafficking	21
	4.1.1 Integrin structure and ligands.....	21
	4.1.1.1 Integrin structure.....	21
	4.1.1.2 Integrin ligands	23
	4.1.2 Integrin activation and recycling.....	26
	4.1.2.1 Integrin activation.....	26
	4.1.2.2 Integrin trafficking to the membrane and recycling loops	27
	4.1.2.3 Integrin trafficking regulation	29
	4.1.2.4 Integrin trafficking functional consequences.....	30
	4.1.2.4.1 Apicobasal polarity	31
	4.1.2.4.2 Cell migration and invasion	31
	4.1.2.5 Integrin glycosylation and its consequences	32
	4.1.3 Integrin adhesion complexes (IACs)	33
	4.1.3.1 Types of IACs	33
	4.1.3.2 Structure of IACs	34
	4.1.3.3 IAC signaling.....	35

4.1.4 Integrins in cancer	36
4.1.4.1 Integrins in tumor initiation	36
4.1.4.2 Integrins in cancer invasion and metastasis	37
4.1.4.3 Targeting integrins for anticancer treatments	37
4.2 Apicobasal polarity of epithelial cells	38
4.2.1 Polarity establishment.....	38
4.2.1.1 Molecular actors.....	38
4.2.1.1.1 Polarity complexes	39
4.2.1.1.2 Phosphoinositides (PIs).....	40
4.2.1.1.3 Rho-GTPases	41
4.2.1.2 Sequence of events and interactions during polarity establishment.....	43
4.2.2 Polarity orientation and maintenance	44
4.2.2.1 ECM contact and subsequent orientation of polarity markers.....	44
4.2.2.2 Trafficking of polarity proteins in the polarity orientation process	45
4.2.2.3 Polarity maintenance.....	46
4.2.3 Inverted polarity	47
4.2.3.1 Inverted polarity in cancer	47
4.2.3.1.1 Consequences of inverted polarity on cancer invasion.....	48
4.2.3.1.2 Consequences of inverted polarity on drug resistance	49
4.2.3.1.3 Consequences of inverted polarity on immune escape	49
4.2.3.1.4 Plasticity of inverted polarity in cancer.....	49
4.2.3.2 Inverted polarity in genetic diseases	50
4.2.3.3 Inverted polarity in pathogen defense	50
4.2.3.4 Inverted polarity in development.....	51

4.3 Biological systems to study polarity and integrin-mediated adhesions	54
adhesions	54
4.3.1 Colorectal adenocarcinomas (CRCs)	54
4.3.1.1 Healthy gut architecture	54
4.3.1.2 Characterization of CRCs	57
4.3.1.2.1 Histopathology	58
4.3.1.2.2 Consensus Molecular Subtypes (CMS)	59
4.3.1.2.3 Developmental pathways	60
4.3.1.3 Metastasis and invasion of CRCs	60
4.3.1.4 Models of CRCs	61
4.3.1.4.1 Cell lines: the example of LS513	61
4.3.1.4.2 Patient-derived xenografts (PDXs)	62
4.3.1.4.3 Patient-derived organoids (PDOs)	62
4.3.2 Human induced pluripotent stem cells (hiPSCs)	63
4.3.2.1 What are hiPSCs?	63
4.3.2.2 Naïve and primed states	64
4.3.2.3 Adhesion and polarity status of the blastocyst	64
4.3.3 Stiffness-insensitive spreading of cancer: the use of TIFs and U2OS	65
4.3.3.1 The role of matrix stiffness in cancer invasion	65
4.3.3.2 The role of matrix composition in cancer invasion	66
4.3.3.3 TIFs and U2OS	66
5 Aims of the PhD	67
6 Material and Methods	68
6.1 Cell culture and organoid formation	68
6.1.1 MUC CRC (II)	68
6.1.1.1 Culture and passaging of patient-derived xenografts (PDXs)	68

6.1.1.2	Generation of tumor spheres.....	69
6.1.1.3	Collagen embedding and culture of tumor spheres	69
6.1.1.4	Generation of a 14P-derived PDO line	70
6.1.1.5	Culture of LS513 and generation of TSIPs	70
6.1.2	hiPSC (IV).....	70
6.1.2.1	Culture of naïve and primed stem cells	70
6.1.2.2	Capacitation.....	71
6.1.2.3	Colony formation assay.....	71
6.2	Protein and gene expressions	72
6.2.1	Western blotting (II)	72
6.2.2	PNGase digestion of lysates (II).....	72
6.2.3	Mass cytometry (II)	73
6.2.4	Whole exome sequencing (II)	73
6.2.5	Analysis of SORLA and ITGB1 gene expression in human tumors (II).....	73
6.2.6	Single cell RNA sequencing (scRNAseq) (IV).....	74
6.3	Quantification of cell-matrix interactions	74
6.3.1	Generation of fluorescent collagen (II & III).....	74
6.3.2	Generation of CNA35 and cloning (II)	75
6.3.3	Peritoneum <i>ex vivo</i> assay (II).....	75
6.3.4	Collagen orientation analysis (II).....	76
6.3.5	Collagen displacement fields (II)	77
6.4	Infections and polarity/trafficking analysis (II)	77
6.4.1	SorLA silencing using shRNA lentiviral transduction	77
6.4.2	SorLA KO using siRNA transient transfection	78
6.4.3	Integrin recycling assay	78
6.5	Stainings and microscopy (II).....	79
6.5.1	Immunofluorescence staining	79
6.5.2	Confocal imaging	80
6.5.3	Immunohistochemistry staining	80

6.6 Statistical analysis and polarity quantification	80
6.6.1 Statistical analysis (II, III & IV)	80
6.6.2 Polarity score (II)	80
6.7 Annexes	81
Table 1 - Antibodies.....	81
Table 2 - siRNA and shRNA.....	84
7 Results	85
7.1 Implication of Integrin-β1 trafficking in the apicobasal polarity orientation of CRC metastasis (II)	85
7.1.1 MUC CRC polarity is regulated by ECM interactions and Focal Adhesion Pathway	85
7.1.2 Collagen-binding integrins regulate polarity establishment in MUC CRC	86
7.1.3 Inverted polarity is linked to altered expression of integrin trafficking regulators	87
7.1.4 The SorLA-dependent integrin trafficking loop is induced by HER2 and HER3	88
7.1.5 The apicobasal polarity orientation allows proper interaction with the matrix	89
7.1.6 Higher HER2/HER3/SorLA expression correlates with a apical-in polarity	90
7.2 Uncoupling stiffness and matrix composition to determine ideal conditions for integrin-dependent cancer cell spreading (III)	91
7.3 Integrin-β1: a cornerstone in hiPSC capacitation (IV)	94
7.3.1 Blocking Integrin- β 1 delays the capacitation process.....	94
7.3.2 Integrin- β 1 is central to a fully primed feature acquisition during capacitation	95

8	Discussion	97
	8.1 Understanding inverted polarity in health and disease (I).....	97
	8.2 A HER2/HER3/SorLA-dependent integrin-β1 recycling loop as a polarity regulator in CRC metastasis (II).....	98
	8.3 Ligand availability and integrin repertoire engagement determine cell behavior and stiffness-independent spreading (III).....	100
	8.4 Integrin-β1 blocking promotes naïve-like features and prevents effective capacitation of hiPSCs (IV).....	101
9	Conclusion	103
	9.1 Original Publication I.....	103
	9.2 Original Publication II.....	103
	9.3 Original Publication III.....	104
	9.4 Original Publication IV	104
10	Acknowledgements	105
11	References	108
12	Original publications	132

1 Abbreviations

AB	Apicobasal
AGAP1	Arf-GAP with GTPase, ANK repeat and PH domain-containing protein 1
AJ	Adherent Junction
AMIS	Apical Membrane Initiation Site
AMOTL2	Angiomotin-like protein 2
Anx2	Annexin-2
AP2- μ	μ subunit of AP2 adaptor complex
APC	Adenomatous polyposis coli
aPKC	Atypical protein kinase C
APP	Amyloid precursor protein
ARE	Apical recycling endosome
ARH	Low Density Lipoprotein Receptor Adaptor Protein 1
ARHGAP15	Rho GTPase Activating Protein 15
AsC	Adenosquamous carcinoma
ASE	Apical sorting endosome
Atoh1	Protein atonal homolog 1
BRAF	v-raf murine sarcoma viral oncogene homolog B1
BRE	Basal recycling endosome
BSE	Basal sorting endosome
β TD	β tail domain
C-ERMAD	C-terminal ERM-association domain
CA	Classic adenocarcinoma
CAF	Cancer-associated fibroblast
CD	Cluster of Differentiation
Cdc42	Cell division control protein 42 homolog
CG	CLIC/GEEC
CGA	Glycoprotein Hormones, Alpha Polypeptide
CIMP	CpG island methylator phenotype
CIN	Chromosomal instability

CLIC	Clathrin-independent carrier
CMS	Consensus Molecular Subtype
Coll.	Collagen
Crb	Crumbs
CRC	Colorectal adenocarcinoma
CRE	Common recycling endosome
CTC	Circulating tumor cell
Dab2	Disabled homolog 2
Dlg	Discs large
DOK1	Docking protein 1
DPPA3	Developmental Pluripotency Associated 3
DSC	Deep secretory cell
ECM	Extracellular matrix
EE	Early endosome
EEC	Enteroendocrine cell
EGF	Epidermal Growth factor
EMT	Epithelial-to-mesenchymal transition
EpCAM	Epithelial cellular adhesion molecule
Eps15	Epidermal growth factor receptor substrate 15
ER	Endoplasmic reticulum
ERM	Ezrin, radixin, moesin
FA	Focal Adhesion
FAK	Focal Adhesion kinase
FB	Fibrillar adhesion
FC	Focal contact
FERM	4.1 protein, ezrin, radixin, moesin
FFPE	Formalin-fixed paraffin-embedded
FILIP1	Filamin-A-interacting protein 1
FMNL2	Formin-like protein 2
Fuc	Fucose
Gal	Galactose
Gal-1	Galectin-1
Gal-3	Galectin-3
GAP	GTPase activating protein
GDP	Guanosine diphosphate
GEEC	GPI-anchored protein-enriched early endosomal compartment
GEF	Guanine nucleotide exchange factor
GlcNAc	N-Acetylglucosamine

GTP	Guanosine triphosphate
HAX-1	HS-1-associated protein X-1
HER2/ERBB2	Receptor tyrosine-protein kinase ErbB-2
HER3/ERBB3	Receptor tyrosine-protein kinase ErbB-3
Hes1	Hairy and enhancer of Split-1
hiPSC	Human induced pluripotent stem cells
HLA-DM	Human leukocyte antigen – DM isotype
HLA-DR	Human Leukocyte Antigen – DR isotype
I-EGF	4 integrin-EGF
IAC	Integrin Adhesion Complex
ICAM-1	Intercellular adhesion protein 1
ICAM-4	Intercellular Cell Adhesion Molecule 4
ICM	Inner Cell Mass
IF	Immunofluorescence
IHC	Immunohistochemistry
ILK	Integrin-linked kinase
ITGB1	Integrin- β 1
JAM	Junctional Adhesion Molecule
KLF17	Krüppel-like factor 17
KLF4	Krüppel-like factor 4
KRAS	Kristen rat sarcoma viral oncogene homolog
L1TD1	LINE1 Type Transposase Domain Containing 1
Lam	Laminin
LDV	L/I-D/E-V/S/T-P/S consensus aminoacid sequence
Lgl	Lethal Giant Larvae
Lgr5	Leucine-rich repeat-containing receptor 5
LIF	Leukemia inhibitory factor
LIMD1	LIM domain Containing protein 1
LLPS	Liquid-liquid phase separation
MDCK	Madin-Darby canine kidney
MeC	Medullary carcinoma
MHC	Major histocompatibility complex
MIA-CID	Multiple intestinal atresia associated with combined immunodeficiency
MIDAS	Metal ion-dependent adhesion site
MiP	Micropapillary carcinoma
MMP	Metalloproteinase
MSI	Microsatellite instable
MT1G	Metallothionein 1G

MT1H	Metallothionein 1H
MUC	Mucinous
MUC1	Mucin 1
MUC2	Mucin 2
MVID	Microvillus inclusion disease
MYO5B	Myosin-Vb
N-WASP	Wiskott-Aldrich syndrome protein
NeC	Neuroendocrine carcinoma
NHERF1	Sodium/Hydrogen exchanger regulatory cofactor 1
OCT4	Octamer-binding transcription factor 4
PALS1	Protein associated with LIN7 1 / MAGUK p55 subfamily member 5
Par3	Partition Defective 3
Par6	Partition Defective 6
PATJ	InaD-like protein
PC	Peritoneal carcinomatosis
Pcx	Podocalyxin
PDO	Patient-derived organoid
PDX	Patient-derived xenograft
PHACTR-1	Phosphatase and actin regulator 1
PI	Phosphoinositide
PI(3,4,5)P3	Phosphatidylinositol 3,4,5-triphosphate
PI(4,5)P2	Phosphatidylinositol 4,5-diphosphate
PI3K	Phosphoinositide 3-kinase
PINCH	Particularly interesting new cysteine-histidine-rich protein
PIP5K	Phosphatidylinositol-4-phosphate 5-kinase
PKD	Polycystic kidney disease
PM	Plasma membrane
PNGase	Peptide-N-Glycosidase
PNRE	Perinuclear recycling endosome
PP2A	Protein Phosphatase 2
PRNRP	Papillary renal neoplasm with reverse polarity
PS	Polarity score
PSI	Plexin-semaphorin-integrin
PTB	F3 phospho-tyrosine binding domain
PtdIns	Phosphatidylinositol
PTEN	Phosphatase and tensin homolog
Rac1	Ras-related C3 botulinum toxin substrate 1
Ras	Rat sarcoma virus

RCP/Rab11fip1	Rab-coupling protein/Rab11 family-interacting protein 1
RGD	Argynyl-glycyl-aspartic acid
RhoGDI	RhoGTPase dissociation inhibitor
ROCK1	Rho-associated, coiled-coil-containing protein kinase 1
RTK	Receptor tyrosine kinase
SA	Sialic acid
Scrib	Scribble
scRNAseq	Single cell RNA sequencing
SeC	Serrated carcinoma
SFK	Src family of kinases
SFRP2	Secreted frizzled related protein 2
SORL1/SorLA	Sortilin-related receptor with A-type repeats
SOX2	SRY-box Transcription factor 2
SPCRP	Solid papillary carcinoma with reverse polarity
SRCC	Signet ring cell carcinoma
STX3	Syntaxin 3
STXBP2	Syntaxin-binding protein 2
Susp.	Suspension
t-SNARE	Target membrane SNAP receptor
TAZ	Transcriptional coactivator with PDZ-binding motif
TBX3	T-box transcription factor 3
TE	Trophectoderm
TEAD	TEA domain family member 1
TFM	Traction Force Microscopy
TGF- β	Transforming growth factor β
TGN	Trans-Golgi network
Tiam1	T-cell lymphoma invasion and metastasis-inducing protein 1
TIF	Telomerase immortalized fibroblasts
TJ	Tight junction
TLR	Toll-like receptor
TME	Tumor microenvironment
TNC	Tenascin C
TNF- α	Tumor necrosis factor α
TNM	Tumor, Node, Metastasis
TSIP	Tumor sphere with inverted polarity
TTC7A	Tetratricopeptide repeat domain 7A
uPA	Urokinase
v-SNARE	Vesicle membrane SNAP receptor

VASP	Vasodilator-stimulated phosphoprotein
VAV2	Vav guanine nucleotide exchange factor 2
VCAM-1	Vascular Cell Adhesion Molecule 1
vWA	Von Willebrand A domain
vWF	Von Willebrand factor
WAVE	WASP-family verprolin-homologous protein
WB	Western Blot
YAP	Yes-associated protein
ZIC2	Zinc finger protein 2
ZO	Zonula occludens

2 List of Original Publications

This dissertation is based on the following publications, that will be referred to by their roman number in the text and enclosed at the end of the thesis.

I- **Pasquier, N., Jaulin, F., & Peglion, F. (2024). Inverted apicobasal polarity in health and disease. *Journal of Cell Science*, 137(5).**

II- **Pasquier N., Isomursu A., Mathieu J., Hamidi H., Härkönen J., Follain G., Desterke C., Barresi V., Fusilier Z., Jaulin F. & Ivaska J., Signaling downstream of tumor-stroma interactions regulates mucinous CRC apicobasal polarity, *manuscript submitted***

III- Conway, J. R., Isomursu, A., Follain, G., Härmä, V., Jou-Ollé, E., **Pasquier, N., Välimäki E., Rantala J. & Ivaska, J. (2023). Defined extracellular matrix compositions support stiffness-insensitive cell spreading and adhesion signaling. *Proceedings of the National Academy of Sciences*, 120(43)**

IV- Taskinen, M., Pasquier N.*, Stubb A.*, Joshi S., Rasila P., Vahlman S., Sokka J., Trokovic R., Lönnberg T., Mikkola L. & Ivaska J., **Inhibition of integrin- β 1 activity and contractility support naïve-like state in human induced pluripotent stem cells, *manuscript submitted***

* equal contribution

The original publications have been reproduced with the permission of the copyright holders.

3 Introduction

Integrins are membrane proteins that link the cell to its direct environment. They act as an adhesion and signaling platform, linking the cytoskeleton (actin and intermediate filaments) to matrix components. They are implicated in many cell processes, such as adhesion, migration and polarity, and they determine the cell state and architecture. Integrins are a wide family of adhesion molecules, and the most common subunit, shared by many distinct ECM-binding heterodimers is integrin- β 1 which this thesis focuses on.

When carcinogenesis occurs, cancer cells go through a series of changes that leads to their reprogramming and modifications in their phenotype, such as changes in their architecture and invasiveness. Cancer clusters can indeed move within different types of extracellular matrix (ECM), adopting a different apicobasal polarity (I) or invade and spread differently to healthy tissues. In both these processes, integrins are involved, but the mechanistic cascade by which they control polarity and spreading in different cancer models is not fully understood.

Integrin- β 1-dependent cell polarity establishment and maintenance during cancer progression remains incompletely understood. Indeed, some carcinomas are composed of cells that maintain a predominantly epithelial signature with a conserved apicobasal polarity. However, this polarity can be misoriented, and the mechanisms underlying the reprogramming of polarity orientation in cancer have not been elucidated yet. Because the polarity status of cancer cells can directly be linked to prognosis and outcome, we investigated the intricacies of polarity orientation in cancer, using a colorectal cancer patient-derived model. We studied the focal-adhesion dependent pathway by which cancer cells orient their polarity and discovered a new integrin-recycling loop, involving SorLA, HER2 and HER3 (II).

Integrins are involved in the architecture of cancer cells and tumors, but also in the way cells migrate throughout the body and invade. This is the main motor of metastasis formation which accounts for most cancer deaths. Because cancer cells efficiently remodel the matrix they migrate on, they have a direct impact on its physical and chemical properties. However, while these parameters have been studied separately, few models comprehensively addressing the joint effects of the

matrix stiffness and composition have been developed across literature. Here we describe a matrix array platform and employ it to test different combinations of stiffnesses and composition, allowing the discovery of matrix compositions supporting integrin-dependent cancer cell spreading independently of ECM stiffness. We found that the collagen/laminin and laminin/tenascin C combinations allow an engagement of a broader repertoire of integrin- β 1 heterodimers facilitating efficient cell-ECM engagement and even on low rigidity (III).

Finally, integrins are not only involved in pathological processes as we have investigated above, but also efficiently participate in the organization and proper architecture and development of tissues. From the very first step of development, integrins play a role in cell-ECM interactions. In this thesis we studied the role of integrins in the maintenance of different stem cell states: the naïve pre-implantation and the primed post-implantation state. This process is key in the development, as it allows the adhesion of the blastocyst to the endometrium. Working with human induced pluripotent stem cells (hiPSCs), we found that the engagement of Integrin- β 1 is necessary for stem cells to exit their naïve state and become primed for differentiation into different lineages (capacitation) and for the reorganization of hiPSC colony morphology and adhesions upon this transition (IV).

Altogether this thesis provides a wide overview of the actions of integrins across different biological process, from development to carcinogenesis and cancer development.

4 Review of the literature

4.1 Integrins: adhesion and trafficking

4.1.1 Integrin structure and ligands

Integrins are a family of heterodimeric receptors that interact with extracellular ligands sensing both their chemical and physical nature. In return, they induce a whole range of biochemical responses through different signaling pathways (Kechagia et al., 2019). Integrins both adhere to the extracellular matrix (ECM) and to other cells and integrate these signals through their connection to the actin cytoskeleton via a set of so-called Integrin adhesion complexes (IACs). Not only are integrins implicated in cell adhesion, but they also regulate crucial parameters such as cell shape, migration and motility (Conway and Jacquemet, 2019). While their role at the plasma membrane is well documented, integrins also play a role in the activation of signaling pathways when endocytosed (Moreno-Layseca et al., 2019).

4.1.1.1 Integrin structure

While integrins are present in all multicellular animals, they display an important diversity amongst species. In mammals, integrins are composed of 18 α and 8 β subunits. These monomers combine to form 24 functional heterodimeric integrin receptors (Humphries, 2000; Hynes, 2002). Since the discovery of the integrin receptor family (Hynes, 1987), the knowledge span has increased, further characterizing the bidirectionality of integrin signaling, both outside-in and inside-out (detailed in **4.1.2.1**). This signaling is mediated by conformational changes both in the extracellular and cytoplasmic regions of the integrin subunit (Hynes, 2002). Both subunits are composed of a cytoplasmic tail, a single α helix inserted within the plasma membrane, and an extracellular or ectoplasmic domain. The latter is composed of a “head” where the binding sites of the ligands are found, as well as a “leg”, which conformation changes upon binding of the ligands (Campbell and

Humphries, 2011). The ~1000 amino acid-long α subunit extracellular domain is composed of Calf-1, Calf-2, Thigh and β -propeller domains. Additionally, about half of α subunits contain an inserted α I domain, which contains a metal ion-dependent adhesion site (MIDAS) with the following gradual affinity for cations: $Mn^{2+} > Mg^{2+} > Ca^{2+}$ and is responsible for ligand binding in these integrins. The ~750 amino acid-long β subunit extracellular domain is composed of β tail (β TD), 4 integrin-EGF (I-EGF), plexin-semaphorin-integrin (PSI), Hybrid and β I domains. MIDAS sites can also be found on the β subunit (Zhang and Chen, 2012) (see Figure 1).

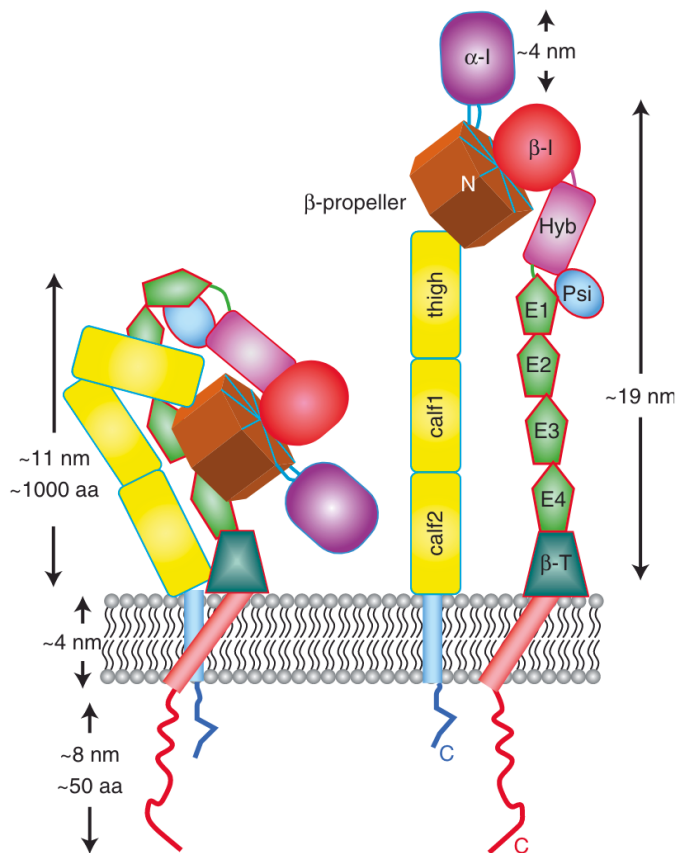


Figure 1- Integrin structure (from Campbell and Humphries, 2011).

Hyb=Hybrid dromain; β -T= β TD

4.1.1.2 Integrin ligands

Integrins have multiple ligands that can bind to their ectoplasmic domain (Chastney et al., 2021) and they can be divided into 5 categories depending on the ligands they bind to (Humphries et al., 2006) (see Figure 2):

→ **RGD-binding integrins** are composed of all five heterodimers of the αV subunit, two heterodimers of the $\beta 1$ subunit ($\alpha 5$ and $\alpha 8$) as well as the $\alpha IIb\beta 3$ heterodimer. Multiple ligands contain an RGD residue (argynyl-glycyl-aspartic acid) including fibrinogen, fibronectin, tenascin, thrombospondin, vitronectin and von Willebrand factor (vWF) (Plow et al., 2000). The RGD-motif interacts at the interface of the α and β subunits, the arginine binding to the β -propeller domain on the α subunit, and the aspartic acid binding to a von Willebrand A domain (vWA) on the β subunit (Whittaker and Hynes, 2002).

→ **LDV-binding integrins** are composed of $\alpha 4\beta 1$, $\alpha 4\beta 7$, $\alpha 9\beta 1$, $\alpha E\beta 7$ and the four heterodimers of the $\beta 2$ subunit. The LDV sequence is functionally close to RGD, can be described by the consensus sequence L/I-D/E-V/S/T-P/S and can be found on several ligands such as fibronectin, osteopontin, tenascin and fibrinogen. Other LDV-containing ligands, such as VCAM-1 (Vascular Cell Adhesion Molecule 1), allow intercellular integrin-dependent interactions. Although structural information is lacking, it is also believed that the LDV residue interacts similarly to RGD, at the interface of the α and β subunits.

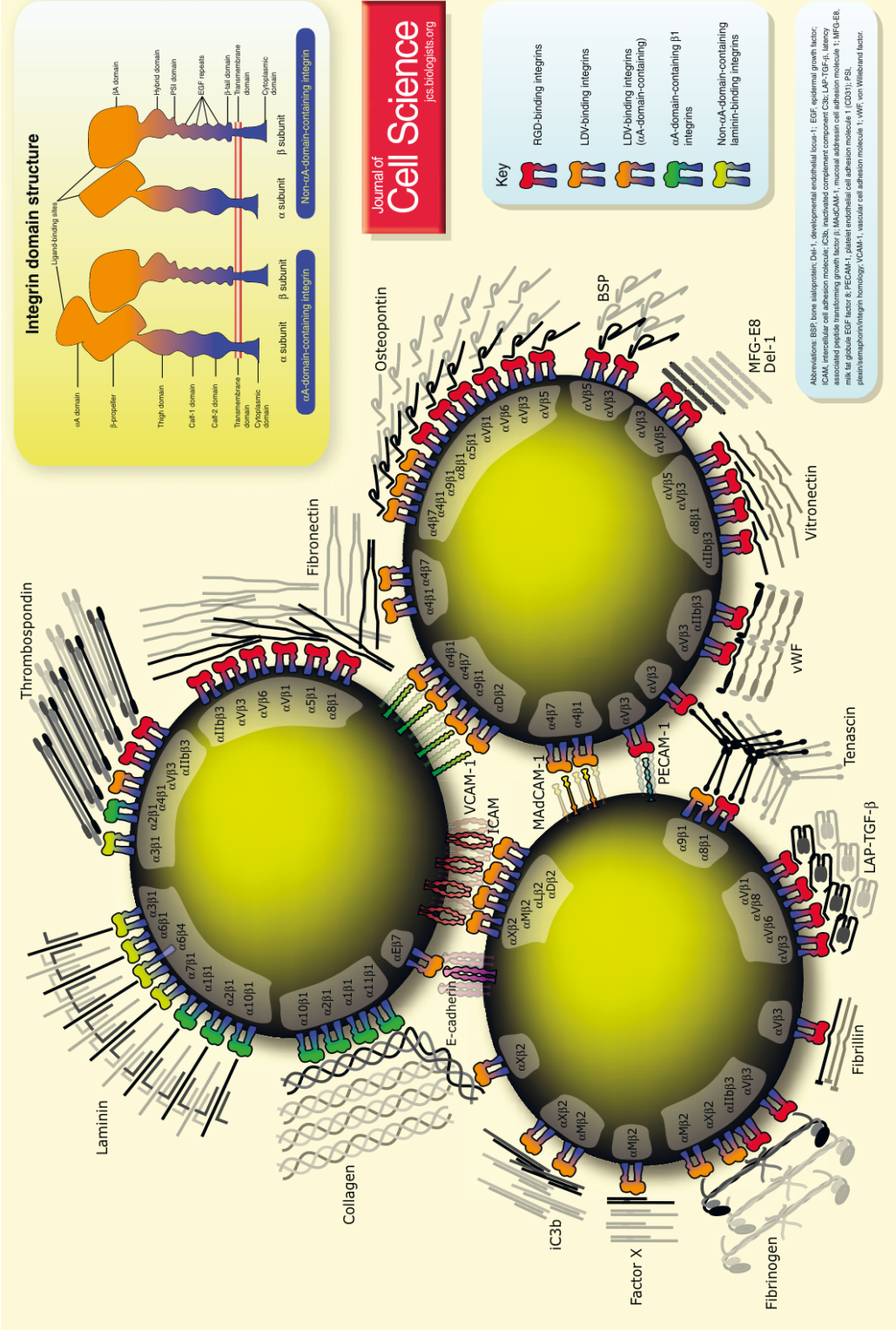
→ **I-domain-containing $\beta 1$ integrins** are composed of integrin heterodimers which α subunit harbours the αI domain described earlier (Lee et al., 1995). These are $\alpha 1\beta 1$, $\alpha 2\beta 1$, $\alpha 10\beta 1$ and $\alpha 11\beta 1$. These form a collagen-binding subgroup, with some receptors reported to bind also laminin. In the case of collagen, a glutamate in a triple-helical GFOGER motif binds to a MIDAS in the αI domain of the $\alpha 2$ subunit (Emsley et al., 2000). The most ubiquitously expressed collagen-binding integrin for fibrillar type I collagen is the $\alpha 2\beta 1$.

→ **Non-I-domain-containing integrins** form a subfamily composed of $\alpha 3\beta 1$, $\alpha 6\beta 1$, $\alpha 7\beta 1$ and $\alpha 6\beta 4$ that selectively bind to laminin, through a different site than that of the I-domain containing $\beta 1$ integrins.

→ **Other integrins** include integrin-ligand interactions with no-ECM ligands. This category also includes integrins mediating intercellular interactions, binding to cell adhesion molecules such as ICAM-4 (Intercellular Cell Adhesion Molecule 4) or E-cadherin (in the case of $\alpha_E\beta_7$) (U Kroneld, 1998).

Amongst all heterodimers, β_1 is the most common subunit. It can dimerize with 12 different α subunits, each with specific ligand binding specificity and signaling activity.

Figure 2- Integrin ligands (from Humphries et al., 2006) – see next page



4.1.2 Integrin activation and recycling

4.1.2.1 Integrin activation

On the plasma membrane, integrins can be either in an inactive or an active state. When inactive, integrins are in a bent shape, not engaging with their ligands (Campbell and Humphries, 2011). This bent conformation is stabilized by integrin inactivators that bind to the integrin cytoplasmic tails and therefore prevent the binding of integrin-binding activating proteins, such as talin or kindlin. For instance, filamin or docking protein 1 (DOK1) are both inactivators that bind to the β subunit cytoplasmic tail and sharpin binds to both tails, stabilizing the inactive conformation (Bachmann et al., 2019; Gao et al., 2019).

Upon activation however, integrins can bind to extracellular ligands. There are two ways these integrins can be activated:

→ **The activation via inside-out signals.** Other cell-surface receptors receive extracellular signals, thus causing the binding of integrin activators such as talin and kindlin to the cytoplasmic tail of β subunits (Watanabe et al., 2008). The binding site of talin is precisely situated at the F3 phospho-tyrosine binding domain (PTB) (Calderwood et al., 2002) and is recruited to focal adhesions (FA – further detailed in 4.1.3) from the cytosol (Rossier et al., 2012) which allows separation of the α/β “inter-legs” (disruption of hydrophobic and electrostatic interactions) and integrin activation through the unfolding of the ligand binding site followed by the “legs” moving apart from each other (Anthis et al., 2009). Kindlin is an important coactivator of integrins and binds to a membrane distal NxxY motif on the β subunit (Harburger et al., 2009). It is not known to activate integrins on its own (Karaköse et al., 2010) and talin-vinculin and talin-actin interactions also influence activation (Banno et al., 2012). Kindlin does not have a binding site to actin and Focal Adhesion Kinase (FAK) acts as an intermediate.

Whereas talin and kindlin have long been established as essential activators of integrins, this idea has been recently challenged, some findings qualifying talin as more of a stabilizer of an active state and suggesting that ligand binding to the bent integrin conformer is a key trigger for rapid activation and extension (Li et al., 2024).

→ **The activation via outside-in signals.** Ligand binding to integrins induces conformation changes that further increases ligand affinity of integrins, leading to increased integrin signaling (Arnaout et al., 2005). Ligand binding leads to clustering

of integrins, consequently activating the autophosphorylation of the Src family of kinases (SFK) (Arias-Salgado et al., 2003). SFK then phosphorylates many components of the IACs triggering signaling. It has also been reported to phosphorylate a tyrosine within the integrin cytoplasmic domain (Law et al., 1999), which changes the strength of the affinity of the bond of integrins with its ligands, but also with other signaling molecules such as kinases, GTPases and adaptors constitutive of focal adhesions (Gahmberg et al., 2009).

The outside-in activation can be regulated internally, either through regulators of talin recruitment, the phosphorylation of integrin cytoplasmic domains or the binding of talin competitors.

4.1.2.2 Integrin trafficking to the membrane and recycling loops

Just like integrin activation, talin is an essential element in the trafficking of integrins to the plasma membrane (PM) after their synthesis (Margadant et al., 2011). Indeed, the binding of talin to integrins in the endoplasmic reticulum (ER) regulates the delivery of newly synthesized integrin heterodimers to the PM through transport along actin filaments (Martel et al., 2000). More precisely, talin binding to integrin exposes the GFFKR sequence that acts as an ER export signal. α subunits associate with the β subunits in the ER and stay dimerized during their whole travel to the plasma membrane through the Golgi (Tiwari et al., 2011).

Once at the PM, integrin trafficking controls the availability of integrin heterodimers via both clathrin-dependent and independent endocytosis pathways (Paul et al., 2015). It has been shown that most integrins are recycled back to the PM, and that only a small proportion is degraded in the lysosomal compartment (Böttcher et al., 2012). Differential trafficking of integrin heterodimers effectively leads to different responses to different ECM cues such as formation of adhesions upon cell spreading (Shafaq-Zadah et al., 2016).

Integrins have been described to traffic through four recycling routes (Powelka et al., 2004; Caswell and Norman, 2006; Pellinen and Ivaska, 2006). The most studied recycling loops are (Mohrmann and Sluijs, 1999) (see Figure 3):

→ A Rab4-dependent **short loop** where integrins are endocytosed through a clathrin/dynamin-dependent mechanism and traffic through a Rab4-positive early endosome (EE) before being recycled to the membrane. The recycling half-time in this loop is of 3 minutes.

→ A Rab11-dependent **long loop** where, after being endocytosed in early endosomes, integrins traffic through a Rab11-positive perinuclear recycling endosome (PNRE) before being recycled to the membrane. The recycling half-time in this loop is of 10 minutes.

Additionally, other recycling routes have been described, including for example:

→ An **Arf6-dependent pathway** that is activated by the addition of serum or specific stimulants such as epidermal growth factor (EGF) (Powelka et al., 2004).

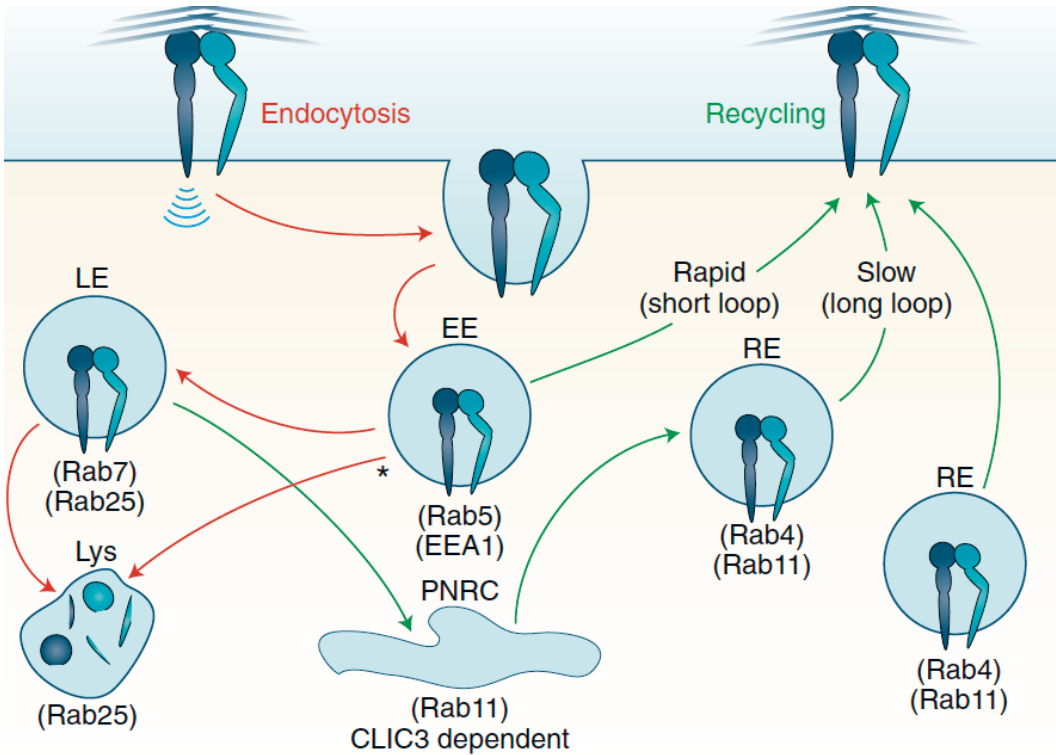
→ An **actin-dependent pathway** characterized by its enhancement by supervillin, an actin-binding and myosin-II binding protein (Puthenveedu et al., 2010).

Both active and inactive integrins are recycled through different compartments at different rates. This has been especially documented for Integrin- β 1 (Arjonen et al., 2012). Inactive β 1 integrins can be endocytosed through a dynamin and clathrin-dependent endocytosis to early endosomes (EE) in a Rab5- and Rab21-dependent manner. This endocytosis is then quickly balanced by the Rab4-dependant recycling to Arf6-positive protrusions. Thus, inactive β 1 integrins predominantly traffic through the previously described short loop.

Active β 1 integrin is endocytosed predominantly via clathrin-independent Rab21 and Swip-1 regulated CLIC/GEEC (CG) – endocytosis (with a minor fraction endocytosed via a clathrin-dependent route) to a Rab5- and Rab21-positive EE (Arjonen et al., 2012; Moreno-Layseca et al., 2019). Recycling via this route is slower and involves Integrin- β 1 being present in Rab11-positive endosomes, therefore predominantly using the long recycling loop (Arjonen et al., 2012), but also involving a step of Eplin α - and actin-dependent endosomal tubulation (Jäntti et al., 2024).

Figure 3- Integrin recycling loops (from Moreno-Layseca et al., 2019) – see next page

LE= late endosome; Lys=lysosome, PNRC=perinuclear recycling compartment



4.1.2.3 Integrin trafficking regulation

Integrin internalization is a continuous process in adherent cell types and the exact triggers of receptor uptake remain poorly understood. Integrin uptake has been linked to focal adhesion turnover. Integrin-ECM interactions induce the formation of focal contacts (FC) leading to the interaction of integrins with F-actin. When the connection to actin is disrupted through the disassembly of FCs, microtubules are targeted to the disassembling adhesions and clathrin adaptors have been implicated in the process (Ezratty et al., 2009, 2005). However, strong evidence for direct integrin uptake from adhesions is lacking. The prevailing view is that unengaged integrins are taken up by endocytosis. These can be, for example, in their active conformation, adhering to ligand fragments still in the endosomes (Alanko et al., 2015; Moreno-Layseca et al., 2019; Nader et al., 2016) or inactive receptors clustered by extracellular glycans at the PM (Lakshminarayan et al., 2014; Shafaq-

Zadah et al., 2016). However, more work is needed to determine exactly what regulates integrin endocytosis in different contexts.

Through their action within recycling loops, Rab and Arf GTPases are both regulators of integrin trafficking. Whereas Rab mostly control the fusion of membrane vesicles, as well as their transportation and that of cargo proteins (Zerial and McBride, 2001), Arf preferentially promotes the recruitment of coating proteins such as clathrin from the cytosol to the membrane (D'Souza-Schorey and Chavrier, 2006). As an example, Rab21 locked in a GDP-bound state causes β 1-integrin accumulation at the PM at FAs. However, when locked in a GTP-bound state, this causes its accumulation in endocytic vesicles (Pellinen et al., 2006; Simpson and Jones, 2005).

GTP-locked Arf6 results in β 1 accumulation in PI(4,5)P2 (phosphatidylinositol diphosphate)-containing macropinocytic vesicles (Brown et al., 2001). Conversely, AGAP1, an Arf6 GAP, promotes the recycling of active integrins to protrusions and drives invasion. This shows that the activation and inactivation of Arf6 is important for integrin trafficking, respectively its endocytosis and its recycling to the membrane (Nacke et al., 2021; Nikolatou et al., 2023).

Several studies have focused on the cytoplasmic domains of β subunits for trafficking regulation. Sequences have been identified on β 1, β 2 and β 3 cytoplasmic tails (Caswell and Norman, 2006). In addition, the cytoplasmic domains of integrin α subunits contain key elements mediating signaling and playing a role in integrin internalization. For instance, the aforementioned Rab21 binds to a conserved sequence found in all integrin α tails to induce endocytosis (Pellinen et al., 2006; Pellinen and Ivaska, 2006). Additionally, AP2- μ has been shown to interact with a specific subset of integrin α tails harboring a classical AP2-binding motif, while Dab2 and ARH interact with integrin β cytoplasmic tails and regulate endocytosis (Caswell et al., 2007; De Franceschi et al., 2016).

4.1.2.4 Integrin trafficking functional consequences

Differential regulation of integrin recycling evidently plays a role on the integrin availability at the PM. This impacts different cell processes, such as polarity and cell migration and invasion.

4.1.2.4.1 *Apicobasal polarity*

Apicobasal polarity will be further discussed in section 4.2. As seen previously, Rab5 and Arf6 are present in multiple integrin recycling loops and respectively activate PI3K and PIP5K. PIP5K's product PI(4,5)P₂ regulates actin remodeling as well as other actin-binding FA proteins such as ezrin, which is a specific apical marker and an apicobasal polarity stabilizer (Shin et al., 2005). Another protein of the Rab family, Rab10, has also been shown to mediate integrin recycling (Jin et al., 2021) and, simultaneously, has been identified around the Trans-Golgi Network (TGN) and involved in the polarized trafficking from basolateral regions (Larocque and Royle, 2022). As such, integrin trafficking plays an important role in apicobasal polarity maintenance.

4.1.2.4.2 *Cell migration and invasion*

Integrin availability modulated by recycling controls cell migration and invasion (Paul et al., 2015). In pancreatic and ovarian carcinoma, preferential recycling of $\alpha 5\beta 1$ over $\alpha V\beta 3$ promotes a switch from mesenchymal to pseudopodial cell migration and cell invasion (Muller et al., 2009). It is important to mention that the impact of integrin endocytosis and recycling is context-dependent and varies between different cancer types. In ovarian cancer, Rab25 associates with $\beta 1$ integrin and increases the recycling of the $\alpha 5\beta 1$ towards the cell surface, thus promoting an invasive phenotype (Caswell et al., 2007). However, in head and neck cancer, cells lacking Rab25 will present an invasive phenotype and detach from the primary tumor (Amornphimoltham et al., 2013). In bladder cancer, a Rab11-coupling protein (RCP or Rab11fip1) enhances the recycling of $\alpha 5\beta 1$ and promotes invasive cell migration (Rainero et al., 2012). Interestingly, $\alpha V\beta 3$ can inhibit the RCP-dependent recycling of $\alpha 5\beta 1$, showing a competitive relationship between integrin heterodimers (Caswell et al., 2008; Christoforides et al., 2012).

Interestingly, the cell's glycocalyx can also play a role on cell invasion via integrin endocytosis. Indeed, the glycocalyx can facilitate integrin clustering (Paszek et al., 2014, 2009) which, through a recycling activation, can cause progression and invasion in cancers such as glioblastoma (Barnes et al., 2018). Cell migration and adhesion in normal epithelial cells and during development has been shown to be regulated by the transport of Integrin- $\beta 1$ from the PM to the TGN to be recycled at the leading edge (Shafaq-Zadah et al., 2016).

Integrin trafficking influences invasion by regulating integrin recycling. For instance, HS1-associated protein X-1 (HAX-1) regulates clathrin-dependent endocytosis of $\alpha v\beta 6$ integrin and facilitates invasion (Ramsay et al., 2007). Integrin internalization through the PKC α - and RhoC-dependent FMNL2 activation promotes integrin internalization and invasion of melanoma cells (Wang et al., 2015).

4.1.2.5 Integrin glycosylation and its consequences

Integrins have multiple N-glycosylation and O-glycosylation sites. The glycosylation profile of integrins change along their journey from the ER to the PM. In the ER, integrins are in a high-mannose state, characterized by a majority of mannose residues on the integrin glycosylation sites. Their glycosylation profile gets more complex when processed in the Golgi and brought to the PM, leading to so-called *hybrid* or *bisected* glycosylations, with sialic acid (SA), N-Acetylglucosamine (GlcNAc), galactose (Gal), and fucose (Fuc) residues.

The glycosylation sites of the $\alpha 5\beta 1$ have been particularly well documented. It contains 26 N-glycosylation sites, amongst which 14 on the α subunit and 12 on the β subunit. The differential glycosylation on these sites has been shown to modulate the interaction with the ECM as well as integrin activation (Janik et al., 2010) and conformational changes (Isaji et al., 2004; Zhao et al., 2008). For instance, hyposialylation (ie. a low proportion of SA residues) of $\beta 1$ -integrin enhances its binding to fibronectin (Passaniti and Hart, 1988; Reddy and Kalraiya, 2006).

Glycosylation of integrins has various functional consequences. One of the most studied examples is the $\beta 1$ subunit. For instance, the removal of N-glycosylations on the βI domain decreases the formation of heterodimers, thus inhibiting cell spreading (Isaji et al., 2009). Direct consequences of glycosylation on endocytosis are a bit more unclear and indirect. Galectin-1 (Gal1) and Galectin-3 (Gal3) both interact with the glycosylated extracellular domain of the $\beta 1$ subunit and control its endocytosis and recycling. For instance, Gal3 promotes mechanical deformation of the plasma membrane and a subsequent clathrin-independent endocytosis. Additionally, Gal1 knockdown leads to intracellular accumulation of $\beta 1$ -integrin (De Franceschi et al., 2016; Fortin et al., 2010; Furtak et al., 2001; Lakshminarayan et al., 2014). This link between glycosylation and recycling goes further, as it has been shown that an integrin- $\beta 1$ cytoplasmic-tail mutant, which is not recognized and recycled by sorting nexin 17, is predominantly degraded in lysosomes resulting in low levels of glycosylated or “mature” forms of Integrin- $\beta 1$ on the plasma membrane. Therefore,

the level of mature, fully glycosylated integrin would correlate with active recycling of endocytosed Integrin- β 1 back to the plasma membrane (Böttcher et al., 2012). Other documented examples can be found in α subunits, such as α 5. α 5 lacking N-glycosylation sites showed increased cell surface localization and delayed internalization of the active form of the α 5 β 1 heterodimer (Hang et al., 2017). It has also been shown that N-glycans on the α 5 β 1 heterodimer allow the clustering of Gal3, which in return clamps it in its bent shape and primes it for endocytosis (Shafaq-Zadah et al., 2023).

4.1.3 Integrin adhesion complexes (IACs)

4.1.3.1 Types of IACs

Integrins are transmembrane proteins, with a short cytoplasmic tail, linking the cell to the ECM, intracellular proteins and the cytoskeleton. This link is permitted by a repertoire of proteins interacting with this cytoplasmic tail and/or each other, as well as with the actin microfilaments. The resulting protein complex, or adhesome, is composed of 147 proteins developing 361 different interactions, and giving rise to structures called Integrin Adhesion Complexes (IAC) (Chastney et al., 2021, 2020; Conway and Jacquemet, 2019). This adhesome is composed of integrins, cargo adaptors, scaffolding proteins, signaling molecules and components of the cytoskeleton. 60 of these proteins are part of a “consensus adhesome” sequence, centered around three axis: ILK-PINCH-kindlin, FAK-paxilin, talin-vinculin and α -actinin-zyxin-VASP (Horton et al., 2016, 2015).

IACs all involve integrins but are of different nature depending on their structure and the other proteins involved in the adhesion. Amongst them, we can find hemidesmosomes (Jones et al., 2017), podosomes (Veillat et al., 2015), invadopodia (Eddy et al., 2017), immunological synapses (Dieckmann et al., 2016) as well as Focal Adhesion (FA)-like structures.

FA-like structures constitute a link between the ECM and actin filaments and can be divided depending on their levels of maturations. From early filopodial adhesions, these IACs mature into nascent adhesions, proper FAs, and finally fibrillar adhesions (FBs). While early adhesions mostly function as a constant sensor of the cell environment, late adhesions are more specialized into other functions such as traction and ECM remodeling (Jacquemet et al., 2019; Zaidel-Bar et al., 2004, 2003). This maturation of FA-like structures is molecularly characterized, with a loss of talin and a recruitment of tensin along the maturation (Rainero et al., 2015).

Maturation and strengthening are also largely mediated by vinculin. Indeed, talin and vinculin are both recruited in early adhesion and the unfolding of the talin rod domain exposes vinculin binding sites. This allows a strengthening of the adhesion by increasing the talin/actin interaction (Atherton et al., 2015; Gingras et al., 2009; Han et al., 2021; Himmel et al., 2009) and via vinculin binding to actin. Vinculin's activity for actin increases with mechanical load, therefore stabilizing the adhesion throughout maturation (Baumann et al., 2023).

4.1.3.2 Structure of IACs

IACs are layered vertically (see Figure 4). Most proximal to the ECM, on the plasma membrane is first a layer of integrins, then a layer of adaptors such as paxillin and Focal Adhesion Kinase (FAK), higher up a layer of force transmitters such as talin, tensin and vinculin, and an actin regulatory layer (Case et al., 2015; Liu et al., 2015). The layering has been shown to change upon adhesion maturation with the position of vinculin moving higher with adhesion maturation in mesenchymal cells (Case et al., 2015) and N to C-terminus orientation of vinculin being distinctly “upside down” in stem cells (Xia et al., 2019; Stubb et al., 2019). While the significance of the altered orientation remains to be fully elucidated, these studies imply that the vertical orientation may be a key determinant of IAC function in specific contexts such as during differentiation. Finally, actin interacting proteins, tropomyosins and α -actinin localize to different layers of IACs and regulate IAC turnover and integrin-mediated cell migration (Kumari et al., 2024).

The structure of IACs are affected by different parameters, such as the integrin heterodimers involved (Schiller et al., 2013) and their activation state (Byron et al., 2015), the ECM ligands (Humphries et al., 2009) and the previously mentioned maturation state (Horton et al., 2015).

The maturation of nascent adhesions into FAs are driven by actomyosin contractility, which generates the necessary forces for adhesion strengthening and signaling (Han et al., 2015; Roca-Cusachs et al., 2013). *In vitro*, liquid-liquid phase separation (LLPS) experiments have shown that p130Cas and FAK are involved in the clustering stage, while LIMD1 is implicated in the recruitment of proteins to IACs during this actomyosin-dependent maturation (Case et al., 2022; Y. Wang et al., 2021).

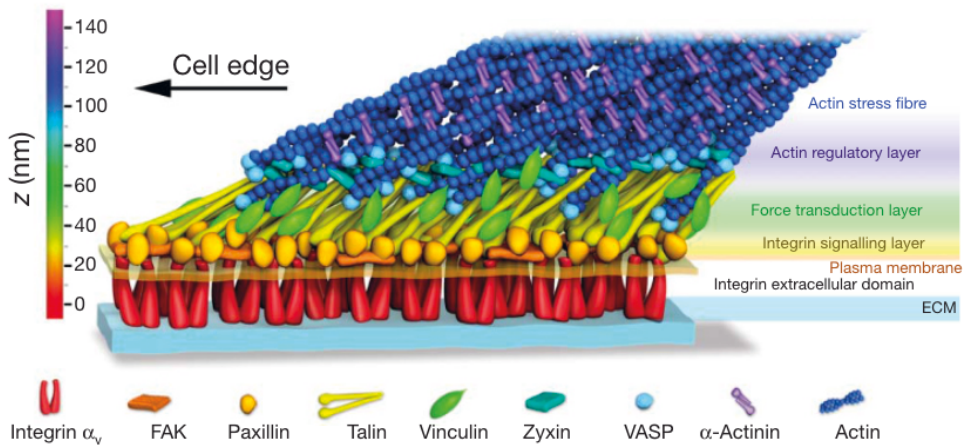


Figure 4- FA structure (from Kanchanawong et al., 2010)

Amongst several studies, FA-mediated adhesion was described using the molecular clutch model. It features a ligand-binding protein (clutch) composed of an ECM-receptor, such as an integrin heterodimer, and its adaptors linking it to the cytoskeleton (Bangasser et al., 2013; Chan and Odde, 2008; Elosegui-Artola et al., 2016; Isomursu et al., 2022). In this model, another unit, called motor, is composed of the actomyosin contractile force. This force is transmitted to the substrate through the clutches, thus enhancing cell spreading.

4.1.3.3 IAC signaling

Through integrins, IAC integrate biochemical and mechanical signals from the environment and mediate durotaxis (cells migrating in response to an ECM stiffness gradient towards increasing rigidity) and haptotaxis (cells migrating in response to an ECM component gradient). Mechanical stimulations sensed by IACs cause YAP and TAZ to translocate to the nucleus where they bind to transcription factors of the TEAD family to regulate gene expression (Charras and Sahai, 2014; Cho et al., 2017; Kechagia et al., 2019).

FAs are phosphorylation platforms, with important roles of kinases and phosphatases like Src and the aforementioned FAK and paxillin (Humphries et al., 2019). The

small GTPases signaling downstream of IACs regulate protrusion, cell contractility and cytoskeleton dynamics in general. This dynamic is finely controlled by the well described RhoA/Rac1 balance and mutual exclusion which controls integrin adhesion, with RhoA promoting cell contraction and Rac1 cell spreading (Bass et al., 2007; Jacquemet et al., 2013). Cells can switch between these two modes and therefore contribute to IAC formation (Lawson et al., 2014). This is discussed in further detail in section 4.2.1.1.3.

IACs are also characterized by their spatiotemporal regulation. They constantly assemble and disassemble, and this process is mediated by several mechanisms including phosphorylation of different integrins and their adaptors, or endocytosis (Ezratty et al., 2009; Wilhelmsen et al., 2007; Zaidel-Bar et al., 2007). This causes a constant regulation in the adhesion strength. For instance, integrins are very motile within FAs and stay immobilized for less than 80 seconds, but this dynamic varies amongst integrin heterodimers (Rossier et al., 2012; Tsunoyama et al., 2018).

4.1.4 Integrins in cancer

Integrins can have an important role in cancer, namely in its initiation and progression. They have also been considered as targets for anti-cancer treatments (Hamidi and Ivaska, 2018).

4.1.4.1 Integrins in tumor initiation

Integrin-mediated interactions influence different cell functions, such as survival and proliferation by modulating signaling pathways such as the PI3K/Akt, Erk/MAPK, and Rho GTPase pathways. In addition, some integrins such as $\alpha 6 \beta 4$ enhance oncogenic signals of receptor tyrosine kinases (RTK). Indeed, it amplifies HER2 signaling and promotes mammary tumorigenesis (Rubashkin et al., 2014). It also potentiates the oncogenic activity of the MET receptor (or HGFR, hepatocyte growth factor receptor) by engaging $\alpha 4 \beta 1$ -integrin and the integrin associated tetraspanin CD151 (Bertotti et al., 2006, 2005).

Conversely, some integrins can act as tumor suppressors. In some occurrences, the $\alpha v \beta 3$ heterodimer has been reported to suppress tumor growth by inducing cell differentiation and apoptosis (Ramovs et al., 2017). Loss of integrin $\alpha v \beta 3$ expression has been associated with increased tumor progression and metastasis. In this way, the role of integrins in tumorigenesis is ambiguous, as integrin-mediated adhesion to the ECM regulates the cellular response to growth factors, which can either inhibit

or promote tumor initiation depending on the cellular context and the involved heterodimers (Alanko et al., 2015).

4.1.4.2 Integrins in cancer invasion and metastasis

Integrins are implicated in cancer cell invasion and metastasis. Indeed, they facilitate ECM degradation, cell motility and invasion by upregulating metalloproteinases (MMPs) and interacting with other proteases (Macedo et al., 2015). For instance, integrin $\alpha_6\beta_1$ promotes invasion in carcinoma cells by upregulating MMP-9, which degrades the ECM and facilitates cancer cell migration (Nardone et al., 2017). Additionally, integrin $\alpha_5\beta_1$ has been implicated in the invasion of breast cancer cells by activating urokinase (uPA), a protease involved in ECM degradation.

Integrins also contribute significantly to ECM remodeling by cancer-associated fibroblasts (CAFs), which generates a stiffer ECM, enhancing cancer cell migration and invasion (Winograd-Katz et al., 2014). Further details will be given in section 4.3.3.1. For example, integrin $\alpha_1\beta_1$ expression in CAFs has been shown to increase ECM stiffness, which promotes an invasive behavior of cancer cells (Cox et al., 2013). Furthermore, integrins play a crucial role during metastasis, supporting various steps such as intravasation, survival of circulating tumor cells (CTCs), extravasation into secondary sites, and colonization of new tissues (Labernadie et al., 2017). Integrin $\alpha_5\beta_1$, for instance, helps the survival of circulating tumor cells by maintaining cell-ECM interactions and activating survival pathways that prevent anoikis (a programmed cell death that occurs when cells detach from the ECM) (Desgrosellier et al., 2009).

During extravasation, heterodimers such as $\alpha_3\beta_1$ facilitate the adhesion of cancer cells to the endothelial cells lining blood vessels, thus increasing their escape rate into surrounding tissues (Labernadie et al., 2017). Integrins also guide the formation of invasive structures such as invadopodia, which are protrusions that degrade the ECM and allow cancer cells to invade surrounding tissues.

4.1.4.3 Targeting integrins for anticancer treatments

Given their significant roles in tumor progression and metastasis, integrins are attractive targets for anti-cancer therapies. Therapeutic strategies include the use of monoclonal antibodies to block integrin function, integrin-directed delivery of therapeutics, and the inhibition of integrin-mediated signaling pathways. For example, the monoclonal antibody etaracizumab targets integrin $\alpha_v\beta_3$ and has shown

promise in inhibiting angiogenesis and tumor growth in preclinical models (Canel et al., 2013).

Another strategy involves the use of integrin antagonists, such as cilengitide, which targets integrins $\alpha v \beta 3$ and $\alpha v \beta 5$ and has demonstrated anti-angiogenic and anti-tumor effects in glioblastoma (Borghi et al., 2010). However, so far, directly targeting integrins in cancer has failed, mostly because of cell plasticity, integrin redundancies and difficulty in patient stratification. Additionally, novel approaches such as integrin-targeted nanoparticles for drug delivery are being developed to improve the specificity and effectiveness of cancer treatments. For instance, integrin-targeted liposomes loaded with chemotherapeutic agents have shown improved delivery to tumor cells, reducing systemic toxicity and enhancing anti-tumor.

4.2 Apicobasal polarity of epithelial cells

A crucial feature of epithelial cells is to present an apicobasal polarity. This can be defined as an asymmetric segregation and distribution of membrane components such as proteins and lipids to distinct membrane sectors. Epithelial cells have an apical membrane facing the outside of the body or internal cavities named lumen, as well as a basolateral membrane on the opposite side featuring cell/ECM-interaction proteins, such as integrins.

This asymmetry allows the emergence of specialized cell functions (Nelson, 2003). The first polarized cells in mammals appear as soon as the 8-to-16 cells division at the blastocyst stage, further leading to a polarized trophectoderm (TE) and an apolar Inner Cell Mass (ICM) (Gerri et al., 2020; Nikas et al., 1996).

4.2.1 Polarity establishment

4.2.1.1 Molecular actors

The polarization process in cells is first initiated by cell-cell contacts (Bryant and Mostov, 2008). The process that polarizes the epithelium following this cue is called polarity establishment. During the formation of nascent cell-cell adhesions, a dimerization of E-cadherins will occur, thus triggering the recruitment of AJ and Tight Junction (TJ) proteins that will act as anchors for polarity proteins.

Three family of molecules have been reported to be a part of this polarity establishment process: polarity complexes, phosphoinositides (PIs) and Rho-GTPases.

4.2.1.1.1 *Polarity complexes*

Three protein polarity complexes have been well characterized across the literature. This molecular machinery is highly conserved in vertebrates.

→ **The Par3/Par6/aPKC complex** defines the apical domain. It is composed of Partition Defective 3 and Partition Defective 6 (Par3 and Par6) as well as atypical protein kinase C (aPKC) (Kemphues et al., 1988). There are three different Par6 proteins that can be found together as complexes or alone depending on the cell type: Par6A/C, Par6B and Par6D/G. Par6D/G is mostly found at TJs, Par6B in the cytosol, and Par6A/C in both. Par6 proteins help the accurate localization of other adhesion proteins and act as a mediator for the interaction between aPKC, Par3 and Lgl (Lethal Giant Larvae). For instance, downregulation of Par6 impairs TJs (Hurd et al., 2003; Joberty et al., 2000).

Two Par3 proteins have been identified: Par3A and Par3B. However, only Par3A binds atypical PKC (aPKC) and plays a role in the polarity complex (Lin et al., 2000). Indeed, after its association with Junctional Adhesion Molecules (JAMs) at nascent junctions, it recruits Par6 and aPKC therefore causing the junction's maturation. Indeed, it has been shown that a dysregulation in Par3 expression causes an incorrect localization of Par6, aPKC and defective TJs maturation (Itoh et al., 2001; Mizuno et al., 2003).

Interestingly, aPKC has been named “atypical” since it features an N-terminal PB1 domain that cannot be found in conventional PKCs. There are two isoforms of aPKC (aPKC λ /1 and aPKC ζ), found to be colocalizing with Par proteins at TJs (Suzuki et al., 2001).

→ **The Crb/PALS1/PATJ complex** also defines the apical domain. First characterized in *Drosophila Melanogaster*, it is composed of Crumbs (or Crb), which interacts with PALS1 and PATJ (Tepass et al., 1990).

Three Crb proteins have been described: Crb1, Crb2 and Crb3. While they present varied localization within tissues, Crb3 is mostly found at the apical domain in epithelial cells. Its FERM domain allows it to interact with the cytoskeleton (Roh and Margolis, 2003) and even with Par6, thus showing an inter-complex interaction profile (Lemmers et al., 2004).

Crb3, PALS1 and PATJ are found at the apical pole and around TJs. PATJ interacts with TJ proteins such as ZO-1, ZO-3 and Claudin-1. While downregulation of PALS1 causes mislocalization of E-cadherin (Wang et al., 2007), dysregulation of PATJ prevents ZO-1, ZO-3 and Claudin-1 from correctly localizing at TJs (Lemmers et al., 2004; Michel et al., 2005; K. Shin et al., 2005), therefore showing the role of this complex as a scaffold for TJ establishment during cell-cell contacts.

→ The **Scrb/Lgl/Dlg complex** defines the basolateral domain. The SCRIB (Scribble planar cell polarity protein), LGL (Lethal giant larvae) and DLG (Disc large) genes have first been discovered in *Drosophila Melanogaster*. Scribble plays a role in excluding apical proteins from the basolateral domain (Bilder and Perrimon, 2000a). While 5 Dlg-family proteins exist in mammals, Dlg1 has been the most extensively studied. It binds to APC, β -catenin and PI3K and is localized at the basolateral domain (Laprise et al., 2004; Matsumine et al., 1996).

The Lgl family presents two proteins: Lgl1 and Lgl2. They bind to the Par6/aPKC complex, after which aPKC phosphorylates Lgl causing its exclusion from the apical domain and its localization to the basolateral domain. This plays a key role in the apicobasal polarity establishment process (Suzuki et al., 2001).

4.2.1.1.2 Phosphoinositides (PIs)

PIs are a subtype of phospholipids that arise from a single precursor named phosphatidylinositol (PtdIns). This precursor can be phosphorylated at three different sites, therefore creating seven different PIs that have a different cellular localization (Di Paolo and De Camilli, 2006). These differentially phosphorylated PIs act as structural and signaling mediators. For instance, phosphatidylinositol-(4,5)-diphosphate ($\text{PI}(4,5)\text{P}_2$) controls the activity of the actin cytoskeleton by regulating the activity of actin-binding proteins (Yin and Janmey, 2003). The distribution of PIs is one of the main apicobasal polarity markers, with $\text{PI}(4,5)\text{P}_2$ being enriched at the apical membrane and phosphatidylinositol-(3,4,5)-triphosphate ($\text{PI}(3,4,5)\text{P}_3$) being enriched at the basolateral domain (Buckley and St Johnston, 2022; Gassama-Diagne et al., 2006; Martin-Belmonte et al., 2007).

→ **$\text{PI}(4,5)\text{P}_2$** is situated at the apical domain. A mechanism has been proposed (Martin-Belmonte and Mostov, 2007), in which PTEN (Phosphatase and tensin homolog deleted on chromosome ten), a phosphatase, converts $\text{PI}(3,4,5)\text{P}_3$ to $\text{PI}(4,5)\text{P}_2$. PTEN is targeted to the apical pole through a β 1-integrin/ECM contact, activating the GTPase Rac1 (see section 4.2.1.1.3). Because PTEN is targeted to the

apical domain, it results in a polarization of PIs. PI(4,5)P₂ at the apical site recruits Annexin-2 (Anx2), which in turn recruits the GTPase Cdc42 (see section 4.2.1.1.3), which acts as a binding platform for proteins of the Par6/aPKC complex, thus further characterizing an apical domain. PI(4,5)P₂ also interacts with other apical markers, such as ezrin, radixin and moesin (Di Paolo et al., 2002) which are polarity stabilizers, linking the apical membrane to the actin cytoskeleton.

→ **PI(3,4,5)P₃** is situated at the basolateral domain. The PI(4,5)P₂/PI(3,4,5)P₃ balance is finely regulated by the previously mentioned PTEN, but also by PI3K (phosphatidylinositol-3 kinase), which phosphorylates PI(4,5)P₂ into PI(3,4,5)P₃. PTEN and PI3K are therefore potent polarity drivers, and have been found to be regulated by localized Ras signaling (see section 4.2.1.1.3) (Sasaki et al., 2004). Insertion of PI(3,4,5)P₃ within the apical domain of MDCK (Madin-Darby canine kidney) cyst is sufficient to localize basolateral molecular markers and inverting polarity (Gassama-Diagne et al., 2006).

4.2.1.1.3 *Rho-GTPases*

GTPases are enzymes that can be described as GTP-dependent molecular switches. They can take two different conformations: one is bound to GTP (Guanosine triphosphate), which is often called “active” or “on” state, while the other is bound to GDP (Guanosine diphosphate), the “inactive” or “off” state. Active GTPases can interact with effector molecules up until they go back to an off state. These GTPases can be divided in five categories: Ras, Rho, Ran and the aforementioned Rab and Arf. Rho-GTPases have been described to play a major role in polarity establishment, which are the ones we will be describing here (Etienne-Manneville and Hall, 2002).

The switch between the active and inactivate states of Rho-GTPases are regulated by activators (GEFs – Guanine nucleotide exchange factors) and inactivators (GAPs – GTPase-activating proteins) (Bos et al., 2007). They can also associate with dissociation inhibitors (RhoGDIs) that keep them in an inactive state (Boulter and Garcia-Mata, 2012). Amongst the twenty identified Rho-GTPases, three are playing an important role in polarity establishment: **RhoA**, **Rac1** and **Cdc42**. Mutations in one of these GTPases is sufficient to trigger loss or misorientation of the apicobasal polarity (O’Brien et al., 2001).

While RhoA, Rac1 and Cdc42 all regulate the actin cytoskeleton and are implicated in apicobasal cell polarity, they each have specific roles (Mack and Georgiou, 2014):

→ **RhoA** is implicated in stress fiber formation, actomyosin contractility and activation of myosin-II. RhoA supports the formation and assembly of actin filaments and generates contractile forces. Linking it to polarity, RhoA regulates AJs and TJs which are crucial to the stability of the epithelium (Ridley and Hall, 1992). RhoA is recruited by the Crb/PALS1/PATJ complex in the first steps of cell-cell contacts and therefore increases cell contractility thanks to its effector ROCK. ROCK activity generates an actin belt in mature AJs. RhoA is therefore mostly localized at the apical domain, and recruits Rac1 GAPs which effectively disable Rac1 activity at the apical domain (Ratheesh et al., 2012). Therefore, the mutual RhoA/Rac1 exclusion is a founding characteristic of the apicobasal polarity establishment.

It should be kept in mind that the RhoA/Rac1 gradients can vary amongst the stages of apicobasal establishment and the maturation stages of cell-cell junctions. While RhoA plays a role in the maturation of the actomyosin belt on the AJs, it is then deactivated at the apical pole by its GAP, p190RhoGAP, but can later on be recruited once again for further maturation of AJs through E-cadherin recycling and activation of Myosin-II (Gomez et al., 2011).

→ **Rac1** is implicated in lamellipodia and membrane protrusion formation. It supports actin polymerization and allows cell migration. Through the establishment of a front-rear polarity, it allows cells to move in a mesenchymal cell migration mode (Ridley and Hall, 1992). Rac1 impacts apicobasal polarity by signaling downstream of Integrin- β 1 and assembling laminins at the basal membrane (O'Brien et al., 2001). It also plays a role at nascent AJs, just like RhoA. Indeed, Rac1 activation causes actin polymerization and membrane protrusions through its effector WAVE (Yamazaki et al., 2007), which causes cell-cell contacts and the formation of AJs. Once AJs are established, Rac1 is activated there by its GEFs: VAV2 and Tiam1 (Fukuyama et al., 2006; Hordijk et al., 1997; Malliri et al., 2004) which have been recruited by the E-cadherins of AJs. Rac1 inhibition has been shown to prevent clathrin-dependent cell-cell adhesion and proper epithelium polarization (Ehrlich et al., 2002).

→ **Cdc42**'s role is a key regulator of polarity as it regulates the localization of polarity complexes such as Par3/Par6/aPKC, and, consequently, the formation of TJs. Cdc42 is crucial in the formation of filopodia and plays a role in the formation of polarized structures in epithelial cells such as microvilli (Ngok et al., 2014). Cdc42 acts by first binding to Anx2 and accurately localizes the Par3/Par6/aPKC (Martin-Belmonte et al., 2007). Cdc42 also localizes the Crb/Pals1/Patj complex through a Rab11-dependant mechanism (Schlüter et al., 2009).

Cdc42 forms filopodia through its activation of Arp2/3, which promotes branching of actin cytoskeleton in an N-WASP-dependent mechanism (Ngok et al., 2014). Just like other Rho-GTPases, Cdc42 activity is temporally and spatially controlled. Indeed, it plays an important role in the early stages of cell-cell junction, but the presence of Cdc42 GAPs such as ARHGAP17 at the apical pole and GEFs such as Tuba at the basal pole indicates that Cdc42 inactivation is necessary for junctional maturation (Elbediwy et al., 2012). The localized concentration and activation of Cdc42 is needed for apical growth, and it has been shown that Cdc42 inhibition prevents the proper growth and polarization of MDCK cysts (Jaffe et al., 2008; Salat-Canela et al., 2023).

4.2.1.2 Sequence of events and interactions during polarity establishment

During polarity establishment, Crb recruits PALS1 through its PDZ domain, which then recruits Par6. These components of the Crb/PALS1/PATJ complex, through Cdc42 and aPKC, mediate the phosphorylation of Par3, Par1 and Lgl. This causes exclusion of Lgl (along with other basolateral proteins such as Dlg and Scrib) from the apical domain. The phosphorylation of Par1 prevents the basal recruitment of apical markers such as Par3. This signaling cascade explains the segregation between Crb and Par complexes at the apical pole, and Scribble complex at the basolateral domain (see Figure 5).

As mentioned before, PIs are also responsible for membrane asymmetries. PTEN is recruited to cell-cell junctions through its interaction with Par3, which causes a higher concentration of PI(4,5)P₂ at the apical domain which in return causes the recruitment of Cdc42 through Anx2. Cdc42 activates aPKC, which closes a signaling loop as it can in return, phosphorylate Par3, Par1 and Lgl.

PI3K is recruited by E-cadherin to basolateral junctions which recruits basal markers such as Dlg, and causes a higher concentration of PI(3,4,5)P₃ (Rodriguez-Boulan and Macara, 2014). In this process, E-cadherin plays a central role as it mediates junction maturation by reducing the surface tension at cell-cell interactions (Slováková et al., 2022; Stachowiak et al., 2012; Winklbauer, 2015). Upon E-cadherin binding, there is a RhoA inactivation and a Rac1 activation, therefore better characterizing the basal domain (Anastasiadis et al., 2000; Yamada and Nelson, 2007).

4.2.2 Polarity orientation and maintenance

4.2.2.1 ECM contact and subsequent orientation of polarity markers

As discussed above, many key steps of the polarity establishment process have been described. Another important aspect is the polarity orientation process, i.e. the correct localization of both basal and apical poles. To detail the timeline of polarity orientation, it is necessary to focus on a specific example. MDCK (Madin-Darby canine kidney) cells can generate polarized cysts and for this model, the sequence of events has been largely elucidated. Early on, through first MDCK cell contacts, podocalyxin (Pcx) (a glycoprotein, member of sialomucins and an apical marker) is distributed at the outer membrane of cysts. It is then endocytosed in a Rab8- and Rab11-dependant manner and delivered to a zone named AMIS (apical membrane initiation site). This is the first step of polarity orientation, as the AMIS is the precursor of what will become the apical membrane (Bryant et al., 2010). Anx2 and Cdc42 associate with the Rab8/Rab11-positive Pcx-transporting vesicles which, upon Cdc42 activation through its GEF, Tuba, initiates the lumenogenesis process. Par6 bridges Cdc42 to the aPKC-Par3 complex, which allows the docking of the apical vesicle to the AMIS. This AMIS evolves to a Pcx-enriched pre-apical patch (PAP) which is where the lumen starts forming. The lumen expansion is allowed by kinase-dependent activation of apical chloride channels (Bryant et al., 2010; Li et al., 2004) (see Figure 5).

Several supplementary polarity actors have been described more recently (Bryant et al., 2014). Pcx forms a complex with NHERF1 (Na⁺/H⁺ Exchanger Regulatory Factor) and Ezrin (which stabilizes Pcx at the apical membrane). In cysts cultured in suspension, the inverted localization (ie. to the outer side) of this Pcx/NHERF1/ezrin complex is stabilized by the phosphorylation of ezrin through ROCK1 (a RhoA effector, member of the aforementioned ROCK family) activity. However, upon ECM sensing via β 1 integrin (likely as α 2 β 1 and α 3 β 1 heterodimers), integrin heterodimers recruit FAK that leads to an activation of p190-RhoGAP which in return inactivates RhoA and causes a decrease in ezrin phosphorylation (Bryant et al., 2014). This, combined with the phosphorylation of Pcx by PKC β II induces a destabilization of the complex and a subsequent endocytosis of Pcx to the AMIS. This is followed by the action of phosphatase PP2A which dephosphorylates Pcx and causes a reassociation of the Pcx/NHERF1/ezrin complex, at the AMIS this time, showing here a sequential timeline of the polarity orientation process.

This ECM-integrin contact also initiates the formation of a basal membrane with the assembly of laminin at the basal pole (O'Brien et al., 2001). This process is IRSp53-

dependent, which also activates factors like WAVE leading to actin polymerization from the basal pole. Blocking Integrin- β 1 forces an inverted-polarity phenotype. Conversely, inhibiting RhoA will support a normal polarity phenotype, and this will be further described in 4.2.3 (Adams et al., 2004; O'Brien et al., 2001; Yu et al., 2008, 2004) and in 7.1.

4.2.2.2 Trafficking of polarity proteins in the polarity orientation process

Polarity orientation goes hand in hand with redistribution of polarity-related molecules. In the case of Crb and Pcx, they are brought from the outer membrane to the AMIS by first being endocytosed in a clathrin-dependent manner. The heterotetramere Adaptor Protein Complex 2 (AP-2) is central here, playing a crucial role for the recognition and selection of polarity proteins that are destined for endocytosis (Bonifacino, 2014). This recognition is simultaneous to the formation of a clathrin triskelion-coated pit. Indeed, proteins such as Eps15 and Epsin interact with both clathrin and AP-2 to stabilize this budding endosome (Rodriguez-Boulan and Macara, 2014). Once in the early endosome (EE), Crb is brought to the AMIS through an Apical recycling endosome (ARE).

Once apically localized, Crb is constantly endocytosed and recycled back to the plasma membrane to maintain its localization. Endocytosis of Crb through ASE (Apical Sorting endosome) is then followed by a retrograde transport to the trans-Golgi network (TGN) through a Common Recycling endosome (CRE). From the TGN, it is recycled back to the apical membrane. In the TGN, the sorting of polarity proteins is helped by the heterotetramer Adaptor Protein Complex 1 (AP-1). However, some studies have shown that the localization of polarity proteins can be AP-independent (Schuck and Simons, 2004).

In a similar fashion, basolateral components traffic through BREs (Basal recycling endosomes) and BSEs (basal sorting endosomes) (Apodaca et al., 2012; Zhang et al., 2023).

After their recruitment via AP-1 and AP-2, the polarity protein-containing vesicles need to be fused at the proper membrane. This is controlled mainly by Anx2 which binds to vesicles containing apical proteins. The fusion is dependent on v-SNARE (on the vesicular side) and t-SNARE (on the target side) proteins, the specific SNAREs involved differs between the apical and basal domains (Gerke et al., 2005; Pocard et al., 2007).

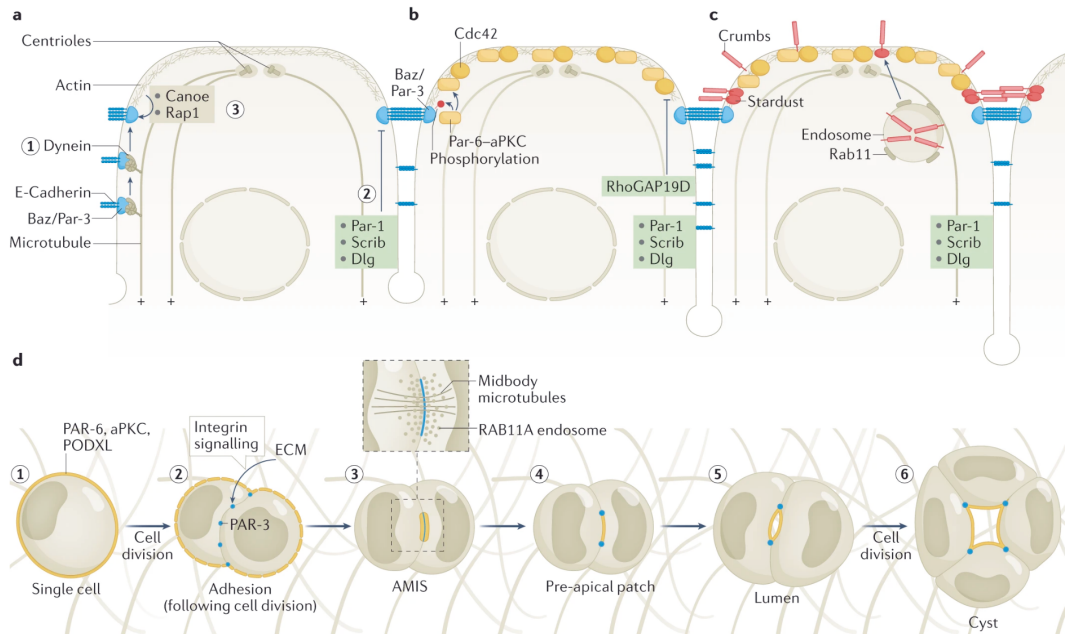


Figure 5- Polarity establishment and orientation (from Buckley and St Johnston, 2022)

a,b,c: Steps of polarity establishment. d: Polarity orientation. Stardust=PALS1, PODXL=podocalyxin

4.2.2.3 Polarity maintenance

Apicobasal polarity is maintained through the action of ERM proteins (for ezrin, moesin, radixin). Indeed, during the polarity orientation, a decrease in the phosphorylation of ezrin causes a destabilization of the Pcx/ezrin/NHERF1 complex and causes a relocalization of polarity markers (Bryant et al., 2014). ERM proteins all contain a plasma membrane-binding domain called the FERM domain (4.1,ezrin,radixin,moesin) and an actin-binding domain called C-ERMAD (C-terminal ERM-association domain). ERM proteins are found in various cells in the mammalian body, but ezrin is exclusively present in epithelial cells. When inactive in the cytoplasm, ERM's FERM and C-ERMAD domain interact and this

intramolecular bond mediates the autoinhibition of the protein. Once recruited to the plasma membrane, phosphorylated by RhoA's effector ROCK1 and bound to PI(4,5)P₂, the autoinhibitory interaction is disrupted, the two domains dissociate and the C-ERMAD domain become available for actin binding (Fehon et al., 2010; Saotome et al., 2004).

In intestinal epithelial cells mostly, ezrin is the only ERM protein expressed and acts as a polarity maintenance key regulator. Being a well polarized molecule, it is often used as a polarity marker (Saotome et al., 2004).

4.2.3 Inverted polarity

Inverted polarity englobes any non-conventional distribution of polarity molecules. It is always described as opposed to what a “normal polarity” would be. The normal polarity, also named “apical-in”, is conventionally defined by an apical domain facing a lumen-like structure and a basolateral domain facing other cells or the ECM. However, inverted polarity sometimes called “reverse polarity” or “apical-out”, is characterized by a reversion of the apical and basolateral domain while the overall polarity axis of the cell/cell cluster remains. In mammals, this inverted polarity occurs in pathological situations, an exception to this being the blastocyst development. More instances of inverted polarity can be found in other animals, such as within the *Drosophila Melanogaster* embryo (Ebnet, 2015). All of these processes are well described in Pasquier et al., 2024 (see Figure 6). The study of inverted polarity has been the focus of **I**, which can be found enclosed at the end of this thesis.

4.2.3.1 Inverted polarity in cancer

For a long time, the loss of apicobasal polarity commonly referred to as EMT (epithelial-to-mesenchymal transition) was thought to be one of the main drivers in carcinoma progression and dissemination. It has been shown that nonpolarized epithelia were more likely to invade (Lee and Vasioukhin, 2008; Macara and McCaffrey, 2013; Peglion and Etienne-Manneville, 2023; Wodarz and Näthke, 2007). However, it has been found through histopathological analysis that some cancers such as colorectal adenocarcinoma present structures with highly conserved AB polarity axis, with epithelial structures surrounding an inner lumen (Libanje et al., 2019).

A subtype of highly invasive carcinoma named micropapillary carcinoma show structures that have a fully inverted AB polarity (Verras et al., 2023). In these tumors,

apical markers such as the membrane-bound glycoprotein MUC1 are found at the outer bound, whereas basolateral markers such as the cell adhesion molecule EpCAM is inside.

These inverted polarized structures can be found in multiple different cancers, such as breast or lung carcinomas (Adams et al., 2004; Hirakawa et al., 2022; Luna-Moré et al., 1994; Nassar et al., 2004; Siriaunkgul and Tavassoli, 1993), colorectal carcinoma (Verdú et al., 2011), cervical carcinoma (Stewart et al., 2018) and thyroid carcinoma (Asioli et al., 2013). Some cancers are even characterized by this inverted polarity, such as breast solid papillary carcinoma with reverse polarity (SPCRP) (Chiang et al., 2016) and papillary renal neoplasm with reverse polarity (PRNRP) (Al-Obaidy et al., 2020, 2019).

Inverted polarity cancer cell clusters have also been found in peritoneal effusions or pleural effusions (Ritch and Telleria, 2022; Zajac et al., 2018), in the lumen of lymphatic vessels or lymph nodes (de Boer et al., 2010; Mohammed et al., 2019) and in pools of mucins within tumors (Sun et al., 2020). These structures have been named TSIPs (Tumor spheres with inverted polarity) and can be described as tumor cell clusters that present an apical domain on their outer membrane. These structures have an apical-out polarity in suspension as expected, since there is no ECM to trigger any polarity establishment. However, in some instances TSIPs placed in matrix maintained an apical-out polarity, therefore demonstrating inverted polarity as a distinct malignant phenotype for some cancer subtypes (Canet-Jourdan et al., 2022; Okuyama et al., 2016; Onuma et al., 2021; Zajac et al., 2018).

4.2.3.1.1 Consequences of inverted polarity on cancer invasion

The presence of TSIP-like structures in cancer has a direct impact on cancer prognosis and invasion. Indeed, micropapillary carcinomas with inverted polarity structures show a high proportion of lymph node metastasis (Kuroda et al., 2004). Because of their inverted polarity, TSIPs lack surface integrins that would allow them to form IACs with the ECM and form actin-based protrusions (Zajac et al., 2018). They propagate from a metastasis or another TSIP, budding from their structure. It has been shown that TSIPs adopt a collective amoeboid mode of migration, moving in a fashion that is similar to immune cells, which depends on friction forces and the contractility of the actomyosin ring at the rear of the cluster (Pagès et al., 2022). A partial inversion of polarity is enough to trigger invasion in a collective amoeboid manner in MDCK spheroids (Bryant et al., 2014).

4.2.3.1.2 *Consequences of inverted polarity on drug resistance*

In colorectal cancer organoids, TSIPs have a better resistance to chemotherapy than apical-in structures which is due to a lower proliferation of apical-out structures, therefore conferring resistance against some chemotherapies such as anti-mitotic drugs (Canet-Jourdan et al., 2022). This can also be linked to a protection that is inherently linked to inverted polarity. Indeed, transporters such as ABCB1 are localized at the outer membrane in TSIPs, causing drug exclusion (Ashley et al., 2019).

4.2.3.1.3 *Consequences of inverted polarity on immune escape*

Proteins necessary for the immune response such as Major histocompatibility complex (MHC) or toll-like receptors (TLRs) are polarized. Indeed, in healthy gut or lung epithelia, MHC-II proteins such as HLA-DR and HLA-DM are polarized at the basolateral domain. This polarization is essential for the regulation of CD4⁺ T-cells which have a well-established anti-tumor role (Hershberg et al., 1998; Speiser et al., 2023; Wosen et al., 2018). In TSIPs with inverted polarity, MHC-II is not localized to the outward membrane. This may be linked to TSIPs escaping immune surveillance and to immunotherapy failure in cancer types with inverted polarity (Axelrod, 2019; Guo et al., 2008).

TLR-3 is also polarized in healthy tissue, as it is basolaterally localized in the intestinal epithelium (Stanifer et al., 2020). Because of this, TSIPs might lack TLR-3 on their outer membrane, therefore causing, once more, an immune escape.

4.2.3.1.4 *Plasticity of inverted polarity in cancer*

While the aforementioned TSIPs show an apical-out polarity in suspension, they can adopt two polarity phenotypes once embedded in an ECM. After culturing them in a collagen matrix, some of them revert to an apical-in polarity. This shift in polarity is not fully understood and has been the main object of this thesis, although an implication of the TGF- β pathway as the main driver of polarity in this system has been described (Canet-Jourdan et al., 2022). Blocking Integrin- β 1 has been shown to prevent the establishment of a normal apical-in polarity in ECM-embedded TSIPs, which shows an implication of the Focal Adhesion Pathway in the polarity establishment process (Canet-Jourdan et al., 2022 and 7.1).

4.2.3.2 Inverted polarity in genetic diseases

Some genetic diseases can cause pathological inverted polarity:

→ **Microvillus inclusion disease (MVID)** is a disease that affects absorption of nutrients through the intestinal epithelium, causing diarrhea. This disease can be caused by several mutations, including MYO5B, STX3 or STXBP2. This results in a loss of apical microvilli and mispolarization of key proteins (Schneeberger et al., 2015).

→ **Multiple intestinal atresia associated with combined immunodeficiency (MIA-CID)** is linked to a mutation in the TTC7A gene. This disease causes complete inversion of polarity in intestinal organoids (Bigorgne et al., 2014).

→ **Polycystic kidney disease (PKD)** is caused by mutations in PKD1 and PKD2 genes. This results in mispolarization of proteins leading to an abnormal cell proliferation and cyst formation (Menezes and Germino, 2019; Wilson Patricia D., 2004) in the kidney. This polarity inversion causes an alteration in fluid absorptions, therefore causing an expansion of these cysts (Li et al., 2022).

4.2.3.3 Inverted polarity in pathogen defense

Inverted polarity in epithelia caused by pathogen infection leads to a signaling to immune system. In chronic liver diseases for instance, damage caused to healthy cells causes a relocalization of ICAM-1, normally localized at the apical domain, to the basal pole. Indeed, TNF- α treatment of healthy hepatocytes is sufficient to invert ICAM-1 localization to the basal domain enhancing T-lymphocyte recruitment (Reglero-Real et al., 2014).

Some examples show that pathogen infection cause a local polarity inversion. Upon *Pseudomonas aeruginosa* infection, the intestinal epithelium cells form protrusions surprisingly enriched in basolateral markers such as PI3K, PI(3,4,5)P₃ and E-cadherin. This causes both a more favorable environment for bacterial colonization, but also triggers immune response signaling, so the effect is dual (Gassama-Diagne et al., 2006; Kierbel et al., 2007; Tran et al., 2014).

Similarly, *Neisseria meningitidis*, the cause of cerebrospinal meningitis, invades thanks to polarity disrupting. At infection sites, its membrane extensions containing

basolateral and apical components destabilizes the endothelium which creates gaps allowing bacterial crossing (Coureuil et al., 2009).

4.2.3.4 Inverted polarity in development

Inverted polarity can also occur in a physiological situation, and more precisely during the early stages of embryonic development. From the 8-cell stage, blastomeres start compacting and develop an apical-out polarity. This inverted polarity is characterized by an increased localization of actin, actin-binding proteins and the Par3/Par6/aPKC polarity complex at the outer membrane (Ducibella et al., 1977; Lehtonen and Badley, 1980; Nikas et al., 1996; Plusa et al., 2005; Reeve and Ziomek, 1981), when basolateral proteins such as the Scrib/Lgl1/Dlg1 are localized at cell/cell contacts (Hirate et al., 2013). Through asymmetrical and symmetrical divisions, polar cells differentiate into a polarized trophectoderm (TE) and an apolar Inner cell mass (ICM). ; Maître, 2017; Maître et al., 2016). The formation of the blastocoele (a lumen-like structure within the blastocyst) is interesting, because the lumen initiation at the basolateral domain obeys different laws than to the apical domain. While the apical domain does not harbor adhesion molecules and therefore makes it a favorable site for fluid accumulation, the blastocoele forming at the basolateral domain is due to the accumulation of fluid-filled microlumens, fusing to each other by Ostwald ripening, therefore creating and increasing the size of the cavity (Dumortier et al., 2019).

There is a marked plasticity in the polarity status of the blastocyst pre- and post-implantation. While the apical-out polarity has been well described pre-implantation, the polarity status adjusts during implantation. TE cells adhere to the endometrium, which requires a polarity adjustment of the blastocyst in order to avoid apical/apical repulsion. It has been shown that the mural blastocyst maintains its apical domain externally, but invert the localization of some integrins to promote the adhesion to the endometrium (Sutherland et al., 1993).

During the menstrual cycle, the polarity of luminal endometrial cells is changed, with the loss of the apical enrichment of the Par complex, the Crb complex and mucins (Whitby et al., 2020). The formation of pinopodes at the surface of the endometrium makes it receptive to implantation (Quinn et al., 2020), via different integrin heterodimers such as $\alpha v \beta 3$. No obvious link has been found between the implantation process and the involvement of integrin- $\beta 1$. Interestingly however, overexpression of Integrin- $\beta 1$ subsequent to a pathological situation, such as infection by *C. trachomatis*, enhances adhesion of the blastocyst within the Fallopian tubes and promotes ectopic pregnancies.

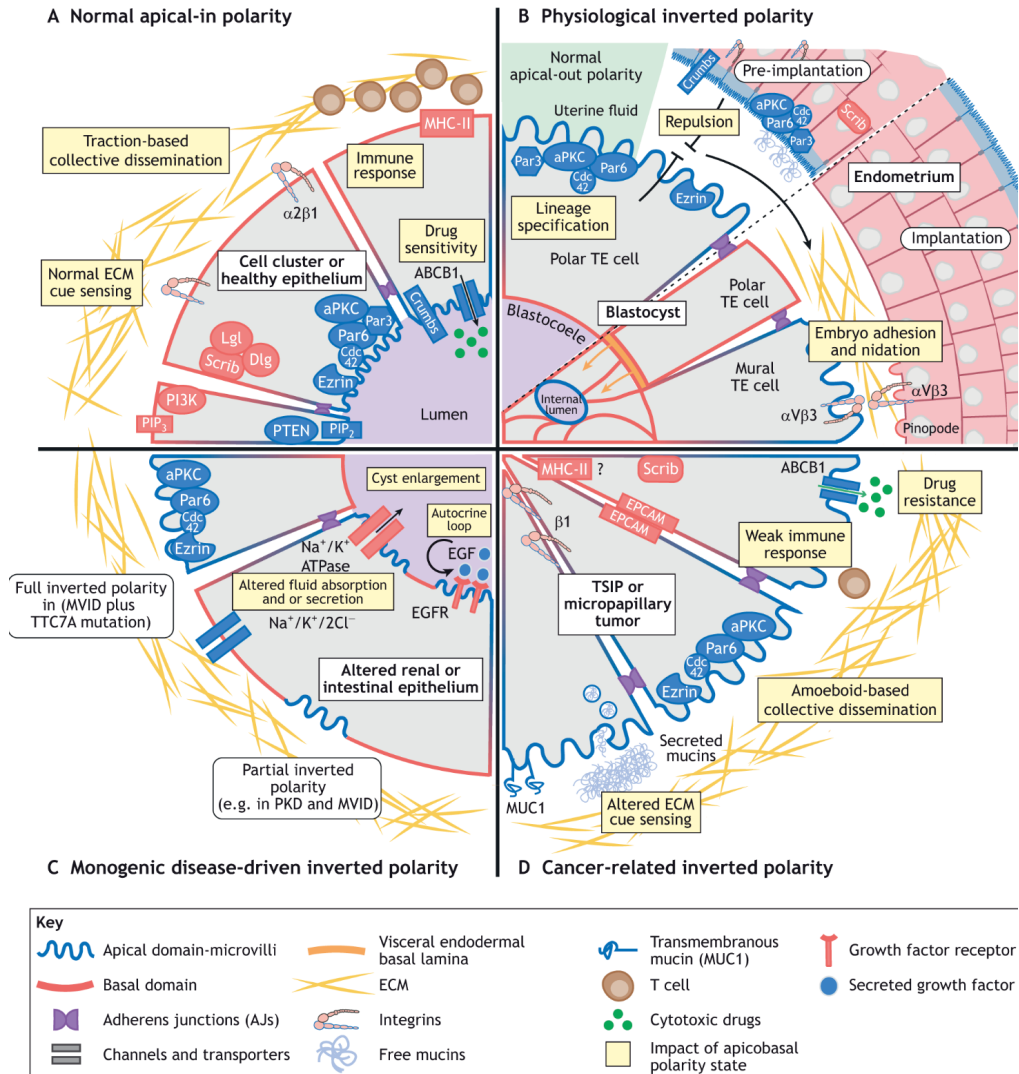


Figure 6- Inverted apicobasal polarity (from Pasquier et al., 2024)

(A) Normal epithelial polarity is regulated by the asymmetric localization of mutually antagonistic complexes. The Par and the Crumbs complexes define the apical pole which is enriched in PIP₂, PTEN and ezrin (proteins marked in blue). Below AJs, the Scribble complex defines the basolateral domain, which is enriched in PIP₃ and PI3K (proteins marked in red). ECM sensing through integrins controls the orientation of apicobasal polarity and ensures traction-based collective migration. Basal localization of MHC-II is thought to promote immune clearance of damaged cells by permitting T cell recruitment. Apical localization of the multidrug resistance transporter ABCB1 allows drugs to persist in lumens of epithelia. PIP₃, phosphatidylinositol 3,4,5-phosphate. (B) The pre-implantation blastula displays apical-out polarity, which prevents adhesion to the uterine wall due to apical–apical repulsion. During the menstrual cycle, to permit successful embryo nidation, apical determinants in the endometrium disappear from the lumen-facing membranes while integrins and pinopodes appear. In parallel, polar throphectoderm (TE) cells invert their polarity in response to emergence of the endodermal basal lamina and mural TE cells express integrins at the periphery of the blastula to promote implantation. (C) MVID enterocytes show partial inverted polarity of microvilli structures. MVID with an additional mutation in *TTC7A* results in fully inverted polarity in these cells. In PKD renal tubules, inverted polarity of ion channels and EGFR contribute to the growth of cysts via altered fluid absorption and secretion. (D) TSIPs arise from micropapillary and mucinous carcinoma. The absence of integrins and presence of mucins at the TSIP periphery prevent cell–ECM interactions resulting in tissue invasion via the collective amoeboid mode of migration. The inverted polarity of ABCB1 enhances cytotoxic drug resistance whereas basolateral localization of MHC-II could limit T cell infiltration and increase immune escape.

4.3 Biological systems to study polarity and integrin-mediated adhesions

4.3.1 Colorectal adenocarcinoma (CRC)

4.3.1.1 Healthy gut architecture

The colon is an organ which function is to uptake nutrients and water from the alimentary bolus. The role is dual, being both a structure of absorption and secretion. It is also an important epithelial barrier against pathogens. Because of all these combined functions, the colon displays a wide variety of cells with different architectures, thus creating a multifunctional epithelium.

Through histological analysis, the colon can be divided in four distinct zones from the lumen to the peritoneum (Maqbool, 2013):

→ **The mucosa** is the outermost layer (on the apical side, at the border with the lumen). This sheet is composed of the cells composing the Lieberkühn crypts, as well as the lamina propria, ie. the connective tissue and inflammatory cells joining the mucosal cells.

→ **The muscularis mucosa**, a thin muscular layer.

→ **The submucosa** is composed of nerves, blood and lymphatic vessels. It is a connective tissue surrounding the muscularis mucosa.

→ **The muscularis externa**, a thin sheet of smooth muscles.

In addition to these layers, **the serosa**, a monolayer of mesothelial cells, is one of the composing sheets of the peritoneum (the visceral layer) surrounding the gut as well most of the organs situated within the abdomen.

As mentioned above, the mucosa is composed of Lieberkühn crypts containing a set of different cells named colonic cells. These crypts increase the surface area of the gut, therefore enhancing secretion and absorption. Different cell types are found in the crypt with specific localization and function (see Figure 7):

→ **Colonic stem cells** are situated at the base of the Lieberkühn crypt. These cells are nonmigratory, undifferentiated and maintain a pluripotent identity. They are

characterized by the expression of stem cell marker Lgr5 (leucine-rich-repeat-containing G-protein-coupled receptor 5) (Barker et al., 2007). Lgr5 acts as a Wnt pathway amplifier by binding to its agonist, R-spondin. Colonic stem cells give rise to other mucosa cells, such as Paneth cells, goblet cells, enteroendocrine cells and tuft cells. This differentiation is finely tuned by a regulator called Notch. Indeed, Notch influences cell fate by activating Hes1, which represses Atoh1 to prevent secretory lineage entry. Hes1 deletion increases secretory cells production, while Atoh1 deletion eliminates them, indicating their crucial regulatory roles (Jensen et al., 2000; Shroyer et al., 2005).

→ **Deep secretory cells (DSCs)** have a similar structure and function to that of Paneth cells in the small intestine. They are issued from the first differentiation stage of colonic stem cells. They act as a protector against pathogens by secreting antimicrobial peptides such as α -defensins. These cells are also nonmigratory. They have a growth factor secretion activity and produce digestive enzymes (Bevins and Salzman, 2011).

→ **Goblet cells** have a protective function through the production of mucins. Mucins in the gut can be of two natures: membrane-bound mucins (mostly MUC1) compose the first layer, which acts as a filter protecting the epithelial cells against pathogens. The second layer is composed of free mucins (mostly MUC2), which acts as a protective layer and allows transport of secreted gut content (Birchenough et al., 2015). These cells progressively migrate from the bottom of the crypt towards the villi (Yang and Yu, 2021).

→ **Enteroendocrine cells (EECs)** mostly play a role in the synthesis of digestive enzymes and present ion transporters and channels allowing fluids and electrolyte transports. EECs also produces hormones that are stored within cytoplasmic granules. Upon signaling reception, these vesicles are released at the basolateral membrane, which triggers nerve endings at the basal membrane or reaches other distant cells through the bloodstream (Gribble and Reimann, 2016; Latorre et al., 2016).

→ **Tuft cells** have been less studied, but their structure is known to be close to that of taste buds on the tongue. Indeed, many molecular markers of the taste transduction pathway were found on tuft cells such as α -gutducin, β -endomorphin, metenkephalin and uroguanylin (Höfer et al., 1996; Luciano and Reale, 1990).

→ **Enterocytes** are the most common cells within the gastrointestinal (GI) tract and compose more than 80% of the gut epithelium. They present structures called microvilli at their apical pole (facing the lumen). Measuring around 1-3 μm long, these structures increase the absorption surface of the gut. These cells also present transporters and channels allowing the absorption of water and nutrients. Akin to goblet cells with mucins, enterocytes produce a membrane-bound mucin-type glycoprotein (Maury et al., 1995).

Enterocytes are mainly responsible for nutrients and water absorption and do so through two different transport pathways:

→ **The transcellular transport** is ensured by channel proteins or carrier proteins. Nutrient uptake can also be performed through endocytosis or pinocytosis (Conner and Schmid, 2003). In this pathway, nutrients travel within the cell.

→ **The intercellular or paracellular transport** relies on the plasticity of TJs which allows the diffusion of small nutrients (Pappenheimer, 2001) in between the cells.

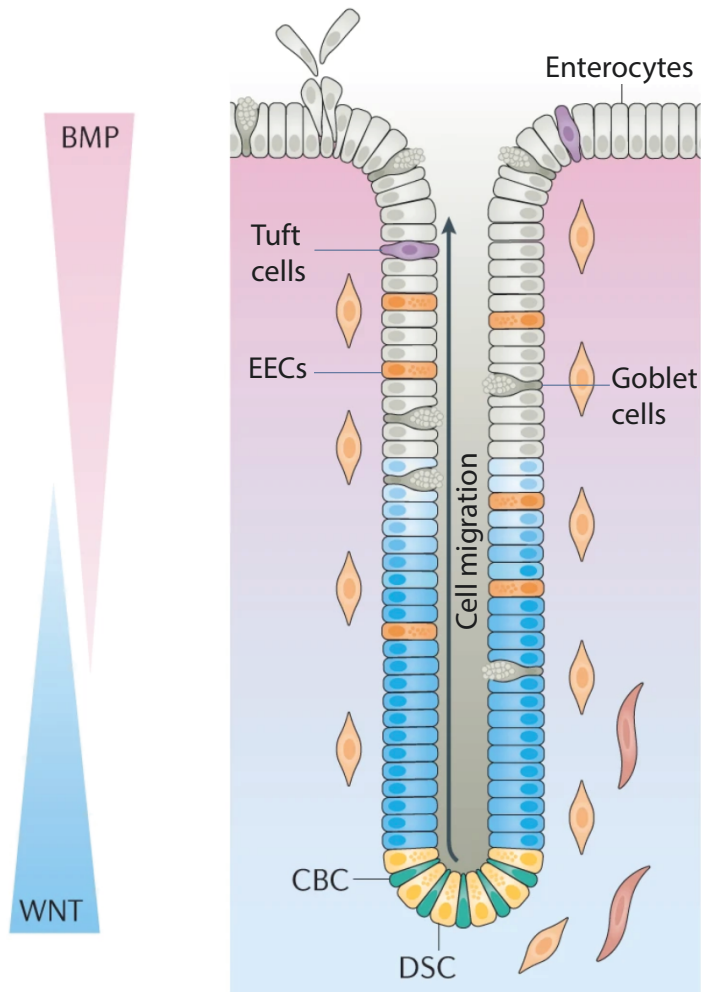


Figure 7- Structure of a crypt (adapted from Beumer and Clevers, 2021)

4.3.1.2 Characterization of CRCs

Colorectal adenocarcinoma (CRC) is the third most common cancer type worldwide as well as the second most common cause of cancer death (Siegel et al., 2023). In more than a half of cases, carcinogenesis can be attributed to specific risk factors, such as smoking, diet, alcohol consumption, physical inactivity or body weight (Islami et al., 2018). Some forms are hereditary, with Lynch syndrome being one of the best documented instances (Lynch et al., 2008).

4.3.1.2.1 *Histopathology*

Beyond conventional scoring such as TNM (Tumor, Node, Metastasis) score and the immune infiltration of tumor microenvironment, CRCs can be analyzed by anatomopathologists subsequently to a biopsy. Therefore, several histological CRC subtypes have been identified:

→ **Classic adenocarcinoma (CA)** is the most common histological subtype of CRC. It accounts for 80-90% of patients (Li et al., 2019; Bagante et al., 2018). They can be further characterized by their glandular status:

→ Well differentiated CA-CRCs have more than 95% of the tumor that is gland-forming.

→ Moderately differentiated CA-CRCs have 50-95% gland formation.

→ Poorly differentiated CA-CRCs have less than 50% gland formation.

→ **Mucinous adenocarcinoma (MUC)** is characterized by more than 50% of the analyzed surface being composed of mucins. Although this has been challenged, MUC-CRC subtypes are correlated with a higher metastatic burden, a higher proportion of peritoneal carcinomatosis (PC) and is linked to a poorer outcome (Hugen et al., 2016; Mekenkamp et al., 2012).

→ **Micropapillary carcinoma (MiP)** is characterized by the presence of tumor clusters within the cancer stroma. They are more invasive than CAs and are associated with a poorer prognosis. Some of these MiP-CRCs keep a highly differentiated profile with the presence of polarized structures (Barresi et al., 2014; Nagtegaal et al., 2020).

→ **Serrated carcinoma (SeC)** is characterized by serrated lesions within the glandular sections of the tumor. It is thought that MUC-CRC actually arise from serrated lesions, therefore relegating these subtypes as two evolution stages of CRCs (Laiho et al., 2007).

→ **Medullary carcinoma (MeC)** are characterized by poorly differentiated clusters showing an eosinophilic cytoplasm, but this subtype can often be confused with the poorly differentiated grade of CA-CRCs (Wick et al., 2005).

→ **Signet ring cell carcinoma (SRCC)** are characterized by the presence of signet ring cells, which are big cells with a large vacuole. They have a high invasiveness towards lymph nodes and have a poor prognosis (Hugen et al., 2015).

→ **Neuroendocrine carcinoma (NeC)** arise from neuroendocrine (which enteroendocrine cells constitute a section of) cells within the gut. A tumor is classified NeC if it contains more than 30% of neuroendocrine cells (Bernick et al., 2004; Nagtegaal et al., 2020).

→ **Adenosquamous carcinoma (AsC)** is the least documented of these subtypes, and presents a very similar phenotype than CAs, with a poorer prognosis (Nagtegaal and Hugen, 2015).

4.3.1.2.2 *Consensus Molecular Subtypes (CMS)*

In addition to histological profiling, a molecular profiling called “Consensus Molecular subtypes” allows to classify different CRCs in 4 different categories (CMS1, 2, 3 and 4). This classification discriminates between different cancer subtypes using multiple criteria detailed below (Fessler and Medema, 2016):

→ **CMS1, or MSI (Microsatellite instable) immune group**, among which tumors are generally associated with a high MSI status, hypermethylation (CpG island methylator phenotype or CIMP) and BRAF^{V600E} mutation. MSI tumors have a dysfunctional mismatch repair (MMR) machinery, causing an accumulation of mutations in the DNA. CIMP phenotype causes many cytosine- and guanine-enriched promoters to be methylated, thus causing a silencing of genes, and most importantly tumor suppressor genes.

→ **CMS2, or canonical subtype**, presents high levels of chromosomal instability (CIN) and an activation of Wnt signaling pathway. CIN phenotype causes an abnormal karyotype, with some chromosomes being aneuploid and showing structural defaults.

→ **CMS3, or metabolic subgroup**, displays KRAS mutations, increase in metabolic pathways, and present a hypomethylated phenotype.

→ **CMS4, or mesenchymal type**, presents an activation of EMT-associated genes, angiogenesis, TGF- β signaling and matrix remodeling.

CMS classification and histopathology do not necessarily coincide. For instance, MUC-CRCs can be found in CMS1, CMS3 and CMS4, but are practically absent from CMS2. Furthermore, 13% of CRCs cannot be stratified using this classification due to mixed phenotypes.

4.3.1.2.3 *Developmental pathways*

Most CRCs arise from polyps, which are precursor lesions arising from colorectal cancer stem cells at the very base of intestinal crypts. A polyp evolves to CRCs in about 10-15 years. CRCs evolve along two distinct developmental pathways (“Comprehensive molecular characterization of human colon and rectal cancer,” 2012; Dekker et al., 2019):

→ **The adenoma-carcinoma pathway** accounts for 70-90% of CRCs. These evolve by the accumulation of CIN and genetic mutations. This sequence is generated by an APC (Adenomatous polyposis coli) mutation, causing its loss of function. This is followed by RAS activation and loss of the anti-cancer TP53. This pathway leads to a tubular adenoma.

→ **The serrated neoplasia pathway** accounts for 10-20% of CRCs. This pathway is often started by genetic mutations of BRAF or KRAS and is characterized by a high CIMP status. This pathway leads to serrated lesions.

4.3.1.3 *Metastasis and invasion of CRCs*

CRCs invade following three main metastatic routes:

→ **The circulatory route** occurs using blood and lymphatic vessels. This cascade starts with the invasion of tumor cells within the surrounding matrix, followed by the intravasation of the tumor cells inside the circulatory system (where they are called circulating tumor cells - CTCs), the circulation of tumor cells, the extravasation from the vessels to the parenchyma and the colonization of distant organs and formation of metastasis (Pretzsch et al., 2019). These CTCs have been shown to be tumorigenic and are able to colonize the liver *in vivo* (Grillet et al., 2017). The main metastatic site of CRCs is the liver, as the cancer cells easily migrate from the gut through the portal system.

→ **The transcoelomic route** is described when tumor cells invade through the digestive wall and through the serosa to reach the peritoneal cavity (in between the two sheets of the peritoneum). The peritoneum surrounds most organs within the abdomen, and this makes it an important route for the transport of fluid and cells within the abdomen. CRC cells easily migrate through the peritoneum and, once they adhere, form metastasis called peritoneal carcinomatosis (PC). It is generally believed that patients harboring PC have a lower prognosis and are in a terminal stage of CRC, although almost half the patients with metastasis present PC without liver metastasis (Aoyagi et al., 2014; Lemoine et al., 2016; Pretzsch et al., 2019).

→ **The perineural route** is the migration of cancer cells along the nerves from the primary tumor site. This dissemination route is associated with a poor prognosis (Krasna et al., 1988; Liebig et al., 2009).

4.3.1.4 Models of CRCs

CRCs can be studied using different models (Rizzo et al., 2021). Although multiple cell lines have been generated, thus representing a large phenotypical diversity (more than 100 CRC cell lines in different cell banks) and present the advantage of consistency and practicality, they do not model the intratumoral cell diversity, and the cell lines easily diverge from the original tumors. To solve these problems, other models can be used, such as Patient-derived xenografts (PDXs) and patient-derived organoids (PDOs).

4.3.1.4.1 Cell lines: the example of LS513

LS513 is a colorectal adenocarcinoma cell line which has been used for this project. It comes from a primary tumor in the caecum of a 64 year old male and presents a KRAS^{G12D} mutation (Suardet et al., 1992). Because of its serrated origins and its CIMP-high, MSS (microsatellite stable) statuses, it recapitulates the MUC-CRC phenotypes well and is classified in the CMS3 category. When cultured on plastic and reaching confluency, the LS513 monolayer starts to bud and releases TSIP-like structures in the medium that present an inverted polarity, which was particularly relevant for our study. Using a cell line allows an easier manipulation for basic biochemistry techniques and a higher throughput (Lopez, 2022). Genetic drift amongst passaging, the immortalization process as well as a culture exclusively *in vitro* are amongst the main limitations to the relevance of the use of such cell lines.

4.3.1.4.2 *Patient-derived xenografts (PDXs)*

Patient-derived xenografts have been used since their first successful report in 1953 (Toolan, 1953). This technique relies on grafting patient tumor tissue in an immunodeficient mouse. PDX are a very relevant technique to reproduce the tumor phenotype, as they correspond to the histopathological features of the original patient tumor (Blomme et al., 2018), as well as its CMS status (Sveen et al., 2018). However, there might still be a genetic divergence along with the increasing number of passages that should be taken into account (Rizzo et al., 2021). The subcutaneous engrafting of patient tumoral material allows to develop a full-grown tumor *in vivo*, and such tumor fragments can be passaged in immunocompromised mice. It must be noted that maintaining PDXs is expensive, slow and technically challenging, especially when it comes to genetic manipulation of the tumoral material *ex vivo*. For this research work, three CRC PDX models have been retrieved from the CReMEC (Center of Resource for Experimental Models of Cancer) consortium, all presenting mucinous characteristics and KRAS mutations (Julien et al., 2012).

4.3.1.4.3 *Patient-derived organoids (PDOs)*

The production of PDOs (Patient-derived organoids) is a good alternative to PDXs' limitations. It is easier to expand the tumoral material and requires a 3D ECM as well as a serum-free medium supplemented with stem cell growth factors. PDOs start with patient tumoral material and follows three main steps: fragmentation and digestion of the tissues, embedment in the ECM and culture in the medium (Cartry et al., 2023; Date and Sato, 2015) (see Figure 8). At every passage, PDOs are digested into small fragments and seeded into fresh ECM and can be expanded this way. Having this small fragment/single cell stage at each passage step makes genetic manipulation of PDOs easier than that of PDXs but might compromise the cell diversity, although this has not been fully investigated.

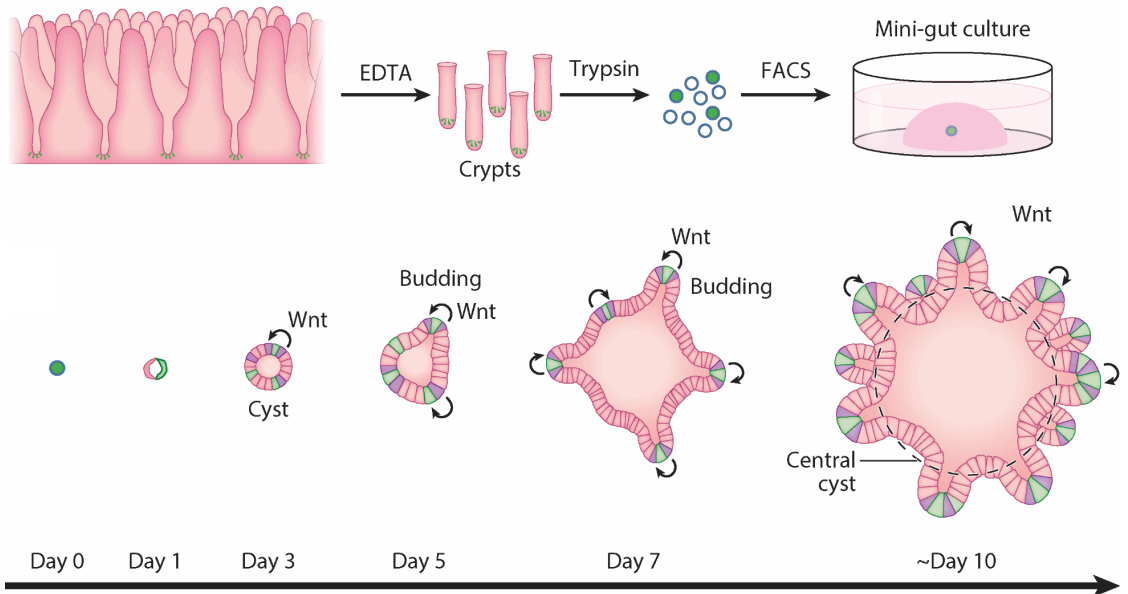


Figure 8- Generation of PDOs (from Date and Sato, 2015). After digestion, digested cells are embedded in Matrigel. From Lgr5+ cells, different cell types differentiate to form a full-grown organoid

4.3.2 Human induced pluripotent stem cells (hiPSCs)

4.3.2.1 What are hiPSCs?

hiPSCs are a type of pluripotent stem cells, which means they have the ability to renew and differentiate into multiple cell types. To avoid the use of embryonic stem cell, it is possible to reprogram human somatic cells for them to revert to pluripotency. These reprogrammed cells are hiPSCs (Takahashi et al., 2007; Takahashi and Yamanaka, 2006), and they overexpress pluripotency and stemness-related genes: OCT3/4, SOX2, KLF4, NANOG and c-Myc.

4.3.2.2 Naïve and primed states

hiPSCs can be described in two different states:

→ Naïve hiPSCs mimic the pre-implantation state of the Inner Cell Mass (ICM). They can give rise to both embryonic and extraembryonic cell lineages, and therefore can be qualified of pluripotent. These cells can be maintained in a naïve state *in vitro* by the addition of leukemia inhibitory factor (LIF).

→ Primed hiPSCs however, have a state which is similar to that of post-implantation of ICM cells. These cells can give rise to the three documented germ layers: the ectoderm, the mesoderm and the endoderm (X. Wang et al., 2021). *In vivo*, primed stem cells surround the amniotic cavity which will contain the growing embryo.

While the transition mechanisms between the naïve and primed states are not fully understood to this day, several protocols are available to revert primed hiPSCs into naïve hiPSCs and to capacitate naïve hiPSCs into primed hiPSCs (Collier et al., 2022; Rostovskaya et al., 2019; Taei et al., 2020). Capacitation can be defined as the process during which naïve hiPSCs gain competence for lineage induction, turning them into primed hiPSCs, which does not require exogenous growth factors but is facilitated by the inhibition of Wnt, which is what was performed *in vitro* (see **6.1.2.2**).

Some cell-state markers help discriminate between the naïve and primed states, namely the naïve markers Krüpel-like factor 17 (KLF17) and T-Box Transcription factor 3 (TBX3), and the primed markers Zix family member 2 (ZIC2) and secreted frizzled related protein 2 (SFRP2).

4.3.2.3 Adhesion and polarity status of the blastocyst

Integrins are crucial to the growth of hiPSCs. Indeed, they grow in colony-like structures, and their colony architecture is dependent on the attachment to the ECM through integrins. When cultured on Matrigel, naïve colonies tend to adopt a dome-shaped structure, while primed colonies tend to have a flatter phenotype. This flattened shape is accompanied by a contractile actin fence at the edge of the colony. These fibers present a specific type of focal adhesions at both ends, named cornerstone focal adhesions, which are enriched in integrin- $\beta 5$ (Närvä et al., 2017; Stubb et al., 2019).

During the implantation of the embryo to the endometrium (and therefore during capacitation), it has been shown that the mouse blastocyst started its polarity orientation process (Bedzhov and Zernicka-Goetz, 2014). Indeed, the tissue epithelialization, and especially the lumen formation is concomitant with the naïve-to-primed transition (Cesare et al., 2022). This polarity establishment has been linked to the subsequent exit of pluripotency, with cells in contact at the basal membrane responding to survival signals, which triggers their differentiation into polarized columnar epithelium (Coucouvani and Martin, 1995). To further understand this process, we have investigated the role of Integrin- β 1 in the capacitation and reversion cascades, and how it translates into the architecture of stem cell colonies (see 7.3).

4.3.3 Stiffness-insensitive spreading of cancer: the use of TIFs and U2OS

4.3.3.1 The role of matrix stiffness in cancer invasion

In solid tumors, the increased tissue stiffness is often seen as a hallmark of cancer and is a direct prognosis factor in different carcinomas such as breast, pancreas and colon (Paszek 2005, Lee 2019, Rice 2017, Baker 2013). Stiffness can also be used as a diagnosis tool, for example during palpation (Boyd et al 2007).

The increase in stiffness is due to the remodeling of the ECM within the tumor microenvironment (TME) which is mainly produced by cancer-associated fibroblasts (CAFs). Increased matrix protein deposition, altered collagen crosslinking and a change in the expression of metalloproteinases (MMP) that degrade ECM components cause dramatic remodeling altering matrix density and its visco-elastic properties. While a stiff ECM can cause the transformation of healthy epithelial cells into cancer cells, it can also influence and support cancer cell invasiveness (Bonnans et al., 2014; Fu et al., 2018; Katara et al., 2018; Najafi et al., 2019). Historically, cancer cells are often cultured on plastic, ie. on a substrate which stiffness is higher than physiological ones. However, it is more and more common to culture cells in more physiological stiffness regimes, where soft matrix is often mimicked with 0.5 kPa ECM coated hydrogels and stiff matrix with hydrogels with a Young Modulus of around 50 kPa (James R. W. Conway et al., 2023).

4.3.3.2 The role of matrix composition in cancer invasion

Matrix remodeling by CAFs is not characterized by a sole change in the physical visco-elastic properties of the ECM, but also in its biochemical composition. Carcinogenesis can be accompanied by altered expression or mutations in collagens, laminin and fibrillin (Bateman et al., 2009; Mao and Bristow, 2001). In addition, just like it is possible to correlate stiffness with prognosis, the matrix composition can also act as a prognostic marker. For instance, higher proportions of collagen VI, tenascin C and fibronectin are correlated with a poorer prognosis (Fernandez-Garcia et al., 2014; Ishihara et al., 1995; Wishart et al., 2020). The mutations and overexpression of MMPs in cancer cells also implicate a change in the TME matrix through selective degradation of some components (Liao et al., 2021). By testing different stiffness and matrix compositions, it has been possible to find conditions that uncouple composition and stiffness in the cancer cell spreading process (James R. W. Conway et al., 2023).

4.3.3.3 TIFs and U2OS

Across our study, we have looked into the impact of the TME ECM composition and physical properties using two cell lines, namely telomerase immortalized fibroblasts (TIFs) and U2OS osteosarcoma cells (from a moderately differentiated sarcoma in a 15-year-old girl). Using these, it was possible to study the effect of the matrix both on the invasiveness of cancer cells and their associated fibroblasts.

5 Aims of the PhD

Integrins are crucial in the establishment of cell states. In the literature review, I have discussed their importance in cell spreading, apicobasal polarity establishment and in the architecture of stem cell colonies during the capacitation process. Therefore, this PhD work is a pan-model study (CRC PDXs and cell lines, osteosarcoma cell lines and hiPSCs) to further investigate a wide panel of the influence of integrin availability, trafficking and signaling in regulation of these three processes. While Integrin- β 1 is the best-studied integrin monomer, owing to its involvement many integrin heterodimers, mechanisms by which it regulates these processes in a context and cell-type specific manner remain unclear. Consequently, the aims of this PhD are:

1. To better understand the underlying events in polarity orientation of inverted polarity structures, both in health and disease (Publication I).
2. To investigate the underlying reasons of the focal-adhesion pathway-dependent polarity reversion in CRC metastasis and the possible role integrin-mediated control of polarity on cancer invasiveness (Publication II).
3. To investigate the role of matrix stiffness and ECM composition on cell spreading using a matrix spot-array screening system (Publication III).
4. To investigate the role of Integrin- β 1 on the architecture of hiPSC stem cell colonies and in the regulation of naïve and primed cell states (Publication IV).

6 Material and Methods

6.1 Cell culture and organoid formation

6.1.1 MUC CRC (II)

6.1.1.1 Culture and passaging of PDXs

Animal experiments performed in France were compliant with French legislation and EU Directive 2010/63. The project was validated by the Ethical Committee (CEEA) no. 26 and was then granted French government authorizations under number 517-2015042114005883 and 2734-2015111711418501. Animal experiments performed in Finland were done in accordance with the Finnish Act on Animal Experimentation (animal license number ESAVI/12558/2021 and ESAVI/6253/2024). Mice were obtained from Charles River France and Germany, housed and bred at the Gustave Roussy animal core facility (accreditation number E-94-076-11) and at TCDM (Turku Center for Disease Modelling). Animals were humanely euthanized according to endpoints that were validated by the Ethical Committee, the French government (Ministère de l'Enseignement Supérieur, de la Recherche et de l'Innovation) and the Finnish government.

Three human colorectal tumors (9C corresponding to LRB-0009C, 12P corresponding to IGR-0012P and 14P corresponding to IGR-014P) from the CReMEC tumor collection were maintained in NSG mice (strain: NOD.Cg-Prkdc^{scid} Il2rg^{tm1Wjl}/SzJ) as described in Canet-Jourdan et al., 2022 and in Julien et al. 2012. Briefly, small tumor fragments were subcutaneously engrafted on both flanks of anesthetized mice (2.5% isoflurane). Tumor growth was measured once to twice a week. When the combined tumor burden reached 1700 mm³, mice were sacrificed, tumors were used for *ex vivo* experiments and 50 mm³ fragments engrafted on the flanks of new mice.

6.1.1.2 Generation of tumor spheres

Organoids were prepared according to Sato and Clevers 2013 and adapted for muco-secreting tumors as follows. The 9C, 12P or 14P tumors between 1200 and 1700 mm³ were retrieved from the mice, minced into small fragments using a sterile scalpel and were incubated for 1 h at 37°C in a final volume of 5 to 10 ml of culture medium (Dulbecco's modified Eagle's medium; DMEM) without fetal bovine serum (FBS) and with 2 mg/ml collagenase (Sigma, C2139). The samples were then mixed with 20 ml of DMEM and filtered on 100 µm mesh size cell strainers (Greiner, EASYstrainer, 542000) and centrifuged 10 min at 277 g. Clusters were isolated from the remaining mucin and single cells by washing in 10 ml of DMEM and pulse centrifugating at 277 g five times. The clusters, now free of mucin and single cells, were maintained for 3 days in ultra-low attachment plates (Corning, CLS3471) in culture medium. Then, organoids were pelleted at 277 g and used for further experiments.

6.1.1.3 Collagen embedding and culture of tumor spheres

Collagen-I (Corning, 354236) was neutralized with 1.0 M NaOH and 10× MEM (Life Technologies, 21430-02) according to the ratio: 1.0:0.032:0.1 (v/v/v). The concentration was then adjusted to 2 mg/ml with 1x DMEM, and the collagen-I was incubated on ice for 1h. The organoids, after spending 3 days in suspension as described previously, were then embedded in neutralized collagen-I and were added on top of pre-coated (using 7µl of the collagen mix per well) wells of an µ-Slide 8 Well ibiTreat slide (Ibidi, 80826) at a concentration of 30–50 organoids/5 µl. The gel was allowed to polymerize for 1h at 37°C. Organoids were then cultured in culture medium supplemented with FBS 10% for up to 6 days (3 days for PDX#3). The drugs were diluted in the medium as follows: AIIB2 (DSHB, AB528306, 1 µg/ml), Heregulin-β1 (Peprotech, 100-03-10UG, 20 ng/ml), Trastuzumab (Herceptin, Roche, 10 µg/ml), Pertuzumab (Perjeta, Genentech, 10 µg/ml), Saracatinib (Selleckchem, S1006, 1 µM), EHT-1864 (R&D Systems, 3872, 5 µM), P1E6 (DSHB, AB2619597, 10 µg/ml), FAK14 (Tocris, 3414, 10 µM).

6.1.1.4 Generation of a 14P-derived PDO line

The clusters obtained from the PDX as described previously were pulsed centrifuged at 277 g and resuspended in Matrigel (Corning, 354230) and plated in 10 x 15 μ l droplets in the bottom of a 6-well plate (Greiner, 657160). Cells were then incubated at 37°C for 15 minutes to let the basement membrane extract polymerize, then culture medium was added as described in Fujii et al 2018, without any human R-spondin1, A83-01 and Afamin-Wnt-3A serum-free condition medium. During the first two days, the organoid expansion medium was supplemented with Y-27632 (Calbiochem, 688000, 10 μ M). This medium was renewed every two days and PDOs were passaged every 7 to 14 days as described in Cartry et al 2023.

6.1.1.5 Culture of LS513 and generation of TSIPs

LS513 cells were obtained from ATCC (#CRL-2134) and cultured in RPMI-1640 medium supplemented with 10% FBS. LS513 were cultured in 10 cm cell culture dish. To generate TSIPs from the LS513 monolayer, the medium was changed every two days until the monolayer reached confluence. After waiting 5 days, the medium was collected and pulse centrifuged at 277g to collect the LS513 TSIPs. These were left for 3 days in suspension in ultra-low attachment plates (Corning, CLS3471), and embedded in collagen as described earlier (using the LS513 medium). For passaging, the monolayer was digested with 1x trypsin when 70% confluence was reached.

6.1.2 hiPSCs (IV)

6.1.2.1 Culture of naïve and primed stem cells

Primed hiPSCs HEL24.3 were a kind gift from Timo Otonkoski (University of Helsinki). They were cultured in Matrigel-precoated plates (354277, Corning) and in Essential 8 Medium (A1517001, ThermoFisher) at +37°C and 5% CO₂. For passaging, 50 mM EDTA in PBS was used until detachment of the edges of the colonies as described in Närvä et al., 2017. The medium was changed daily. To culture naïve hiPSCs, a monolayer of feeder cells was prepared. For this, inactivated mouse embryonic fibroblasts (iMEFs, A24903, Life Technologies) were

cultures on 0.1% gelatin-precoated (07903, StemCell Technologies) dishes in DMEM/F12 (11320033, Gibco) supplemented with 10% FBS at 37°C, 5% CO₂. Naïve hiPSCs were obtained after reversion of the primed HEL24.3 using the NaïveCult Induction Kit (05580, StemCell Technologies). They were then cultured on the feeder cell monolayer after washing it twice with PBS and cultured in NaïveCult Expansion Medium (StemCell Technologies). The medium was changed daily. The cells were cultured at 37°C, 5%CO₂ and 5% O₂. For passaging, cells were dissociated with TrypLE Express (12604-21, Gibco), and re-plated on a feeder-cell monolayer in culture medium - supplemented with 10 µM ROCK inhibitor Y-27632 (72302, StemCell Technologies) during the first 24 hours. In cells cultured with Mab13 (in-house, 10 µM), the antibody was added 24h after passaging and introduced in the freshly changed medium every day.

6.1.2.2 Capacitation

For the capacitation process, naïve hiPSCs were first plated on a Matrigel-precoated plates (354277, Corning) supplemented with 10 µM Y-27632 (72302, Stemcell Technologies). After two days, the NaïveCult medium was changed to capacitation medium, called N2B27, as described in Rostovskaya et al., 2019 (DMEM/F12 [1:2; 11320033, Gibco], Neurobasal medium [1:2; 21103049, Gibco], N2 supplement [in house], 1 mM l-glutamine [Sigma-Aldrich] and 0,1 mM ²-mercaptoethanol [M3148, Sigma-Aldrich]) medium supplemented with 2 µM XAV-939 (Tocris Bio-Techne, 3748) at +37°C, 5 % CO₂ (Guo et al. 2017). N2 was prepared by supplementing DMEM/F12 with 0.4 mg/ml insulin (I9278, Sigma-Aldrich), 10 mg/ml apo-transferrin (3188-AT-001G, R&D systems), 3 µM sodium selenite (S5261, Sigma-Aldrich), 1.6 mg/ml putrescine (P5780-5G, Sigma-Alrich) and 2 µg/ml progesterone (P8783, Sigma-Aldrich). Depending on the experiment, the cells were capacitated for 2 to 5 days. The capacitation process was followed with an Incucyte S3 live-cell analysis instrument (Sartorius).

6.1.2.3 Colony formation assay

Similarly to what is described in Rostovskaya et al., 2019, previously capacitated cells were passaged according to that of the Naïve cell passaging protocol into Matrigel-precoated 12 well plates at a density of 4x10³ cells/well. Depending on the conditions, cells were cultured in NaïveCult Medium (reversion) or E8 medium (control), supplemented with 10 µM Y-27632 for the first 24 hours.

After 7 days, colonies were fixed and stained with Crystal Violet. Pictures of the whole plate were taken and analyzed using the ImageJ Colony Area plugin (Guzmán et al., 2014).

6.2 Protein and gene expressions

6.2.1 Western blotting (II)

Spheres embedded in collagen were first released from the matrix by incubation of DMEM without serum supplemented with 2 mg/ml collagenase (Sigma, C2139) for 45 minutes. After pulse centrifugating at 277g, spheres were washed with PBS and pulse centrifugated at 277 g twice. Spheres were then lysed in TXLB buffer [50 mM Hepes, 1% Triton X-100, 0.5% sodium deoxycholate, 0.1% SDS, 0.5 mM EDTA, 50 mM NaF, 10 mM Na₃VO₄, and protease inhibitor cocktail (cOmplete Mini, EDTA-free, Roche)]. Cells cultured in 2D were washed twice with PBS and directly lysed with TXLB. Separation was performed by gel electrophoresis (Mini-PROTEAN TGX Precast Gels 4-20%, Bio-Rad, 4561096), before transferring onto a nitrocellulose membrane (Trans-Blot Turbo Transfer System, Bio-Rad) and blocking with AdvanBlock-Fluor (Advansta, R-03729-E10). Primary antibodies in AdvanBlock-Fluor were incubated overnight at 4°C with the dilutions mentioned in Table 2. Membranes were washed thrice between primary and secondary antibody treatments with Tris-buffered saline with 0.1% Tween 20 (TBST). IRDye secondary antibodies (see Table 2) were incubated for at least 1 hour at RT, before detection on an Odyssey fluorescence imager CLx (LI-COR). Densitometry analysis was performed in Fiji by normalizing the signal to GAPDH, which was used as a loading control.

6.2.2 PNGase digestion of lysates (II)

For PNGase digestion, cell lysates were prepared in a SDS-free buffer [50 mM Hepes, 1% NP-40, 0.5% sodium deoxycholate, 0.5 mM EDTA, 50 mM NaF, 10 mM Na₃VO₄, and protease inhibitor cocktail (cOmplete Mini, EDTA-free, Roche)]. 9 µl of lysate was mixed to 1 µl of Glycoprotein Denaturing Buffer 10X (NEB, B1704S). The lysate was denatured at 100°C for 10 minutes, then chilled on ice. 2 µl GlycoBuffer 2 (10X) (NEB, B3704S), 2 µl 10% NP-40 (NEB, B2704S), 5 µl H₂O and 1 µl PNGase F (NEB, P0704S) were then added to the lysate, and mixed gently.

The lysate was then incubated at 37°C for 1h. From there, the samples were prepared and run as described before.

6.2.3 Mass cytometry (II)

Spheroids in collagen for 3/6 days underwent collagen digestion by incubation of DMEM without serum supplemented with 2 mg/ml collagenase (Sigma, C2139) for 45 minutes. After resuspending in DMEM + 10% FBS and pulse centrifugating at 277g, they were collected. Spheroids cultured in suspension, clusters obtained from PDX digestion or spheroids released from collagen as described previously were washed with PBS thrice and pulsed centrifuged at 277 g thrice in order to keep the clusters/spheroids and get rid of any single cells and secreted mucins. The spheres were then digested in Cell Dissociation Buffer Enzyme-Free PBS-based (gibco, 13151-014) supplemented with 2 mg/ml collagenase (Sigma, C2139) and incubated for 1h at 37°C with occasional mechanical dissociation by pipetting. After addition of DMEM+10% FBS to quench the collagenase, cells were centrifuged at 200 g for 3 minutes and washed thrice with PBS. They were then resuspended in 1 ml cold PBS and filtered through a 5 ml polystyrene round bottom tube with Cell-Strainer cap (Falcon, 352235), and kept on ice until analysis. The sample was then run through a HeliosØ Mass Cytometer and the data analyzed with Cytobank and clustered through SPADE and viSNE analysis.

6.2.4 Whole exome sequencing (II)

DNA was extracted using the DNeasy ikit (Qiagen, Cat. No. 69504) from organoids either after 3 days in suspension (wash one time in PBS supplemented with Ca²⁺ and Mg²⁺ as mentioned above). Whole exome analysis was performed by Integrigen SA (France), comparing the three samples (9C, 12P and 14P) to a PON (panel of normal) and analyzed with MERCURYØ .

6.2.5 Analysis of SORLA and ITGB1 gene expression in human tumors (II)

Preprocessed TCGA colon adenocarcinoma cohort RNAseq data and raw RSEM-counts were downloaded from <https://gdc.cancer.gov/node/905/> and

https://gdac.broadinstitute.org/runs/stddata__2016_01_28/data/, respectively. CMSCaller (Eide et al., 2017) was used to infer consensus molecular subtypes (CMS) from RSEM-counts, excluding calls with FDR > 0.05. The samples were categorized as mucinous and control cases based on previously conducted characterization (Nguyen et al., 2021). Associations between SORLA and ITGB1 gene expression were assessed with the preprocessed normalized log₂ mRNA expression data by computing linear regression within each CMS group.

6.2.6 Single cell RNA sequencing (scRNAseq) (IV)

Naïve hiPSCs were seeded on Matrigel-coated 6 well plates at a density of 10⁴ cells/well (354277, Corning), with or without Mab13 (inhouse, 10 µM) in naïve conditions as previously described. After two days of culture, selected plates were put in normoxia in capacitation medium as detailed earlier, for 2 days. Similarly, HEL24.3 cells were cultured on Matrigel-coated 6 well plates at a density of 10⁴ cells/well, with or without Mab13, in primed conditions for 4 days.

After the 4 full days, cells were detached with EDTA (for primed hiPSCs) or TryPLE express (for naïve hiPSCs) as previously described. For each condition, 3 wells were used. Cells were washed thrice with PBS and resuspended in 15 µl 0.04% BSA in PBS. The sequencing and analysis were carried by the Single-Cell Omics facility at the University of Turku.

6.3 Quantification of cell-matrix interactions

6.3.1 Generation of fluorescent collagen (II & III)

To fluorescently label rat tail type I collagen (~4.24 mg/mL, 354236, Corning), 1.65 mL was mixed with 450 µL of Milli-Q water and 500 µL of neutralizing buffer (20 mM NaH₂PO₄, 112 mM Na₂HPO₄·2H₂O, 0.4 M NaCl, and 46 mM NaOH) and incubated at 37 °C for 30 min. The polymerized collagen was then washed thrice with PBS for 10 min. Then, 3 mL of Milli-Q water and 1 mL of bicarbonate buffer [1 M NaHCO₃ (pH 8), raised dropwise to pH 8.3 using 1.17 M Na₂CO₃ (pH 11)] were added to the collagen gel before addition of the Alexa Fluor[®] 647 NHS Ester (Succinimidyl Ester) dye (A20006, Invitrogen) in 100 µL of PBS. After incubating the collagen mix overnight at 4 °C, the dye was then removed, and the collagen was washed with PBS with rotation at room temperature for 30 min,

changing the PBS five times. Stained collagen was then depolymerized through the addition of 2 mL HCl (20 mM) and gentle rotation at 4 °C overnight. The collagen was finally centrifuged at 20,000 g for 10 min, collecting the labeled collagen from the supernatant. The fluorescent collagen was then used at a 1:1000 concentration in the previously described neutralized collagen gel.

6.3.2 Generation of CNA35 and cloning (II)

Molecular cloning and recombinant protein purification. To generate the CNA35-mScarlet construct, pET28a-CNA35-EGFP (A kind gift from Maarten Merckx (Eindhoven University of Technology, MB Eindhoven, The Netherlands), Addgene plasmid #61603) was digested with NheI/EcoRI and ligated with a NheI/EcoRI digested mScarlet gene fragment (IDT) to generate pET28a-mScarlet-CNA35. This was validated by analytical digestion and sequencing. Recombinant protein purification for CNA35-mScarlet was performed as described in James R. W. Conway et al., 2023.

6.3.3 Peritoneum *ex vivo* assay (II)

Peritoneum samples were collected from mice and decellularized by incubating them in a 1M NH₄OH solution for 1h at RT. After washing thrice with PBS for 15 minutes, peritoneum samples were left to incubate with PBS and penicillin-streptomycin (1:100) at 4°C overnight. After washing thrice with PBS for 15 minutes, the peritoneum was sectioned in 1cmx1cm pieces and adhered (using Tissue Adhesive, 3M, 1469SB) to the bottom of plastic transwell inserts (Greiner, Thincerts, 8 um pore size, 662638) after removing the filter with a scalpel. 100 tumor spheres were resuspended in 100 ml of DMEM+10%FBS and placed in the well with AIIB2 (DSHB, AB528306, 1 µg/ml), Y27632 (Calbiochem, 688000, 25 µM), Heregulin-β1 (Peprotech, 100-03-10UG, 20 ng/ml), Trastuzumab (Herceptin, Roche, 10 µg/ml), Pertuzumab (Perjeta, Genentech, 10 µg/ml) for 6 days. The fixing and IF staining was performed as described previously. Peritoneum bits were placed upside-down on a glass bottom dishes (Cellvis, D35-14-1-N), and imaged as described previously, using the x20 objective.

6.3.4 Collagen orientation analysis (II)

Type I collagen gels with 14P and 12P spheroids were prepared on glass bottom dishes (Cellvis, D35-14-1-N). 80 μ l of PureCol EZ Gel (Advanced BioMatrix, 5074) was spread on the glass bottom using a micropipette tip and allowed to polymerize at +37 °C for 1 h. Next, 14P or 12P spheroids were pulse centrifuged at 277 g to remove the mucin and single cells. Approximately 100 spheroids were mixed with 80 μ l of PureCol EZ Gel and pipetted on top of the previously polymerized collagen layer, after which the mixture was allowed to polymerize at +37 °C for 1 h. Spheres were treated with AIIB2 (DSHB, AB528306, 1 μ g/ml), Y27632 (Calbiochem, 688000, 25 μ M), Heregulin- β 1 (Peprotech, 100-03-10UG, 20 ng/ml), Trastuzumab (Herceptin, Roche, 10 μ g/ml), Pertuzumab (Perjeta, Genentech, 10 μ g/ml). One day before the samples were imaged, the cultures were supplemented with 1:1000 SiR-actin (Sprichrome, SC001) and ~40 μ g/ml of mScarlet-conjugated collagen probe CNA35 (Aper et al 2014).

The spheroids were imaged live using a Marianas spinning disk confocal microscope, 20x objective, Orca Flash4 sCMOS camera, and 2x2 binning (see Microscopy for details). 60-80 μ m stacks were acquired around the center (z) of each spheroid. In order to analyze collagen fiber orientation around the spheroids, ca. 4 μ m substacks were acquired near the center of each spheroid and used for creating maximum intensity projections. Next, 200x200 μ m regions of interest depicting CNA35 directly proximal to each spheroid, but excluding any dense collagen aggregates on the spheroid surface, were selected from the projections for analysis. If the matrix surrounding the spheroid was obviously heterogeneous, the region was selected to maximize the local alignment.

The selected regions were analyzed with ImageJ plugin OrientationJ, using cubic spline gradient and a local window size of 4 pixels. In the color survey, hue represented orientation and saturation represented coherency. All the local orientations were exported and analyzed using a custom R script to yield fiber orientation indices (Ferdman et al 1993, Taufalele et al 2019). Briefly, the orientations (-90°...+90°) representing each region were normalized, i.e., their distribution was centered around zero based on the peak of the histogram. Next, orientation indices (S) were calculated such that

$$S = 2 \langle \cos^2 \alpha \rangle - 1$$

where α is the angle between an individual (fiber) orientation and the average orientation of the entire region, and $\langle \cos^2 \alpha \rangle$ is the averaged square cosine of all α

per analyzed region. An index of 0 represents a random distribution, and an index of 1 represents a perfectly aligned distribution.

6.3.5 Collagen displacement fields (II)

In order to measure transient displacements exerted on the collagen matrix by the 14P and 12P spheroids, the spheroids were prepared and embedded in type I collagen, as described above. The spheroids were grown in the gels for 6 days and supplemented with 1:1000 SiR-actin and ~40 $\mu\text{g/ml}$ mScarlet-CNA35 one day before the imaging. 60-80 μm stacks were acquired around/near the center of each spheroid, before and after the cells and matrix were relaxed by adding 10 μM latrunculin B and incubating for ca. 20 minutes. Marianas spinning disk confocal microscope, 20x objective, Orca Flash4 sCMOS camera, and 2x2 binning were used for the imaging (see Microscopy for details). 3D displacement fields were calculated using TFMLAB (Barrasa-Fano et al 2021a, Sanz-Herrera et al 2021, Barrasa-Fano et al 2021b), a traction force microscopy toolbox implemented in MATLAB R2022a (MathWorks). The spheroids were segmented using actin images, variable threshold adjustment and a minimum object size of 10^4 voxels. Rigid image registration was done using the default phase correlation-based algorithm. The displacements were calculated from CNA35 images using 10x10x10 μm grid spacing, default registration metric and optimizer (normalized correlation coefficient, adaptive stochastic gradient descent) and post-shift correction. The results were visualized using ParaView v5.11.0 (Ahrens et al 2005).

6.4 Infections and polarity/trafficking analysis (II)

6.4.1 SorLA silencing using shRNA lentiviral transduction

During passaging of the 14P-generated PDO line as described previously, 10^5 cells were resuspended in 36 μl of organoid expansion medium were infected with 4M TU [62 μl of the virus (Origene, TL309181V)], 1 μl polybrene (Merck, TR-1003-G, stock solution at 1 mg/ml) and 1 μl Y-27362 (Calbiochem, 688000, 10 μM , stock solution 1 mM), in a U-bottom 96-well plate (Falcon, 351177) for 6 hours at 37°C. 1 ml of DMEM+10%FBS was added, and cells were centrifugated at 200 g for 3 minutes. Cells were then resuspended in 60 μl Matrigel (Corning, 354230) and

4x15 μ l droplets were poured in a 24 well cell culture plate (Cellstar, 662 160) and left at 37°C degrees to polymerize for 15 minutes. 1 ml organoid expansion medium (supplemented with 10 μ M Y-27362 for the first two days). The medium was changed every two days and organoids left to grow for 7 days. For polarity assays, the well was first washed thrice with PBS, before adding 1 ml of Cell Recovery Solution (Corning 354253). Cells were then left to incubate at 4°C for 20 minutes; Mechanical dissociation was then applied with a p1000 pipette until Matrigel was completely dissolved. 4 ml of PBS was added and spheroids were pulse centrifuged at 277 g. The spheres, now free of Matrigel, were maintained for 3 days in ultra-low attachment plates (Corning, CLS3471) in PDX culture medium. Then, organoids were pelleted at 277 g and used for further experiments.

6.4.2 SorLA KO using siRNA transient transfection

LS513 were plated in a 6 well plate at 80% confluency. Transient siRNA transfections were performed using Lipofectamine RNAiMAX reagent (Invitrogen, 56532) according to the manufacturer's instructions. SORLA-targeting siRNAs were ON-TARGETplus obtained from Dharmacon—siSORLA #1 (J-004722-08), siSORLA #2 (J-004722-06). For controls, Allstars negative control (Qiagen, Cat. No. 1027281) was used. siRNA concentrations used were all 20 nM and cells were transfected with siRNAs 72 h prior to experiments.

6.4.3 Integrin recycling assay

Surface biotinylation-based integrin trafficking assays in SorLA-silenced LS513 cells were performed based on previously published methods (Farage et al., 2021; Arjonen et al. 2012), with some modifications. Nunc MaxiSorb 96-well plates (Thermo Fischer, 44-2404-21) Enzyme-linked immunosorbent assay (ELISA) plates were coating with anti- β 1-integrin antibody mix (5 μ g/ml of AIIB2 (in-house) and anti-CD29 (BD Bioscience #610468)) in TBS (50 μ l per well) overnight at +4 °C. The wells were blocked with 5% BSA in TBS for 2 h at 37 °C, (100 μ l per well). LS513 cells were silenced three days before the experiment as described earlier. 2 hours prior to the experiment, the medium was changed to prewarmed RPMI with 10% FBS to induce receptor traffic. The cells were placed on ice and washed once with cold PBS. Cell surface proteins were labelled with 0.13 mg/ml EZ-link cleavable sulfo-NHS-SS-biotin (Thermo Scientific, 21331) in serum-free RPMI

medium for 30 min at +4 °C. Any unbound biotin was removed by washing with cold medium and pre-warmed RPMI+10% FBS with or without 100 µM primaquine (Sigma, 160393) was added to the cells. The biotin-labelled surface proteins were allowed to traffic at +37 °C for 15 or 30 minutes. Cells were placed on ice, washed once with cold PBS and cold cell surface reduction buffer (50 mM Tris-HCl, pH 8.6 and 100 mM NaCl). Cell surface biotin was cleaved with non-membrane permeant reducing reagent MesNa (30 mg/ml, sodium 2-mercaptoethanesulfonate; Fluka, 63705) in cell surface reduction buffer 20 min at 4 °C, followed by quenching with 100 mM iodoacetamide (Sigma, I3750) for 15 min on ice. For the 0 min internalization, cells were maintained on ice in serum-free RPMI until cell surface reduction with MesNA. The cells were lysed by scraping in lysis buffer (1.5% octylglucoside, 1% NP-40, 0.5% BSA, 1 mM EDTA, and protease and phosphatase inhibitors) and incubation at +4 °C for 20 min with rotation and cleared by centrifugation (16,000g, 10 min, 4 °C). To detect the biotinylated integrins, 50 µl volumes of the cell lysates were incubated in duplicate wells at +4 °C overnight, washed extensively with TBST, incubated for 2 h at 4 °C with 1:1,000 horseradish peroxidase-coupled streptavidin (Fisher, 21130), washed and detected with antibody for ELISA detection.

6.5 Stainings and microscopy (II)

6.5.1 Immunofluorescence staining

After incubation for 3 days in suspension or for 3 to 6 days in collagen, the apicobasolateral polarity of organoids was quantified. Cells were washed thrice with PBSCM (PBS supplemented with CaCl₂ (0.1 mM) and MgCl₂ (1 mM)), fixed with 4% paraformaldehyde (PFA) for 5 minutes (for spheres in suspension) or 45 minutes (for spheres in collagen) at RT. Spheres fixed in suspension were then embedded in collagen for imaging as previously described. Permeabilization was then performed in PBSCM supplemented with 0.5% Triton X-100 for 45 minutes. Spheres were incubated with primary antibodies overnight at 4°C with the dilutions mentioned in Table 2 in PBSCM supplemented with 10% FBS and 0.1% Triton X-100. After washing thrice with PBSCM supplemented with 0.05% Tween, spheres were incubated with secondary antibodies and phalloidin for 2h at RT with the dilutions mentioned in Table 2, as well as with DAPI (1 µg/ml). Spheres were then washed thrice with PBSCM supplemented with 0.05% Tween. The gel was then immersed in PBS before imaging.

6.5.2 Confocal imaging

Images were acquired either using a SpinningDisk CSU-W1 microscope (Yokogawa) with a ZylasCMOC camera piloted with an Olympus X83, or with a 3i CSU-W1 spinning disk confocal microscope with Hamamatsu CMOS (x40 water immersion objective). Images were processed using ImageJ.

6.5.3 Immunohistochemistry staining

Histology CRC and peritoneum specimens obtained after surgical resection were formalin fixed and paraffin embedded according to routine protocols. Sections (3 μm) of formalin-fixed and paraffin-embedded samples were deparaffinized, unmasked (pH 8) and rehydrated before HES or Alcian Blue (pH 2.5) staining, immunohistochemistry or immunofluorescence. Immunohistochemistry Sections were immunostained for SORLA, HER2, HER3 or with anti-CK20 mouse monoclonal antibody (see Table 2). Slides were imaged using Axioscan Z1, Zeiss (x20) and analysed using QuPath.

6.6 Statistical analysis and polarity quantification

6.6.1 Statistical analysis (II, III & IV)

All statistical comparisons were performed using Prism 7 (GraphPad software), as indicated in the figure legends, repeating all experiments at least three times independently.

6.6.2 Polarity score (II)

To quantify polarity, a polarity score was established by computing three parameters:

→ the absence/presence of a lumen (1 if one or more lumen, 0 if none).

→ The quantification of protrusions through the measure of corrected circularity (1-circularity) using the phalloidin signal (varying from 0 if no protrusions, to 1)

→ The quantification of the ezrin fluorescence signal ratio R (varying from 0 if cortical signal only, 1 if luminal signal only). If there is no lumen but a strongly polarized ezrin signal, this is set to 0.

By adding these parameters, we get a score varying from 0 (apical-out) to 3 (apical-in). If there is no lumen and no polarized ezrin signal, the score is set to 1.5.

6.7 Annexes

Table 1 - Antibodies

Protein	Company	Catalog Number	Application	Concentration
Ezrin	DHSB	AB-210031	IF	1 : 400
SorLA	C.M. Petersen (Aarhus U)		IF	1:200
RAB11FIP1 (RCP)	ThermoFischer	PA5-55276	IF/WB	1 :400 / 1 :1000
HER2	ThermoFischer	MA5-14057	IF/WB/IHC	1 :400/1 :1000/1 :400
HER3	Cell Signaling	12708S	IF/WB	1 :1000/1 :100
P5D2 (Total integrin-β1)	Abcam	Ab193592	IF	1 :500
12G10 (Active integrin-β1)	Abcam	Ab202641	IF	1 :500
WGA-lectin	GeneTex	GTX01502	IF	1 :500
CNA-35	In-house		IF	40 ug/ml
Phalloidin 488	Invitrogen	A12379	IF	1 :1000
Phalloidin 647	Sigma	65906	IF	1 :1000
Phalloidin 750	Sigma	07373	IF	1 :1000
SorLA	BD Biosciences	624084	WB	1 :500
Anti-ms 568	Invitrogen	A10037	IF	1 :500
Anti-ms 488	Invitrogen	A21202	IF	1 :500
Anti-rbt 488	Invitrogen	A21206	IF	1 :500
Anti-rbt 561	Invitrogen	A10042	IF	1 :500
GAPDH	HyTest	5G4MAB6C5	WB	1 :2000
Integrin-β1	Abcam	Ab52971	WB	1 :500
Erk	Cell Signaling	4696S	WB	1 :500
p-Erk	Cell Signaling	4370S	WB	1 :500
Src	Cell Signaling	2108S	WB	1 :500
p-Src (active)	Cell Signaling	2101S	WB	1 :500

Ms sec 650	Azure Biosystems	AC2166	WB	1 :1000
Ms sec 800	Azure Biosystems	AC2135	WB	1 :1000
Rbt sec 650	Azure Biosystems	AC2165	WB	1 :1000
Rbt sec 800	Azure Biosystems	AC2134	WB	1 :1000
HER3	Dako	DAK-H3-IC	IHC	1 :50
SorLA	Atlas	HPA031321	IHC	1 :400
Pan-CK	Invitrogen	MA5-13203	IHC	1 :400
P1E6 (Integrin- α 2)	DHSB	AB2619597	FB	10 μ g/ml
AIIB2 (Integrin- β 1)	DHSB	AB528306	FB	1 μ g/ml
AIIB2 (Integrin- β 1)	In-house		ELISA	5 μ g/ml
CD29	BD Bioscience	610468	ELISA	5 μ g/ml
89 Y-Integrin- α IIb	AH Diagnostics	3089004B	MC	1 :100
141 Pr-EpCAM	AH Diagnostics	3141006B	MC	1 :100
142 Nd-PETA-3	AH Diagnostics	3142011B	MC	1 :100
143 Nd-N-Cadherin	AH Diagnostics	3143016B	MC	1 :100
145 Nd-Syndecan-1	AH Diagnostics	3145003B	MC	1 :100
146 Nd-Integrin- β 3	AH Diagnostics	3145011B	MC	1 :100
148 Nd-HER2	AH Diagnostics	3148011A	MC	1 :100
149 Sm-CD34	AH Diagnostics	3149013B	MC	1 :100
150 Nd-Integrin- α v β 3	AH Diagnostics	3150026B	MC	1 :100
151 Eu-ICAM-2	AH Diagnostics	3151015B	MC	1 :100
156 Gd-Integrin- β 1	AH Diagnostics	3156007B	MC	1 :100
158 Gd-E-cadherin	AH Diagnostics	3158018B	MC	1 :100
159 Tb-CD98	AH Diagnostics	3159022B	MC	1 :100

¹⁶⁰ Gd-Integrin- α 5	AH Diagnostics	3160015B	MC	1 :100
¹⁶¹ Dy-Integrin- α 2	AH Diagnostics	3161012B	MC	1 :100
¹⁶² Dy-Integrin- β 7	AH Diagnostics	3162026B	MC	1 :100
¹⁶³ Dy-Integrin- α 1	AH Diagnostics	3163015B	MC	1 :100
¹⁶⁴ Dy-Integrin- α 6	AH Diagnostics	3164006B	MC	1 :100
¹⁶⁵ Ho-Notch2	AH Diagnostics	3165026B	MC	1 :100
¹⁶⁶ Er-CD44	AH Diagnostics	3166001B	MC	1 :100
¹⁶⁸ Er-Integrin- α 9 β 1	AH Diagnostics	3168013B	MC	1 :100
¹⁶⁹ Tm-CD24	AH Diagnostics	3169004B	MC	1 :100
¹⁷⁰ Er-ICAM-1	AH Diagnostics	3170014B	MC	1 :100
¹⁷¹ Yb-CD9	AH Diagnostics	3171009B	MC	1 :400
¹⁷³ Yb-Integrin- β 4	AH Diagnostics	3173008B	MC	1 :100
¹⁷⁴ Yb-Integrin- α 4	AH Diagnostics	3174018B	MC	1 :100
¹⁷⁶ Yb-NCAM	AH Diagnostics	3176001B	MC	1 :100
²⁰⁹ Bi-CD47	AH Diagnostics	3209004B	MC	1 :100
¹¹² Cd-EGFR	Biolegend	352902	MC	1 :50
¹¹⁴ Cd-Integrin- α V	R&D Systems	MAB1219	MC	1 :50
¹¹¹ Cd-Integrin- α 3	Sigma	MAB1952Z	MC	1 :50
¹⁶⁶ Cd-HER4	R&D Systems	MAB11311	MC	1 :50
¹¹⁰ Cd-HER3	R&D Systems	MAB3481	MC	1 :50
¹⁰⁶ Cd-Integrin- α 11	R&D Systems	MAB4235	MC	1 :50
¹⁴⁴ Nd-Syndecan-4	R&D Systems	MAB29181	MC	1 :50
¹⁵² Sm-Integrin- α V β 5	R&D Systems	MAB2528	MC	1 :50
¹⁵⁵ Gd-Integrin- α 8	R&D Systems	MAB6194	MC	1 :50

¹⁷⁵ Lu-Integrin- β8	R&D Systems	MAB4775	MC	1 :50
¹⁵³ Eu-Integrin- β6	R&D Systems	MAB4155	MC	1 :50
¹⁴⁷ Sm-CD166	Biologend	343902	MC	1 :200
¹⁵⁴ Sm-Notch-1	Biologend	352102	MC	1 :50
¹⁶⁷ Er-Notch-3	Biologend	345407	MC	1 :50
¹⁷² Yb- Neuropilin-1	Biologend	354502	MC	1 :50
¹¹³ Cd-CD10	Biologend	312223	MC	1 :50

Table 2 - siRNA and shRNA

Reagent	Catalog number	Company
siSORL1 #1	J-004722-08	Dharmacon
siSORL1 #2	J-004722-06	Dharmacon
AllStar	1027281	Qiagen
shSCR	TL309181V	Origene
shSORLA #A	TL309181V	Origene

7 Results

7.1 Implication of Integrin- β 1 trafficking in the apicobasal polarity orientation of CRC metastasis (II)

This project was the main project during my PhD work; therefore, the results will be detailed thoroughly in the following sections.

7.1.1 MUC CRC polarity is regulated by ECM interactions and Focal Adhesion Pathway

Inverted polarity in cancer has been reported multiple times before (Onuma and Inoue, 2022; Zajac et al., 2018) with the occurrences of TSIPs for instance. However, the mechanisms of polarity orientation of TSIPs once embedded in a matrix is unclear. Being able to decipher this process is clinically relevant, since it had been shown that a higher burden of apical-out structures is associated with a poorer prognosis (Canet-Jourdan et al., 2022). By using MUC-CRC PDXs from the CreMEC bank (Julien et al., 2012), we were able to use clinically relevant models to further investigate the polarity orientation process, in two primary tumor models (12P and 14P) and one PC model (9C). Through generation of tumoroids from these three PDXs and culturing them in suspension or in a collagen-I matrix, we were able to observe two polarity phenotypes. While all these tumoroids are apical-out in suspension, 14P tumoroids revert to an apical-in polarity once embedded in collagen (II, Fig. 1A). 12P and 9C tumoroids remain apical-out in the matrix. All these IF observations (through actin and ezrin staining) were backed up with the computation of a polarity score (described in 6.6.2 and II, Fig.S1A), and by the staining of mucin, which secretion also happens to be polarized (II, Fig. S1B). This polarity score is based on the quantification of protrusions (through the measure of the circularity of the tumoroid), the presence or absence of a lumen, and the ezrin fluorescence ratio

between the cortical and the luminal membranes. By computing these parameters, we establish a polarity score varying from 0 (perfect apical-out) to 3 (perfect apical-in). While all models in suspension and collagen (except the 14P in collagen) presented a polarity score (PS) lower than 0.75, the 14P in collagen harbored a PS of almost 2, showing a unique polarity shift solely in the 14P upon contact with the collagen matrix (II, Fig. 1B). Live imaging of 14P in collagen allowed to see lumen-like structures and beginnings of protrusions as early as 5 hours after embedding (II, Fig. 1B).

Since previously performed transcriptome analysis (GSE152299) on these three models reported an upregulation of the KEGG Focal Adhesion pathway in the collagen-embedded 14P tumoroids, we decided to investigate this pathway deeper. To illustrate this, we plotted the 45 most upregulated genes in 14P in collagen compared to the other conditions (II, Fig.S1C and S1D). Inhibition of key regulators of this pathway, namely Rac, FAK and Src all prevented the polarity reversion of 14P (II, Fig.1D and 1E). Concordantly, we observed a Src phosphorylation in 14P upon embedding in collagen (II, Fig. S1E and S1F).

7.1.2 Collagen-binding integrins regulate polarity establishment in MUC CRC

Because the $\alpha 2\beta 1$ integrin heterodimer, which is the best documented collagen-interactor, is upstream of the FA pathway, we investigated the relative levels and localization of this integrin in our PDXs. IF staining with P5D2 and 12G10 antibodies has shown that the localization of both total and active Integrin- $\beta 1$ receptors changed upon collagen embedding in the 14P. While integrins are mostly intercellular in suspension, they strongly localize on the cortex, at the cell/ECM interface in collagen in 14P (II, Fig. 2A). Through single-cell mass cytometry (CyTOF) of our models, we were able to see that the surface expressions of $\beta 1$ and $\alpha 2$ were higher in the 14P PDX than in the other PDXs (II, Fig. 2B and S2A, S2B and S2C). When generating tumoroids from these PDXs, we noticed that embedding 14P in collagen showed an increase in the surface expression of these two subunits (II, Fig. 2C and S2D). Upon blocking them with AIIB2 (anti- $\beta 1$ -integrin) and P1E6 (anti- $\alpha 2$ -integrin) blocking antibodies, we significantly inhibited the polarity reversion of 14P tumoroids (II, Fig.2D and 2E). It was also possible to observe this through live imaging (II, Fig. S2E and S2F).

7.1.3 Inverted polarity is linked to altered expression of integrin trafficking regulators

Motivated by the observation that the polarity status was correlated to a differential surface expression of integrins and was functionally dependent on integrin-ECM interaction, we decided to investigate this more precisely. Cell surface levels of integrins are largely controlled by the balance of constant integrin endocytosis and recycling (Bridgewater et al., 2012; Caswell and Norman, 2006; Moreno-Layseca et al., 2019) as explained in 4.1. By screening through well-documented integrin traffic regulators, we were able to identify two interesting targets that were respectively down- and up-regulated in the collagen-embedded 14P: RAB11FIP1 (or RCP) and SORL1 (II, Fig. 3A and 3B). RAB11FIP1 encodes for a Rab associated protein which has been shown to be a positive regulator of β 1-integrin recycling in different cancer cell types (Caswell et al., 2008; Eva et al., 2010; Machesky, 2019). SORL1 encodes for the SorLA protein which has been implicated in the rapid recycling of β 1-integrins in breast cancer (Pietilä et al., 2019). Western-blots and IF stainings of these two proteins showed a downregulation of RCP in all three models upon embedding in collagen, while SorLA was upregulated upon collagen embedding, but only in 14P (II, Fig. 3C, 3E, 3G and S3B). Interestingly, this was accompanied by an elevated Erk phosphorylation in 14P tumoroids in collagen, which was sensitive to Integrin- β 1 blocking through function blocking antibodies (II, Fig 3H, 3I, S3C and S3D). These data suggested the possibility that in 14P, integrin recycling might undergo a switch from a Rab11fip1-mediated Rab11-dependent long recycling loop to a SorLA-driven rapid recycling loop, contributing to increased cell surface integrin levels compared to that of the other models.

To explore this in more detail, we blotted for Integrin- β 1. Although the total level of integrins does not significantly change in the different tumoroids between the suspension and collagen conditions, we observe an increase in the mature, heavier glycoform of Integrin- β 1 in 14P in collagen (II, Fig. 4A). We were able to validate this result by digesting the used lysates with PNGase (an enzyme cocktail removing N-glycosylations from the extracellular domain of integrins, as seen in II, Fig.S4A). The ratio of mature/immature integrin- β 1 has previously been linked to alterations in integrin traffic with a higher ratio of the mature form being correlated to increased β 1-integrin recycling (Böttcher et al., 2012). Studying integrin- β 1 trafficking in tumoroids has proven technically challenging, and we therefore had to find a relevant alternative. Our choice was LS513 cells, a mucinous CRC cell line which generates TSIPs in the medium upon confluency when cultured in 2D. These LS513 TSIPs

replicate the 14P polarity phenotype well, with a polarity reversion and a SorLA upregulation when embedded in collagen (II, Fig. S4B, S4C and S4D). Previous studies have shown that impaired recycling of β 1-integrin can lead to its accumulation inside of the cell (Sahgal et al., 2019). Through SorLA silencing of LS513 and performing a cell-surface biotinylation-based integrin uptake assay, we were able to determine that SorLA silencing increases the intracellular levels of cell surface-derived endocytosed β 1-integrin, indicative of defective recycling in CRCs (II, Fig.4C). We then aimed at reproducing these results in 14P. Because efficient silencing SorLA in 14P tumoroids turned out to be technically challenging, we generated a PDO line from the 14P PDXs. Passaging these PDOs transiently goes through a single-cell stage which facilitated the efficacy of shSORLA lentiviral infection. This approach enabled us to generate SorLA-silenced organoids of 14P, which showed a clearly reduced polarity reversion in comparison to the control (II, Fig. 4D and 4E), further demonstrating that SorLA is necessary for polarity reversion in CRC spheroid response to collagen.

7.1.4 The SorLA-dependent integrin trafficking loop is induced by HER2 and HER3

Human epidermal growth factor receptor 2 and 3 (HER2 and HER3) are two transmembrane receptor tyrosine kinase (RTKs) which have been shown to interact with SorLA. By doing so, SorLA stabilizes the HER2/HER3 heterodimer, increasing protein levels of the two receptors, and supports its rapid recycling in breast and gastric cancer (Al-Akhrass et al., 2021). Through IF staining and Western-Blotting, we have found that only the 14P model showed a simultaneous increase in HER2 and HER3 upon collagen embedding (II, Fig. 5A, 5B, 5C and S5A). Similar to the collagen-induced SorLA expression, HER2 and HER3 upregulation were also integrin-dependent in 14P tumoroids in collagen (II, Fig. 5D, 5E and S5B). As it was shown in Al-Akhrass et al., 2021, the HER2/HER3 signaling via the Erk pathway induces a transcriptional regulation of SorLA. In return, SorLA regulates HER3 at a post-transcriptional level, as it was shown that the expression of ERBB3 is unchanged upon SorLA overexpression or silencing in breast cancer.

We have performed HER2/HER3 signaling inhibition using a Pertuzumab/Trastuzumab cocktail (which prevents respectively HER2/HER3 heterodimerization and HER2/HER2 homodimerization) and are both clinically in use in breast cancer (Swain et al., 2015). Upon inhibition, we prevented the 14P tumoroid polarity reversion in collagen, which shows an important functional role of HER2/HER3 signaling in the polarity reversion process (II, Fig. 5F and 5G).

Conversely, activating this signalization through Heregulin- β 1 (the main HER3 ligand) treatment of 12P (which was thus far blind to the matrix and stays apical-out in a collagen matrix) initiates a polarity-reversion process, turning them apical-in (II, Fig.5H and 5I). Upon HER3 stimulation with Heregulin- β 1, SorLA was also found to be upregulated in 12P (II, Fig. 5J and S5E). The 9C model however does not respond to Heregulin- β 1 stimulation (II, Fig. S5C and S5D) which correlates well with its aforementioned low HER3 expression level. These results show the validity of the HER2/HER3/SorLA feed-forward loop, as the stimulation with Heregulin- β 1 in 12P leads to a SorLA upregulation which, in returns, regulates HER3 at a post-transcriptional level (Al-Akhrass et al., 2021). The upregulation of SorLA consequently leads to an activation of the SorLA-dependent Integrin- β 1 recycling loop, therefore allowing 12P to sense the matrix and orient its polarity accordingly.

7.1.5 The apicobasal polarity orientation allows proper interaction with the matrix

The HER2/HER3/SorLA complex seems to play a cornerstone role in the apicobasal polarity orientation in our MUC CRC tumoroids. It was possible to correlate it to their interaction with the matrix. Through Traction Force Microscopy (TFM) and collagen-labelling, we were able to visualize the collagen fibers orientation as well as their displacement. Embedding 14P in a collagen matrix causes marked fiber displacement compared to 12P, showing a higher matrix interaction which goes hand in hand with an apical-in polarity and a basal localization of integrins (II, Fig. 6C, 6D, 6E and S6C). Upon blocking Integrin- β 1 or blocking HER2/HER3 signaling, we were able to see a decrease in collagen-fiber orientation, once more indicating a reduced tumoroid/ECM interaction which correlates with the decrease in polarity reversion. Conversely, activating HER2/HER3 signaling in 12P results in a higher alignment in collagen fibers proximal to the tumoroid (II, Fig.6A, 6B, S6A and S6B). To better visualize this interaction with the matrix and the stroma, we performed *ex vivo* invasion assays of 12P and 14P tumoroids on decellularized peritoneum. We observed a efficient spreading of 14P tumoroids, which goes well with a basal localization of integrins. Blocking Integrin- β 1 or HER2/HER3 reduces this spreading. Conversely, activating HER2/HER3 in 12P increases the spreading area on the peritoneum (II, Fig. 6F, 6G and 6H).

7.1.6 Higher HER2/HER3/SorLA expression correlates with apical-in polarity

We eventually wanted a more clinical readout of HER2/HER3/SorLA expression. By using previously characterized MUC CRC cohort (Canet-Jourdan et al., 2022), we stained Formalin-fixed paraffin-embedded (FFPE) tumor sections for HER2, HER3 and SorLA. We observed a higher expression of HER2 in apical-in structures than in apical-out structures, corresponding well with our in vitro observations (II, Fig. 7A, 7C and S7B). This correlates well with the relative HER2 expression in 14P vs. 12P. in the PDX FFPEs (II, Fig. S7A). In all structures, a positive correlation between HER2 and HER3, as well as between HER2 and SorLA, was seen (II, Fig. 7B). Interestingly, by analysing a CRC cohort (Nguyen et al., 2021) and dividing them into two groups (mucinous and non-mucinous), we were able to see a positive correlation between ITGB1 and SORLA expression both in CMS1 and CMS3 solely for mucinous CRCs, which was not the case for the non-mucinous (II, Fig. 7D and S7C).

Cumulatively, using cell- and mechanobiology methods to interrogate CRC PDX tumors ex-vivo and patient samples we report a novel polarity determination (see Figure 9) mechanism whereby HER2/HER3/SORLA-controlled β 1-integrin traffic control tumor-ECM interactions, ECM rearrangements and invasion into the peritoneum.

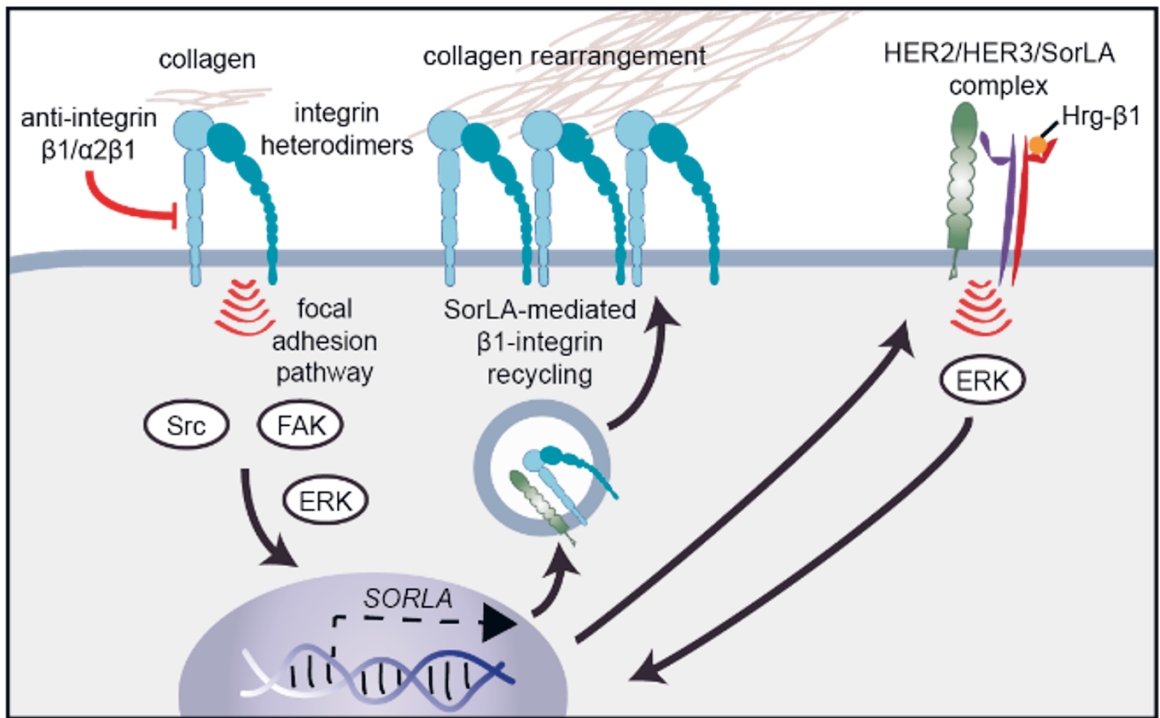


Figure 9 - HER2/HER3/SorLA-dependent Integrin-β1 recycling (from II)

7.2 Uncoupling stiffness and matrix composition to determine ideal conditions for integrin-dependent cancer cell spreading (III)

This project was a side project during my PhD work; therefore an emphasis will be put on my contribution to this work (see Figure 10).

Cell spreading is one of the mechanisms by which cancer cells invade their direct environment (Augoff et al., 2020). While different models show differential spreading depending on the ECM composition (equivalent to a healthy or a diseased ECM state), the coupling of such results with physical properties of the matrix, such as stiffness, is still unclear. To unravel this, we established a high-throughput ECM

array with different compositions and stiffnesses. This aimed at better understanding the invasiveness and spreading of cancer cells, taking into account both chemical and physical parameters.

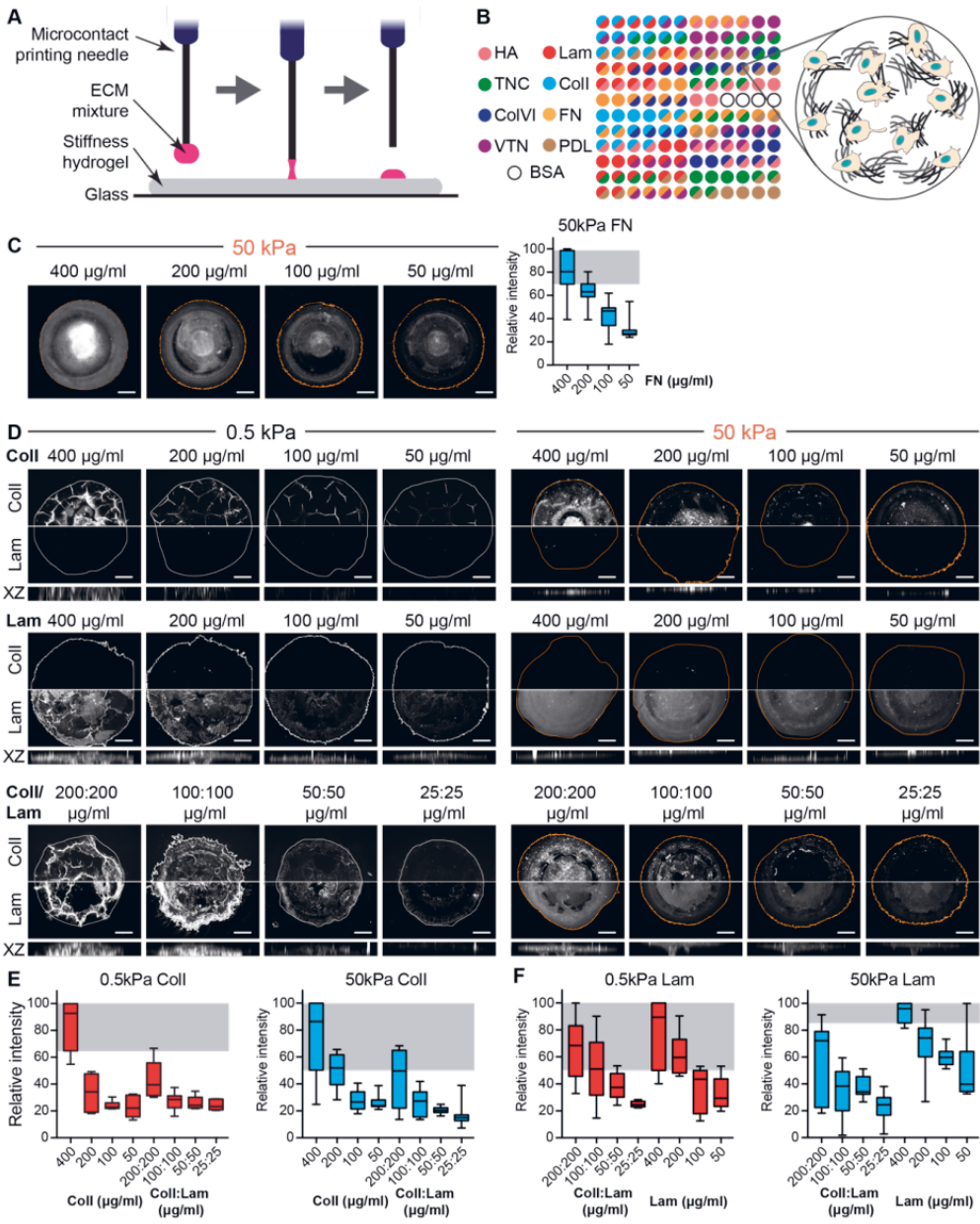
To answer this question, different ECM compositions were printed on polyacrylamide (PA) gels with two different stiffnesses: 0.5 kPa (soft) and 50 kPa (stiff). This was made possible by finding that all these components adhere on PA with no cratering or defaults after printing, using fluorescent collagen (III, Fig. S1, reported here in Figure 10). Chosen concentrations for further experiments were 400 $\mu\text{g/ml}$.

Through the analysis of cell spreading, it was possible to find matrix compositions that uncoupled stiffness and ligand repertoire, and enhanced U2OS and TIF spreading even on soft substrates: Collagen and Laminin (Coll/Lam), as well as Laminin and Tenascin C (Lam/TNC) (III, Fig.1 and Fig.2). This can be explained by an increase of molecular clutches at the cell surface. Indeed, TIFs on soft Coll/Lam substrates present more zyxin- and vinculin-positive foci, which can explain a better adhesion to the substrate (III, Fig.3). Additionally, because TIFs and U2OS present both collagen-binding ($\alpha 2\beta 1$ and $\alpha 11\beta 1$) and laminin-binding ($\alpha 3\beta 1$, $\alpha 6\beta 1$, $\alpha 6\beta 4$) integrins at their surface, they are able to engage a broader integrin repertoire for ECM interaction in a Coll/Lam matrix than on collagen or laminin alone (III, Fig.3). This goes hand in hand with an increase in integrin signaling (III, Fig.4).

It was thus possible to find matrix compositions that engaged a higher diversity of integrins, and therefore initiate a higher number of molecular clutches on the cancer cell surface, therefore creating stiffness-independent conditions for cancer cell spreading and invasion.

Figure 10- Fig. S1 from III (see next page).

(A) Schematic of the microcontact printing technique applied to print the ECM mixtures as spots on hydrogels of different stiffness. (B) Schematic of the ECM spot array following microcontact printing on the different polyacrylamide hydrogels. (C) Representative images (left) and quantification (right) from initial FN test spots on 50 kPa stiffness gels ($n=4$ biological replicates; 4 spots/mixture/replicate; equal protein concentrations printed by making each mixture up to 400 $\mu\text{g/ml}$ total protein with BSA; scale bars, 50 μm). (D to F) Representative images (D; whole spots imaged with half presented from each channel) and quantification of Collagen-I-647 (Coll-647) signal (E) or Lam staining (F) after spotting stiffness gels (0.5 and 50 kPa) with different dilutions of Coll-647, Lam or Coll-647/Lam ($n=4$ 5 biological replicates; 2 spots/mixture/replicate; equal protein concentrations printed by making each mixture up to 400 $\mu\text{g/ml}$ total protein with BSA; scale bars, 50 μm ; XZ maximum projections given below representative XY images).



7.3 Integrin- β 1: a cornerstone in hiPSC capacitation (IV)

This project was a side project during my PhD work; therefore an emphasis will be put on my contribution to this work (see IV, Figures 4 and 6).

7.3.1 Blocking Integrin- β 1 delays the capacitation process

The action of Integrin- β 1 on the blastocyst implantation and on the priming process which enables primed hiPSCs to evolve from naïve hiPSCs is still poorly understood, which is what has been the core of our research here.

While capacitation has already been molecularly characterized (Rostovskaya et al., 2019), the impact of Integrin- β 1 on this process has not been studied. After growing naïve hiPSC colonies in NaïveCult for 48h with or without Mab13 (an integrin- β 1-blocking antibody), the medium was changed to capacitation medium (N2B27 + 2 μ M XAV-939) and the growth was monitored with an IncuCyte. Colonies both adopt naïve-like features with a dome rounded shape in NaïveCult. After 48h in capacitation medium, colonies cultured without Mab13 lose their naïve-specific architecture and spread on the plastic, while the colonies cultured with Mab13 maintained a very similar phenotype to that of naïve hiPSCs. After 120 hours of capacitation, both conditions present a similar primed-like phenotype, lose their dome-shaped architecture and spread (IV, Fig.4A).

To further investigate the capacitation, we performed a colony count assay similar to the one described in Rostovskaya et al., 2019. Naïve hiPSCs were either capacitated for 48h (2d) or 120h (5d), both with or without Mab13. Cells were then passaged on a Matrigel-coated plate and cultured in either NaïveCult (to revert them to a naïve state) or E8 (to maintain them in a primed state) for 7 days (IV, Fig.4B). Colonies were then fixed and stained with CrystalViolet, and the colony area ratio between the NaïveCult and the E8 conditions was assessed from brightfield microscopy pictures. For both conditions, with or without Mab13, we normalized this area ratio to the area of non-capacitated colonies (IV, Fig.4C). Without Mab13, we noticed a significant decrease in the colony area ratio in naïve hiPSCs capacitated for 5 days as opposed to the ones capacitated for 2 days, indicating that during the 5 days of capacitation, the cells have exited their naïve state and are no longer able to grow in NaïveCult. However, when cultured in presence of Mab13, the area ratio remains unaltered despite the capacitation duration, indicating that Mab13 attenuated

exit from the naïve state, such that after 5 days the cells remain capable of growing and renewing in NaïveCult.

Taken together, these data suggest that blocking Integrin- β 1 using Mab13 delays the capacitation process both on a phenotypical and molecular level. In this sense, integrin- β 1 is essential for the capacitation process.

7.3.2 Integrin- β 1 is central to a fully primed feature acquisition during capacitation

To further understand the genetic changes cause by capacitation, we performed single cell RNA sequencing (scRNAseq) using 6 different conditions: naïve hiPSCs cultured with (d0_Mab13) or without (d0) Mab13, previously capacitized (for 48h) naïve hiPSCs with (d2_Mab13) or without (d2) Mab13, and primed hiPSCs cultured with (HEL24.3_Mab13) or without (HEL24.3) Mab13. The U-map of these 6 groups shows that clustering patterns of naïve cells cultured without Mab13 is similar to that of capacitated cells cultured without Mab13, while the d0_Mab13 and d2_Mab13 groups also cluster alike. Primed HEL24.3 cells clustering is identical whether with or without Mab13 (IV, Fig. 6A). The overlaid SFRP2 expression (IV, Fig. 6B) shows a consistent pattern considering the capacitation process: as a primed marker, it is increasingly expressed with the capacitation stage and maximal in primed cells.

To better understand the effect of Mab13 on the capacitation process, we plotted the top up- and down-regulated genes in the d2 condition compared to the d0 condition (IV, Fig. 6C). From this geneset, we identified three populations: genes that remained downregulated in d2_Mab13 compared to d0_Mab13 (written in blue), genes that remained upregulated in d2_Mab13 compared to d0_Mab13 (written in red), and genes that were differentially regulated in the absence of Mab13 but not in d2_Mab13 compared to d0_Mab13 (written in green). DPPA3 and L1TD1, two well characterized naïve markers (Palangi et al., 2017; Rostovskaya et al., 2019; Zhao et al., 2019) and therefore logically downregulated during capacitation seemed to be impacted by Integrin- β 1 function blocking. Indeed, upon addition of Mab13, their expression stays unchanged upon capacitation. The case of Mab13-sensitive upregulation of MT1G and MT1H upon capacitation is interesting, as these metallothioneins have been reported to be upregulated during the differentiation process of cardiomyocytes (Branco et al., 2019) but also as part of naïve genesets in other studies (Liu et al., 2020; Molè et al., 2021) (IV, Fig.6D). Interestingly, CGA which is involved in the embryo attachment to the endometrium (Idelevich and Vilella, 2020) and therefore upregulated upon capacitation (IV, Fig.6D), was slightly

downregulated after integrin- β 1 blocking, once more underlining the strong inhibitory effect of Mab13 on the capacitation process.

Taken together, these data show the impact of Integrin- β 1 function blocking on the capacitation with Mab13-treatment inhibiting capacitated cells to fully display a primed-like expression profile.

8 Discussion

8.1 Understanding inverted polarity in health and disease (I)

Inverted apicobasal polarity plays crucial roles in developmental processes, ranging from embryo implantation to immune surveillance. Conversely to the EMT paradigm, inverted polarity can also be a hallmark of invasive cancer progression. The significance of polarity inversion in the pathophysiology and molecular origins of these diseases is therefore becoming evident.

Our research compiles observations from cancer subtypes and genetic diseases to explain the development of inverted apicobasal polarity. It focuses on cellular responses to polarizing ECM cues, actomyosin contractility, and changes in membrane trafficking. Many of these molecular mechanisms have been identified through *in vitro* studies on cellular spheroids within standardized 3D matrices. However, to identify key molecular targets more precisely, more complex systems involving co-culture with stromal cells are necessary.

Recent advancements in manipulating cell polarity orientation, such as those reported by Watson et al., 2023, are needed to bridge the knowledge gap required for therapeutic interventions in diseases characterized by inverted polarity. These advancements will greatly help in developing targeted treatments to either restore normal cell polarity or induce polarity inversion as needed, enhancing our ability to modulate immune detection, drug responsiveness or cell migration. Overall, understanding and manipulating cell polarity dynamics hold significant promises for improving outcomes in a range of diseases, and especially cancer treatment.

8.2 A HER2/HER3/SorLA-dependent Integrin- β 1 recycling loop as a polarity regulator in CRC metastasis (II)

A prevailing view has been that the normal apicobasal polarity of epithelial tissues is progressively lost during carcinogenesis via the EMT process. However, this idea has increasingly been challenged with the occurrence of well polarized cancer structures (Diepenbruck and Christofori, 2016). Our study reveals a new mechanism through which CRC metastasis orient their polarity. We show a new interaction network involving integrins, HER-family RTKs and SorLA, explaining the efficient trafficking of Integrin- β 1 in a collagen matrix and explaining the consequent apicobasal polarity orientation of MUC CRC metastasis. In this polarity regulation pathway, HER2/HER3/SorLA-regulated Integrin- β 1 trafficking influences the interaction between tumor tissues and the ECM, as well as the ECM rearrangement and the peritoneal invasion of PC. We also show a correlation between the polarity phenotype and HER2, as well as an expression correlation between HER2, HER3 and SorLA in a MUC CRC cohort.

SorLA is a known sorting protein that regulates membrane traffic of amyloid precursor protein (APP) in neurons, insulin receptor in adipocytes and HER2/HER3 in HER2-positive breast cancer. Silencing SorLA has also been previously correlated with a lower Integrin- β 1 recycling in breast cancer (Al-Akhrass et al., 2021; Andersen et al., 2006, 2005; Klinger et al., 2011; Pietilä et al., 2019; Schmidt et al., 2016; Spoelgen et al., 2009; Whittle et al., 2015). However, SorLA has not been previously shown as being implicated in CRC polarity regulation. Our findings indicate that SorLA is crucial for polarity orientation in MUC CRC tumoroids. SorLA levels are low in TSIPs cultured in suspension but increase in TSIPs showing a high surface-integrin expression. These TSIPs can form initial contacts with collagen and adopt an apical-in polarity once embedded in the matrix. ECM contact triggers two feed-forward loops:

→ the increased integrin- β 1 recycling maintains an apical-in polarity phenotype.

→ the increased HER2/HER3 signaling induces SorLA expression.

We have found that inhibiting integrin- β 1 or HER2/HER3 signaling, as well as silencing SorLA, prevents a normal apicobasal polarity orientation of MUC CRC TSIPs. These findings enhance our understanding of MUC CRC TSIP behavior during metastatic invasion and their functional consequences. Indeed, inverted

polarity has been correlated with a shift in the cell migration mode (from collective mesenchymal to collective amoeboid as explained in Pagès et al., 2022) and in anti-cancer drug sensitivity (Ashley et al., 2019).

As we have extensively described in 4.1, integrins constantly traffic between the PM and endosomes, both in normal and cancer cells. Most of these integrins are recycled back to the membrane (Moreno-Layseca et al., 2019; Paul et al., 2015). This integrin trafficking is central to cancer invasion, as it promotes metastasis in many carcinomas such as breast and pancreas. The role of Rab11fip1 in this process has also been described as it promotes integrin- β 1 recycling and consequent cancer cell motility (Caswell et al., 2008; Caswell and Norman, 2006; Jacquemet et al., 2013; Machesky, 2019; Muller et al., 2009; Rainero et al., 2012). Interestingly, in our MUC CRC system, collagen interaction effectively reduces Rab11fip1 expression. We hypothesize that this is followed by a downregulation of the Rab11-dependent long loop of integrin recycling. The CRC-ECM contact upregulates SorLA, which implies that integrin- β 1 trafficking switches to a short SorLA-dependent loop. This loop, supported by HER2/HER3 signaling, allows a proper localization of Integrin- β 1 at the PM which signals for a normal polarity orientation.

CRCs show altered integrin expression compared to that of normal cells. Indeed, the laminin-binding α 6 β 4 heterodimer is overexpressed in cancer (Beaulieu, 2020). We have efficiently shown that both the α 1 β 1 and α 2 β 1-collagen binding heterodimers were expressed in our CRCs, which we have decided to investigate. While the α 1 β 1 dimer has been shown to be upregulated in 65% of CRC cases (Boudjadi et al., 2016), the role of α 2 β 1 in CRC invasion has not been extensively studied. Normally polarized CRC tissues harbor a higher surface expression of both α 2 and β 1-integrins than apical-out CRC tissues. Conversely, blocking α 2 and β 1 integrins prevents the polarity reversion. α 2 blocking alone is enough for a normal polarity orientation, showing that α 1 β 1-collagen interaction does not support polarity reversion.

While HER2-targeting therapy is extensively used in HER2 amplified breast cancer with substantial clinical benefit, there is no such clinically validated therapy for CRC (Nowak, 2020; Ye et al., 2022). Interestingly, HER2 amplified CRC as well as high levels of Heregulin- β 1 are correlated with a resistance to anti-EGFR therapy (Martin et al., 2013; Yonesaka et al., 2011). Because polarity effectively changes the way cancer cells react to anti-cancer drugs (Ashley et al., 2019), and inverted polarity has been correlated with a poorer prognosis (Canet-Jourdan et al., 2022), the way the HER2/HER3/SorLA signaling pathway and subsequent integrin-trafficking loop functions requires further investigation in order to decipher the clinical implications of polarity orientation in MUC CRCs. Further studies may for example facilitate patient stratification for targeted therapy.

8.3 Ligand availability and integrin engagement determine cell behavior and stiffness-independent spreading (III)

While it is now known that cancer cells remodel the substrate by changing the ECM stiffness and composition, few studies have aimed at uncoupling these parameters to further understand the underlying causes of cancer cell invasion (Najafi et al., 2019). Indeed, the adhesion maturation caused by talin unfolding and vinculin recruitment explains adhesions on rigid substrates, but it does not explain cell migration on compliant matrixes (Atherton et al., 2015; Friedland et al., 2009). Here, we developed a composite ECM spot array system to analyze cellular responses to matrix composition and its mechanical properties. We uncovered two ECM compositions promoting stiff-like behavior on compliant substrates. These findings align with observations that cells in soft tissues migrate without rigid support, mostly depending on ligand density and the affinity of specific integrin heterodimers to specific ligands (Su et al., 2016). For instance, the expression of integrin heterodimers with varied affinities to fibrillar and non-fibrillar collagen (Lerche et al., 2020; Tiger et al., 2001; Tulla et al., 2001) shows the implication of a varied integrin repertoire within the same ligand-binding family. The nature of the expressed integrin families explains why some of the matrix combinations we found promoted cancer cells spreading on compliant substrates when others did not.

A computational motor-clutch model was applied to simulate cell spreading on soft substrates as a function of ECM ligand availability and motor activity, showing that a higher number of molecular clutches could compensate for the lack of mechanical support, promoting cell spreading. Experimental verification confirmed that cell spreading on soft ECM depends on the balance between available clutches and motor activity. However, mechanical adhesion reinforcement is less likely on soft substrates, which suggests that ligand density and integrin affinities play a larger role in cell adhesion on compliant matrixes (Elosegui-Artola et al., 2016; Su et al., 2016). The current platform focuses on a limited set of ECM proteins and mechanical properties. To address these limitations, future research should aim to refine the model and validate findings in more complex 3D systems. This will enhance our understanding of ECM dynamics and improve the relevance of drug screening platforms, ultimately leading to better therapeutic strategies for diseases such as cancer, where the ECM plays a critical role in tumor progression and treatment response. Indeed, matrix compliance has been shown to be implicated in treatment resistance in breast cancer (Drain et al., 2021).

8.4 Integrin- β 1 blocking promotes naïve-like features and prevents effective capacitation of hiPSCs (IV)

Although the establishment of naïve hiPSCs, their chemical reversion and their capacitation into a primed state has been documented (Hassani et al., 2019; Rostovskaya et al., 2019; Taei et al., 2020), the influence of Integrin- β 1 in this process has been widely overlooked. In this study, we show that inhibition of Integrin- β 1 supports naïve-like features and architecture in hiPSC cells and reproduces well the maintenance state of the early blastocyst ICM cells.

Across this publication, we have shown that integrin- β 1 inhibition downregulates Angiotensin-Like 2 (AMOTL2) in primed hiPSCs. AMOTL2 is known as a negative regulator of YAP and YAP inhibition is crucial for the differentiation process of PSCs. Therefore, we suggest the importance of Integrin- β 1 signaling into the priming and differentiation process of stem cells, although some more information on its action and that of AMOTL2 on the establishment of primed hiPSC colony architecture and morphology is needed (Pagliari et al., 2021; Wang et al., 2011; Zhao et al., 2011). Upon Integrin- β 1 blocking in naïve hiPSCs, we have shown an upregulation of actin regulators such as Phosphatase Actin Regulator-1 (PHACTR-1) and Filamin A-Binding Protein (FILIP1) which regulate actomyosin assembly, lamellipodium formation and cell migration (Allain et al., 2012; Jarray et al., 2011; Nagano et al., 2002; Wenzel et al., 2012), but deeper studies should be done to further grasp their impact on the maintenance of naïve-like features.

We also show that Integrin- β 1 is crucial for the capacitation of hiPSCs, ie. the transition from the naïve to primed state. Blocking integrin- β 1 seems to effectively delay capacitation, support a naïve-like morphology and induce a higher growth ability in naïve condition. Capacitation is accompanied by the upregulation of primed markers, such as secreted frizzled related protein 2 (SFRP2) and by the downregulation of naïve markers, namely DPPA3 and L1TD1 (Messmer et al., 2019; Rostovskaya et al., 2019; Yilmaz and Benvenisty, 2019). However, blocking Integrin- β 1 prevents the shift towards a fully primed signature, with equal levels of these two markers in Mab13-treated capacitated cells to that of naïve cells. Furthermore, integrin- β 1 inhibition prevents the upregulation of metallothioneins (MT1G and MT1H) upon capacitation. This is an interesting lead to follow in the future as altered metallothionein expression have been linked to cell state transitions. Altogether, we show a crucial role of Integrin- β 1 in the exit from naïve cell. Integrin- β 1 inhibition delays and a full capacitation of hiPSCs and supports a naïve-like

phenotype. This moves the understanding of cell state transition one step forward and puts Integrin- β 1 as a key regulator in the early embryonic development.

9 Conclusions

The aim of this thesis was to understand the role of integrins, and especially integrin- β 1 in different cell processes, namely apicobasal polarity orientation, stiffness-independent cancer cell invasion on different substrates and capacitation of hiPSCs. While these projects had very different outcomes and readouts, they allowed to identify Integrin- β 1 as a cornerstone in the establishment of cell states and morphology. Through this study, we uncovered a previously unknown HER2/HER3/SorLA-dependent Integrin- β 1 recycling loop, matrix compositions allowing a stiffness-independent spreading of cancer cells and further uncovered the role of Integrin- β 1 in the early phases of development.

9.1 Original Publication I

Here we explain the role of inverted polarity in health and disease, studying different examples. Inverted polarity can be considered as a relatively newly described hallmark of cancer, and effectively impacts cancer invasion and growth, treatment resistance and its immune escape. Inverted polarity is also seen in genetic diseases and immune response to pathogen defense. Because inverted polarity is not necessarily pathological, we have also focused on the blastocyst polarity, which shows a perfect example of apicobasal inverted polarity at the pre-implantation stage.

Altogether this work allows to further understand the current knowledge on inverted apicobasal polarity, its molecular mechanisms and its pathological implications.

9.2 Original Publication II

We discovered here a Focal Adhesion pathway-dependent mechanism by which MUC CRC metastasis orient their apicobasal polarity. Indeed, we show that upon embedding tumoroids in collagen, a Rab11-dependent long Integrin- β 1 recycling

loops is downregulated and replaced by a SorLA-dependent short loop. This loop is induced by HER2 and HER3 signaling, which initiates positive feedback as the upregulation of SorLA further stabilizes HER2 and HER3 at the membrane. This newly described Integrin- β 1 recycling loop is responsible for the proper localization of integrin heterodimers at the membrane of MUC CRC metastasis, allowing interactions with the matrix and proper orientation of the apicobasal polarity. These data show relevance clinically, since the polarity status correlates with HER2 expression *in vivo* and HER2, HER3 and SorLA levels show a positive correlation in MUC CRC tissues. Because the polarity status of such tumors has been correlated with survival, this unlocks interesting opportunities for further polarity-oriented anti-cancer targets.

9.3 Original Publication III

Here we explained how osteosarcoma cells and fibroblasts spread in a stiffness-independent fashion on the substrate, and we explain it by the increase in the number of molecular clutches to form interactions with the matrix. By expressing a specific repertoire of specific-ligand binding integrins, cancer cells invaded compliant substrates in a stiff-like fashion. We identified two matrix compositions which supported this: Collagen and Laminin (Coll/Lam), as well as Laminin and Tenascin C (Lam/TNC). Because ECM physical and chemical properties can influence anti-cancer treatment response and resistance, this study impacts in a relevant way by further explaining stiff-like spreading of cancer cells on soft substrates.

9.4 Original Publication IV

Here we unravel how integrin- β 1 acts in the capacitation process of hiPSCs. Integrin- β 1 blocking supports naïve-like features in primed hiPSCs related to their architecture and gene expression patterns. It also maintains a naïve-like state in naïve hiPSCs through the enhancement of cell clustering. Integrin- β 1 blocking effectively delays and weakens the capacitation process and promotes cell growth once back in naïve medium. By changing the expression profile of naïve and primed markers, we show that Integrin- β 1 is a key regulator of capacitation, and therefore a cornerstone in the early development.

10 Acknowledgements

I would first like to thank Riitta Lahesmaa, director of Turku Bioscience, and Fabrice Barlesi, director of the Gustave Roussy Institute, where I carried my PhD project as a cotutelle. Both these places have been incredible research environments, fostering interactions with brilliant scientists who taught me a lot.

I am also addressing my gratitude to Léa Poisot and Nina Lehtimäki, the coordinators of both my doctoral schools (namely CBMS and DPT), who have always been here to answer my numerous questions and made this cotutelle peaceful on an administrative point of view. I am also grateful to Eevi Rintamäki and Eric Deutsch, both directors of my doctoral schools, for having me in your exciting and stimulating research programs. Additionally, I am addressing special thanks to Sanna Ranto and Jyrki Heino, respectively Chief Academic Officer and Research Director at the University of Turku.

My research project was co-supervised by Johanna Ivaska (University of Turku) and Fanny Jaulin (Institut Gustave Roussy). To Johanna, I would like to address my deepest gratitude for the huge opportunity you gave me when hiring me as an intern in your lab in 2020, and for accepting to supervise my PhD project after that. You've been a true inspiration as a scientist, and I have always been impressed and honored by your endless involvement and excitement in my project. I need to put an emphasis on the time you give to each of your PhD students, including me. You actively assisted me in the progress of my project, and I owe you my gratitude. To Fanny, I am grateful for letting me work on this exciting CRC metastasis polarity project, for trusting me along my research path and for giving relevant feedback on my work. Your lab is a very inspirational environment for every scientist and gave me the opportunity to gain insight on a more clinical side of research, which taught me a lot. I am inspired by your scientific career, which made you a true mentor to me.

I could not write this section without mentioning Charlotte Canet-Jourdan, who supervised me during the first months of my PhD and whose project I decided to carry on. You taught me a lot on a technical point of view and I've always valued

your feedback and advice so much! This period of time was short, but I deeply enjoyed working by your side.

I would like to address special thanks to Hellyeh Hamidi and Jacques Mathieu, research coordinators in the Ivaska Lab and the Jaulin lab respectively. Thank you both for your involvement in my project, your always relevant feedback and your patience.

I have had the privilege to be followed by Jacques Mathieu and David Bryant as part of my annual follow-up committee. Thank you both for your precious advice and scientific mentoring during these sessions. I would also like to thank Julie Pannequin and Jean-Léon Maître for accepting to be the reviewers of this thesis, as well as Patrick Caswell for agreeing to be my opponent with regard to the University of Turku during the defense. My jury will also be composed of David Bryant, Guillaume Montagnac and Emilia Peuhu, which I truly feel grateful for.

During my PhD project, I have had the honor to work with talented collaborators and co-authors, namely Hussein Al-Akhrass, James Conway, Aleksii Isomursu, Gautier Follain, Ville Härmä, Eva Jou-Ollé, Eetu Välimäki, Juha Rantala, Florent Pégliion, Jacques Mathieu, Hellyeh Hamidi, Jouni Härkönen, Christophe Desterke, Valeria Barresi, Zoé Fusilier, Aki Stubb, Paula Rasila, Sonja Vahlman, Joonas Sokka and Ras Trokovic. I truly enjoyed working with you.

Both my labs were very exciting and fruitful environments to work in. Every single member has helped me in completing this PhD work, and for this I am deeply grateful. From the Ivaska Lab, I would like to address my gratitude to Martina, Johanna L., Mitro, Siiri, Gautier, Michal, James, Jenni, Petra, Hellyeh, Mathilde, Megan, Niklas, Omkar, Paulina, Meri, Veli-Matti, Eva, Michalis and Huayi. It was always fun and exciting to work by your side. I would also like to address special thoughts, gratitude and appreciation to Jasmin and Maria who have been an incredible emotional support, and I thank you for your friendship. From the Jaulin Lab, I would like to thank Jérôme, Raphaël, Emilie, Sabrina, Charlotte, Jean-Baptiste, Jacques, Joël, Emmanuel, Elise, Grégoire, Diane-Laure, Léa, Clémence, Ali, Alice, Anaïs, Florent, Ioanna, Ryme, Oliviano, Maximiliano and Xihong. I am also addressing special thanks to Aurore for being such a kind and supporting co-PhD student, often from afar! I also thank the whole Montagnac team, I had a lot of fun working by your side.

I would like to address my gratitude to all the technical staff for your help during these projects: thank you Petra and Jenni for your precious help, your patience and your kindness! I also could not have succeeded without the amazing help from Heli, Katri and Nina from the Turku Center for Disease Modelling, and from Mélanie from the Gustave Roussy Institute. Your help with all the mouse work was precious and I could not have done it without you.

To my family, I address my deepest gratitude. Thank you for always being by my side and for always supporting me, bringing me all the strength I needed in the hardest times of my PhD. I thank you for putting up with the distance during my time in Finland. I feel so grateful to have such a loving and understanding family. I am therefore sending lots of love to my mum Martine, my sister Charlotte, my brother Olivier and my stepdad Jean-Pierre. My dad Michel is always in my thoughts and in my heart. I also want to mention my friends, both in France and Finland, who being far away from at different times wasn't always easy. Thank you for the laughs, for your support and for your love; and to the Turku squad, thank you for introducing me to the best Finland has to offer and for being patient with my weak Finnish and Swedish skills. This has truly been the experience of a lifetime!

Lastly, I want to thank the Fondation Philantropia, the Turku University Foundation and the Pentti and Tyyni Ekbom Fund for funding my PhD work.

11 List of references

- Adams, S.A., Smith, M.E.F., Cowley, G.P., Carr, L.A., 2004. Reversal of glandular polarity in the lymphovascular compartment of breast cancer. *J. Clin. Pathol.* 57, 1114–1117. <https://doi.org/10.1136/jcp.2004.016980>
- Al-Akhrass, H., Conway, J.R.W., Poulsen, A.S.A., Paatero, I., Kaivola, J., Padzik, A., Andersen, O.M., Ivaska, J., 2021. A feed-forward loop between SorLA and HER3 determines heregulin response and neratinib resistance. *Oncogene* 40, 1300–1317. <https://doi.org/10.1038/s41388-020-01604-5>
- Alanko, J., Mai, A., Jacquemet, G., Schauer, K., Kaukonen, R., Saari, M., Goud, B., Ivaska, J., 2015. Integrin endosomal signalling suppresses anoikis. *Nat. Cell Biol.* 17, 1412–1421. <https://doi.org/10.1038/ncb3250>
- Allain, B., Jarray, R., Borriello, L., Leforban, B., Dufour, S., Liu, W., Pamonsinlapatham, P., Bianco, S., Larghero, J., Hadj-Slimane, R., Garbay, C., Raynaud, F., Lepelletier, Y., 2012. Neuropilin-1 regulates a new VEGF-induced gene, *Phactr-1*, which controls tubulogenesis and modulates lamellipodial dynamics in human endothelial cells. *Cell. Signal.* 24, 214–223. <https://doi.org/10.1016/j.cellsig.2011.09.003>
- Al-Obaidy, K.I., Eble, J.N., Cheng, L., Williamson, S.R., Sakr, W.A., Gupta, N., Idrees, M.T., Grignon, D.J., 2019. Papillary Renal Neoplasm With Reverse Polarity: A Morphologic, Immunohistochemical, and Molecular Study. *Am. J. Surg. Pathol.* 43, 1099. <https://doi.org/10.1097/PAS.0000000000001288>
- Al-Obaidy, K.I., Eble, J.N., Nassiri, M., Cheng, L., Eldomery, M.K., Williamson, S.R., Sakr, W.A., Gupta, N., Hassan, O., Idrees, M.T., Grignon, D.J., 2020. Recurrent KRAS mutations in papillary renal neoplasm with reverse polarity. *Mod. Pathol.* 33, 1157–1164. <https://doi.org/10.1038/s41379-019-0362-1>
- Amornphimoltham, P., Rechache, K., Thompson, J., Masedunskas, A., Leelahavanichkul, K., Patel, V., Molinolo, A., Gutkind, J.S., Weigert, R., n.d. Rab25 Regulates Invasion and Metastasis in Head and Neck Cancer. *Clin. Cancer Res.*
- Anastasiadis, P.Z., Moon, S.Y., Thoreson, M.A., Mariner, D.J., Crawford, H.C., Zheng, Y., Reynolds, A.B., 2000. Inhibition of RhoA by p120 catenin. *Nat. Cell Biol.* 2, 637–644. <https://doi.org/10.1038/35023588>
- Andersen, O.M., Reiche, J., Schmidt, V., Gotthardt, M., Spoelgen, R., Behlke, J., von Arnim, C.A.F., Breiderhoff, T., Jansen, P., Wu, X., Bales, K.R., Cappai, R., Masters, C.L., Gliemann, J., Mufson, E.J., Hyman, B.T., Paul, S.M., Nykjær, A., Willnow, T.E., 2005. Neuronal sorting protein-related receptor sorLA/LR11 regulates processing of the amyloid precursor protein. *Proc. Natl. Acad. Sci.* 102, 13461–13466. <https://doi.org/10.1073/pnas.0503689102>
- Andersen, O.M., Schmidt, V., Spoelgen, R., Gliemann, J., Behlke, J., Galatis, D., McKinstry, W.J., Parker, M.W., Masters, C.L., Hyman, B.T., Cappai, R., Willnow, T.E., 2006. Molecular Dissection of the Interaction between Amyloid Precursor Protein and Its Neuronal Trafficking Receptor SorLA/LR11. *Biochemistry* 45, 2618–2628. <https://doi.org/10.1021/bi052120v>
- Anthis, N.J., Wegener, K.L., Ye, F., Kim, C., Goult, B.T., Lowe, E.D., Vakonakis, I., Bate, N., Critchley, D.R., Ginsberg, M.H., Campbell, I.D., 2009. The structure of an integrin/talin complex reveals the basis of inside-out signal transduction. *EMBO J.* 28, 3623–3632. <https://doi.org/10.1038/emboj.2009.287>

- Aoyagi, T., Terracina, K.P., Raza, A., Takabe, K., 2014. Current treatment options for colon cancer peritoneal carcinomatosis. *World J. Gastroenterol.* WJG 20, 12493–12500. <https://doi.org/10.3748/wjg.v20.i35.12493>
- Apodaca, G., Gallo, L.I., Bryant, D.M., 2012. Role of membrane traffic in the generation of epithelial cell asymmetry. *Nat. Cell Biol.* 14, 1235–1243. <https://doi.org/10.1038/ncb2635>
- Arias-Salgado, E.G., Lizano, S., Sarkar, S., Brugge, J.S., Ginsberg, M.H., Shattil, S.J., 2003. Src kinase activation by direct interaction with the integrin $\alpha 2$ cytoplasmic domain. *Proc. Natl. Acad. Sci.* 100, 13298–13302. <https://doi.org/10.1073/pnas.2336149100>
- Arjonen, A., Alanko, J., Veltel, S., Ivaska, J., 2012. Distinct Recycling of Active and Inactive $\alpha 2$ Integrins. *Traffic* 13, 610–625. <https://doi.org/10.1111/j.1600-0854.2012.01327.x>
- Arnaout, M.A., Mahalingam, B., Xiong, J.-P., 2005. INTEGRIN STRUCTURE, ALLOSTERY, AND BIDIRECTIONAL SIGNALING. *Annu. Rev. Cell Dev. Biol.* 21, 381–410. <https://doi.org/10.1146/annurev.cellbio.21.090704.151217>
- Ashley, N., Ouaret, D., Bodmer, W.F., 2019. Cellular polarity modulates drug resistance in primary colorectal cancers via orientation of the multidrug resistance protein ABCB1. *J. Pathol.* 247, 293–304. <https://doi.org/10.1002/path.5179>
- Asioli, S., Erickson, L.A., Righi, A., Lloyd, R.V., 2013. Papillary thyroid carcinoma with hobnail features: histopathologic criteria to predict aggressive behavior. *Hum. Pathol.* 44, 320–328. <https://doi.org/10.1016/j.humpath.2012.06.003>
- Atherton, P., Stutchbury, B., Wang, D.-Y., Jethwa, D., Tsang, R., Meiler-Rodriguez, E., Wang, P., Bate, N., Zent, R., Barsukov, I.L., Goult, B.T., Critchley, D.R., Ballestrem, C., 2015. Vinculin controls talin engagement with the actomyosin machinery. *Nat. Commun.* 6, 10038. <https://doi.org/10.1038/ncomms10038>
- Augoff, K., Hryniewicz-Jankowska, A., Tabola, R., 2020. Invadopodia: clearing the way for cancer cell invasion. *Ann. Transl. Med.* 8, 902. <https://doi.org/10.21037/atm.2020.02.157>
- Bachmann, M., Kukkurainen, S., Hytönen, V.P., Wehrle-Haller, B., 2019. Cell Adhesion by Integrins. *Physiol. Rev.* 99, 1655–1699. <https://doi.org/10.1152/physrev.00036.2018>
- Bagante, F., Spolverato, G., Beal, E., Merath, K., Chen, Q., Akgül, O., Anders, R.A., Pawlik, T.M., 2018. Impact of histological subtype on the prognosis of patients undergoing surgery for colon cancer. *J. Surg. Oncol.* 117, 1355–1363. <https://doi.org/10.1002/jso.25044>
- Bangasser, B.L., Rosenfeld, S.S., Odde, D.J., 2013. Determinants of Maximal Force Transmission in a Motor-Clutch Model of Cell Traction in a Compliant Microenvironment. *Biophys. J.* 105, 581–592. <https://doi.org/10.1016/j.bpj.2013.06.027>
- Banno, A., Goult, B.T., Lee, H., Bate, N., Critchley, D.R., Ginsberg, M.H., 2012. Subcellular Localization of Talin Is Regulated by Inter-domain Interactions *. *J. Biol. Chem.* 287, 13799–13812. <https://doi.org/10.1074/jbc.M112.341214>
- Barker, N., van Es, J.H., Kuipers, J., Kujala, P., van den Born, M., Cozijnsen, M., Haegebarth, A., Korving, J., Begthel, H., Peters, P.J., Clevers, H., 2007. Identification of stem cells in small intestine and colon by marker gene Lgr5. *Nature* 449, 1003–1007. <https://doi.org/10.1038/nature06196>
- Barnes, J.M., Kaushik, S., Bainer, R.O., Sa, J.K., Woods, E.C., Kai, F., Przybyla, L., Lee, M., Lee, H.W., Tung, J.C., Maller, O., Barrett, A.S., Lu, K.V., Lakin, J.N., Hansen, K.C., Obernier, K., Alvarez-Buylla, A., Bergers, G., Phillips, J.J., Nam, D.-H., Bertozzi, C.R., Weaver, V.M., 2018. A tension-mediated glycoalyx–integrin feedback loop promotes mesenchymal-like glioblastoma. *Nat. Cell Biol.* 20, 1203–1214. <https://doi.org/10.1038/s41556-018-0183-3>
- Barresi, V., Branca, G., Vitarelli, E., Tuccari, G., 2014. Micropapillary Pattern and Poorly Differentiated Clusters Represent the Same Biological Phenomenon in Colorectal Cancer: A Proposal for a Change in Terminology. *Am. J. Clin. Pathol.* 142, 375–383. <https://doi.org/10.1309/AJCPFEA7KA0SBBNA>
- Barret, C., Roy, C., Montcourrier, P., Mangeat, P., Niggli, V., 2000. Mutagenesis of the Phosphatidylinositol 4,5-Bisphosphate (Pip2) Binding Site in the Nh2-Terminal Domain of Ezrin Correlates with Its Altered Cellular Distribution. *J. Cell Biol.* 151, 1067–1080. <https://doi.org/10.1083/jcb.151.5.1067>
- Bass, M.D., Roach, K.A., Morgan, M.R., Mostafavi-Pour, Z., Schoen, T., Muramatsu, T., Mayer, U., Ballestrem, C., Spatz, J.P., Humphries, M.J., 2007. Syndecan-4–dependent Rac1 regulation

determines directional migration in response to the extracellular matrix. *J. Cell Biol.* 177, 527–538. <https://doi.org/10.1083/jcb.200610076>

Bateman, J.F., Boot-Handford, R.P., Lamandé, S.R., 2009. Genetic diseases of connective tissues: cellular and extracellular effects of ECM mutations. *Nat. Rev. Genet.* 10, 173–183. <https://doi.org/10.1038/nrg2520>

Baumann, H., Schwingel, M., Sestu, M., Burcza, A., Marg, S., Ziegler, W., Taubenberger, A.V., Muller, D.J., Bastmeyer, M., Franz, C.M., 2023. Biphasic reinforcement of nascent adhesions by vinculin. *J. Mol. Recognit.* 36, e3012. <https://doi.org/10.1002/jmr.3012>

Beaulieu, J.-F., 2020. Integrin $\alpha 4$ in Colorectal Cancer: Expression, Regulation, Functional Alterations and Use as a Biomarker. *Cancers* 12, 41. <https://doi.org/10.3390/cancers12010041>

Bedzhov, I., Zernicka-Goetz, M., 2014. Self-Organizing Properties of Mouse Pluripotent Cells Initiate Morphogenesis upon Implantation. *Cell* 156, 1032–1044. <https://doi.org/10.1016/j.cell.2014.01.023>

Bellis, S.L., 2004. Variant glycosylation: an underappreciated regulatory mechanism for $\alpha 1$ integrins. *Biochim. Biophys. Acta BBA - Biomembr.* 1663, 52–60. <https://doi.org/10.1016/j.bbame.2004.03.012>

Bernick, P.E., Klimstra, D.S., Shia, J., Minsky, B., Saltz, L., Shi, W., Thaler, H., Guillem, J., Paty, P., Cohen, A.M., Wong, W.D., 2004. Neuroendocrine Carcinomas of the Colon and Rectum. *Dis. Colon Rectum* 47, 163–169. <https://doi.org/10.1007/s10350-003-0038-1>

Bertotti, A., Comoglio, P.M., Trusolino, L., 2006. Beta4 integrin activates a Shp2-Src signaling pathway that sustains HGF-induced anchorage-independent growth. *J. Cell Biol.* 175, 993–1003. <https://doi.org/10.1083/jcb.200605114>

Bertotti, A., Comoglio, P.M., Trusolino, L., 2005. Beta4 integrin is a transforming molecule that unleashes Met tyrosine kinase tumorigenesis. *Cancer Res.* 65, 10674–10679. <https://doi.org/10.1158/0008-5472.CAN-05-2827>

Bevins, C.L., Salzman, N.H., 2011. Paneth cells, antimicrobial peptides and maintenance of intestinal homeostasis. *Nat. Rev. Microbiol.* 9, 356–368. <https://doi.org/10.1038/nrmicro2546>

Bigorgne, A.E., Farin, H.F., Lemoine, R., Mahlaoui, N., Lambert, N., Gil, M., Schulz, A., Philippet, P., Schlessler, P., Abrahamson, T.G., Oymar, K., Davies, E.G., Ellingsen, C.L., Leteurtre, E., Moreau-Massart, B., Berrebi, D., Bole-Feysot, C., Nischke, P., Brousse, N., Fischer, A., Clevers, H., Basile, G. de S., 2014. *TTCTA* mutations disrupt intestinal epithelial apicobasal polarity. *J. Clin. Invest.* 124, 328–337. <https://doi.org/10.1172/JCI71471>

Bilder, D., Perrimon, N., 2000. Localization of apical epithelial determinants by the basolateral PDZ protein Scribble. *Nature* 403, 676–680. <https://doi.org/10.1038/35001108>

Birchenough, G.M.H., Johansson, M.E., Gustafsson, J.K., Bergström, J.H., Hansson, G.C., 2015. New developments in goblet cell mucus secretion and function. *Mucosal Immunol.* 8, 712–719. <https://doi.org/10.1038/mi.2015.32>

Blomme, A., Van Simaey, G., Doumont, G., Costanza, B., Bellier, J., Otaka, Y., Sherer, F., Lovinfosse, P., Boutry, S., Palacios, A.P., De Pauw, E., Hirano, T., Yokobori, T., Hustinx, R., Bellahcène, A., Delvenne, P., Detry, O., Goldman, S., Nishiyama, M., Castronovo, V., Turtoi, A., 2018. Murine stroma adopts a human-like metabolic phenotype in the PDX model of colorectal cancer and liver metastases. *Oncogene* 37, 1237–1250. <https://doi.org/10.1038/s41388-017-0018-x>

Bonifacio, J.S., 2014. Adaptor proteins involved in polarized sorting. *J. Cell Biol.* 204, 7–17. <https://doi.org/10.1083/jcb.201310021>

Bonnans, C., Chou, J., Werb, Z., 2014. Remodelling the extracellular matrix in development and disease. *Nat. Rev. Mol. Cell Biol.* 15, 786–801. <https://doi.org/10.1038/nrm3904>

Borghi, N., Lowndes, M., Maruthamuthu, V., Gardel, M.L., Nelson, W.J., 2010. Regulation of cell motile behavior by crosstalk between cadherin- and integrin-mediated adhesions. *Proc. Natl. Acad. Sci.* 107, 13324–13329. <https://doi.org/10.1073/pnas.1002662107>

Bos, J.L., Rehmann, H., Wittinghofer, A., 2007. GEFs and GAPs: critical elements in the control of small G proteins. *Cell* 129, 865–877. <https://doi.org/10.1016/j.cell.2007.05.018>

Böttcher, R.T., Stremmel, C., Meves, A., Meyer, H., Widmaier, M., Tseng, H.-Y., Fässler, R., 2012. Sorting nexin 17 prevents lysosomal degradation of $\alpha 1$ integrins by binding to the $\alpha 1$ -integrin tail. *Nat. Cell Biol.* 14, 584–592. <https://doi.org/10.1038/ncb2501>

- Boudjadi, S., Carrier, J.C., Groulx, J.-F., Beaulieu, J.-F., 2016. Integrin $\alpha 1^2 1$ expression is controlled by c-MYC in colorectal cancer cells. *Oncogene* 35, 1671–1678. <https://doi.org/10.1038/onc.2015.231>
- Boulter, E., Garcia-Mata, R., 2012. Analysis of the Role of RhoGDI1 and Isoprenylation in the Degradation of RhoGTPases, in: Rivero, F. (Ed.), *Rho GTPases: Methods and Protocols*. Springer, New York, NY, pp. 97–105. https://doi.org/10.1007/978-1-61779-442-1_7
- Branco, M.A., Cotovio, J.P., Rodrigues, C.A.V., Vaz, S.H., Fernandes, T.G., Moreira, L.M., Cabral, J.M.S., Diogo, M.M., 2019. Transcriptomic analysis of 3D Cardiac Differentiation of Human Induced Pluripotent Stem Cells Reveals Faster Cardiomyocyte Maturation Compared to 2D Culture. *Sci. Rep.* 9, 9229. <https://doi.org/10.1038/s41598-019-45047-9>
- Bridgewater, R.E., Norman, J.C., Caswell, P.T., 2012. Integrin trafficking at a glance. *J. Cell Sci.* 125, 3695–3701. <https://doi.org/10.1242/jcs.095810>
- Brown, F.D., Rozelle, A.L., Yin, H.L., Balla, T., Donaldson, J.G., 2001. Phosphatidylinositol 4,5-bisphosphate and Arf6-regulated membrane traffic. *J. Cell Biol.* 154, 1007–1018. <https://doi.org/10.1083/jcb.200103107>
- Bryant, D.M., Datta, A., Rodríguez-Fraticelli, A.E., Peränen, J., Martín-Belmonte, F., Mostov, K.E., 2010. A molecular network for de novo generation of the apical surface and lumen. *Nat. Cell Biol.* 12, 1035–1045. <https://doi.org/10.1038/ncb2106>
- Bryant, D.M., Mostov, K.E., 2008. From cells to organs: building polarized tissue. *Nat. Rev. Mol. Cell Biol.* 9, 887–901. <https://doi.org/10.1038/nrm2523>
- Bryant, D.M., Rognot, J., Datta, A., Overeem, A.W., Kim, M., Yu, W., Peng, X., Eastburn, D.J., Ewald, A.J., Werb, Z., Mostov, K.E., 2014. A Molecular Switch for the Orientation of Epithelial Cell Polarization. *Dev. Cell* 31, 171–187. <https://doi.org/10.1016/j.devcel.2014.08.027>
- Buckley, C.E., St Johnston, D., 2022. Apical–basal polarity and the control of epithelial form and function. *Nat. Rev. Mol. Cell Biol.* 23, 559–577. <https://doi.org/10.1038/s41580-022-00465-y>
- Burridge, K., 2005. Foot in mouth: do focal adhesions disassemble by endocytosis? *Nat. Cell Biol.* 7, 545–547. <https://doi.org/10.1038/ncb0505-545>
- Byron, A., Askari, J.A., Humphries, J.D., Jacquemet, G., Koper, E.J., Warwood, S., Choi, C.K., Stroud, M.J., Chen, C.S., Knight, D., Humphries, M.J., 2015. A proteomic approach reveals integrin activation state-dependent control of microtubule cortical targeting. *Nat. Commun.* 6, 6135. <https://doi.org/10.1038/ncomms7135>
- Calderwood, D.A., Yan, B., De Pereda, J.M., Alvarez, B.G., Fujioka, Y., Liddington, R.C., Ginsberg, M.H., 2002. The Phosphotyrosine Binding-like Domain of Talin Activates Integrins. *J. Biol. Chem.* 277, 21749–21758. <https://doi.org/10.1074/jbc.M111996200>
- Campbell, I.D., Humphries, M.J., 2011. Integrin Structure, Activation, and Interactions. *Cold Spring Harb. Perspect. Biol.* 3, a004994. <https://doi.org/10.1101/cshperspect.a004994>
- Canel, M., Serrels, A., Frame, M.C., Brunton, V.G., 2013. E-cadherin–integrin crosstalk in cancer invasion and metastasis. *J. Cell Sci.* 126, 393–401. <https://doi.org/10.1242/jcs.100115>
- Canet-Jourdan, C., Pagès, D.-L., Nguyen-Vigouroux, C., Cartry, J., Zajac, O., Desterke, C., Lopez, J.-B., Gutierrez-Mateyron, E., Signolle, N., Adam, J., Raingeaud, J., Polrot, M., Gonin, P., Mathieu, J.R.R., Souquere, S., Pierron, G., Gelli, M., Dartigues, P., Ducreux, M., Barresi, V., Jaulin, F., 2022. Patient-derived organoids identify an apico-basolateral polarity switch associated with survival in colorectal cancer. *J. Cell Sci.* 135, jcs259256. <https://doi.org/10.1242/jcs.259256>
- Cartry, J., Bedja, S., Boilève, A., Mathieu, J.R.R., Gontran, E., Annereau, M., Job, B., Mouawia, A., Mathias, P., De Baère, T., Italiano, A., Besse, B., Sourrouille, I., Gelli, M., Bani, M.-A., Dartigues, P., Hollebecque, A., Smolenschi, C., Ducreux, M., Malka, D., Jaulin, F., 2023. Implementing patient derived organoids in functional precision medicine for patients with advanced colorectal cancer. *J. Exp. Clin. Cancer Res.* 42, 281. <https://doi.org/10.1186/s13046-023-02853-4>
- Case, L.B., Baird, M.A., Shtengel, G., Campbell, S.L., Hess, H.F., Davidson, M.W., Waterman, C.M., 2015. Molecular mechanism of vinculin activation and nanoscale spatial organization in focal adhesions. *Nat. Cell Biol.* 17, 880–892. <https://doi.org/10.1038/ncb3180>
- Case, L.B., De Pasquale, M., Henry, L., Rosen, M.K., 2022. Synergistic phase separation of two pathways promotes integrin clustering and nascent adhesion formation. *eLife* 11, e72588. <https://doi.org/10.7554/eLife.72588>

- Caswell, P.T., Chan, M., Lindsay, A.J., McCaffrey, M.W., Boettiger, D., Norman, J.C., 2008. Rab-coupling protein coordinates recycling of $\pm 5^2$ 1 integrin and EGFR1 to promote cell migration in 3D microenvironments. *J. Cell Biol.* 183, 143–155. <https://doi.org/10.1083/jcb.200804140>
- Caswell, P.T., Norman, J.C., 2006. Integrin Trafficking and the Control of Cell Migration. *Traffic* 7, 14–21. <https://doi.org/10.1111/j.1600-0854.2005.00362.x>
- Caswell, P.T., Spence, H.J., Parsons, M., White, D.P., Clark, K., Cheng, K.W., Mills, G.B., Humphries, M.J., Messent, A.J., Anderson, K.I., McCaffrey, M.W., Ozanne, B.W., Norman, J.C., 2007. Rab25 Associates with $\pm 5^2$ 1 Integrin to Promote Invasive Migration in 3D Microenvironments. *Dev. Cell* 13, 496–510. <https://doi.org/10.1016/j.devcel.2007.08.012>
- Cesare, E., Urciuolo, A., Stuart, H.T., Torchio, E., Gesualdo, A., Laterza, C., Gagliano, O., Martewicz, S., Cui, M., Manfredi, A., Di Filippo, L., Sabatelli, P., Squarzone, S., Zorzan, I., Betto, R.M., Martello, G., Cacchiarelli, D., Luni, C., Elvassore, N., 2022. 3D ECM-rich environment sustains the identity of naive human iPSCs. *Cell Stem Cell* 29, 1703-1717.e7. <https://doi.org/10.1016/j.stem.2022.11.011>
- Chan, C.E., Odde, D.J., 2008. Traction Dynamics of Filopodia on Compliant Substrates. *Science* 322, 1687–1691. <https://doi.org/10.1126/science.1163595>
- Charras, G., Sahai, E., 2014. Physical influences of the extracellular environment on cell migration. *Nat. Rev. Mol. Cell Biol.* 15, 813–824. <https://doi.org/10.1038/nrm3897>
- Chastney, M.R., Conway, J.R.W., Ivaska, J., 2021. Integrin adhesion complexes. *Curr. Biol.* 31, R536–R542. <https://doi.org/10.1016/j.cub.2021.01.038>
- Chastney, M.R., Lawless, C., Humphries, J.D., Warwood, S., Jones, M.C., Knight, D., Jorgensen, C., Humphries, M.J., 2020. Topological features of integrin adhesion complexes revealed by multiplexed proximity biotinylation. *J. Cell Biol.* 219, e202003038. <https://doi.org/10.1083/jcb.202003038>
- Cheng, K.W., Lahad, J.P., Kuo, W., Lapuk, A., Yamada, K., Auersperg, N., Liu, J., Smith-McCune, K., Lu, K.H., Fishman, D., Gray, J.W., Mills, G.B., 2004. The RAB25 small GTPase determines aggressiveness of ovarian and breast cancers. *Nat. Med.* 10, 1251–1256. <https://doi.org/10.1038/nml125>
- Chiang, S., Weigelt, B., Wen, H.-C., Pareja, F., Raghavendra, A., Martelotto, L.G., Burke, K.A., Basili, T., Li, A., Geyer, F.C., Piscuoglio, S., Ng, C.K.Y., Jungbluth, A.A., Balss, J., Pusch, S., Baker, G.M., Cole, K.S., von Deimling, A., Batten, J.M., Marotti, J.D., Soh, H.-C., McCalip, B.L., Serrano, J., Lim, R.S., Siziopikou, K.P., Lu, S., Liu, X., Hammour, T., Brogi, E., Snuderl, M., Iafrate, A.J., Reis-Filho, J.S., Schnitt, S.J., 2016. IDH2 Mutations Define a Unique Subtype of Breast Cancer with Altered Nuclear Polarity. *Cancer Res.* 76, 7118–7129. <https://doi.org/10.1158/0008-5472.CAN-16-0298>
- Cho, S., Irianto, J., Discher, D.E., 2017. Mechanosensing by the nucleus: From pathways to scaling relationships. *J. Cell Biol.* 216, 305–315. <https://doi.org/10.1083/jcb.201610042>
- Christoforides, C., Rainero, E., Brown, K.K., Norman, J.C., Toker, A., 2012. PKD Controls $\pm v^2$ 3 Integrin Recycling and Tumor Cell Invasive Migration through Its Substrate Rabaptin-5. *Dev. Cell* 23, 560–572. <https://doi.org/10.1016/j.devcel.2012.08.008>
- Collier, A.J., Bendall, A., Fabian, C., Malcolm, A.A., Tilgner, K., Semprich, C.I., Wojdyla, K., Nisi, P.S., Kishore, K., Roamio Franklin, V.N., Mirshekar-Syahkal, B., D’Santos, C., Plath, K., Yusa, K., Rugg-Gunn, P.J., 2022. Genome-wide screening identifies Polycomb repressive complex 1.3 as an essential regulator of human naïve pluripotent cell reprogramming. *Sci. Adv.* 8, eabk0013. <https://doi.org/10.1126/sciadv.abk0013>
- Comprehensive molecular characterization of human colon and rectal cancer, 2012. *Nature* 487, 330–337. <https://doi.org/10.1038/nature11252>
- Conner, S.D., Schmid, S.L., 2003. Regulated portals of entry into the cell. *Nature* 422, 37–44. <https://doi.org/10.1038/nature01451>
- Conway, James R. W., Dinç, D.D., Follain, G., Paavolainen, O., Kaivola, J., Boström, P., Hartiala, P., Peuhu, E., Ivaska, J., 2023. IGFBP2 secretion by mammary adipocytes limits breast cancer invasion. *Sci. Adv.* 9, eadg1840. <https://doi.org/10.1126/sciadv.adg1840>
- Conway, James R. W., Isomursu, A., Follain, G., Härmä, V., Jou-Ollé, E., Pasquier, N., Välimäki, E.P.O., Rantala, J.K., Ivaska, J., 2023. Defined extracellular matrix compositions support

- stiffness-insensitive cell spreading and adhesion signaling. *Proc. Natl. Acad. Sci.* 120, e2304288120. <https://doi.org/10.1073/pnas.2304288120>
- Conway, J.R.W., Jacquemet, G., 2019. Cell matrix adhesion in cell migration. *Essays Biochem.* 63, 535–551. <https://doi.org/10.1042/EBC20190012>
- Coucouvani, E., Martin, G.R., 1995. Signals for death and survival: A two-step mechanism for cavitation in the vertebrate embryo. *Cell* 83, 279–287. [https://doi.org/10.1016/0092-8674\(95\)90169-8](https://doi.org/10.1016/0092-8674(95)90169-8)
- Coureuil, M., Mikaty, G., Miller, F., Lécuyer, H., Bernard, C., Bourdoulous, S., Duménil, G., Mège, R.-M., Weksler, B.B., Romero, I.A., Couraud, P.-O., Nassif, X., 2009. Meningococcal Type IV Pili Recruit the Polarity Complex to Cross the Brain Endothelium. *Science* 325, 83–87. <https://doi.org/10.1126/science.1173196>
- Cox, T.R., Bird, D., Baker, A.-M., Barker, H.E., Ho, M.W.-Y., Lang, G., Erler, J.T., 2013. LOX-Mediated Collagen Crosslinking Is Responsible for Fibrosis-Enhanced Metastasis. *Cancer Res.* 73, 1721–1732. <https://doi.org/10.1158/0008-5472.CAN-12-2233>
- Date, S., Sato, T., 2015. Mini-Gut Organoids: Reconstitution of the Stem Cell Niche. *Annu. Rev. Cell Dev. Biol.* 31, 269–289. <https://doi.org/10.1146/annurev-cellbio-100814-125218>
- de Boer, M., van Dijck, J.A.A.M., Bult, P., Borm, G.F., Tjan-Heijnen, V.C.G., 2010. Breast Cancer Prognosis and Occult Lymph Node Metastases, Isolated Tumor Cells, and Micrometastases. *JNCI J. Natl. Cancer Inst.* 102, 410–425. <https://doi.org/10.1093/jnci/djq008>
- De Franceschi, N., Arjonen, A., Elkhatib, N., Denessiouk, K., Wrobel, A.G., Wilson, T.A., Pouwels, J., Montagnac, G., Owen, D.J., Ivaska, J., 2016. Selective integrin endocytosis is driven by interactions between the integrin α -chain and AP2. *Nat. Struct. Mol. Biol.* 23, 172–179. <https://doi.org/10.1038/nsmb.3161>
- Dekker, E., Tanis, P.J., Vleugels, J.L.A., Kasi, P.M., Wallace, M.B., 2019. Colorectal cancer. *The Lancet* 394, 1467–1480. [https://doi.org/10.1016/S0140-6736\(19\)32319-0](https://doi.org/10.1016/S0140-6736(19)32319-0)
- Desgrosellier, J.S., Barnes, L.A., Shields, D.J., Huang, M., Lau, S.K., Prévost, N., Tarin, D., Shattil, S.J., Cheresh, D.A., 2009. An integrin α v β 3-c-*Src* oncogenic unit promotes anchorage-independence and tumor progression. *Nat. Med.* 15, 1163–1169. <https://doi.org/10.1038/nm.2009>
- Di Paolo, G., De Camilli, P., 2006. Phosphoinositides in cell regulation and membrane dynamics. *Nature* 443, 651–657. <https://doi.org/10.1038/nature05185>
- Di Paolo, G., Pellegrini, L., Letinic, K., Cestra, G., Zoncu, R., Voronov, S., Chang, S., Guo, J., Wenk, M.R., De Camilli, P., 2002. Recruitment and regulation of phosphatidylinositol phosphate kinase type 1 β by the FERM domain of talin. *Nature* 420, 85–89. <https://doi.org/10.1038/nature01147>
- Dieckmann, N.M.G., Frazer, G.L., Asano, Y., Stinchcombe, J.C., Griffiths, G.M., 2016. The cytotoxic T lymphocyte immune synapse at a glance. *J. Cell Sci.* 129, 2881–2886. <https://doi.org/10.1242/jcs.186205>
- Diepenbruck, M., Christofori, G., 2016. Epithelial–mesenchymal transition (EMT) and metastasis: yes, no, maybe? *Curr. Opin. Cell Biol., Differentiation and disease* 43, 7–13. <https://doi.org/10.1016/j.ccb.2016.06.002>
- Drain, A.P., Zahir, N., Northey, J.J., Zhang, H., Huang, P.-J., Maller, O., Lakins, J.N., Yu, X., Leight, J.L., Alston-Mills, B.P., Hwang, E.S., Chen, Y.-Y., Park, C.C., Weaver, V.M., 2021. Matrix compliance permits NF- κ B activation to drive therapy resistance in breast cancer. *J. Exp. Med.* 218, e20191360. <https://doi.org/10.1084/jem.20191360>
- D’Souza-Schorey, C., Chavrier, P., 2006. ARF proteins: roles in membrane traffic and beyond. *Nat. Rev. Mol. Cell Biol.* 7, 347–358. <https://doi.org/10.1038/nrm1910>
- Ducibella, T., Ukena, T., Karnovsky, M., Anderson, E., 1977. Changes in cell surface and cortical cytoplasmic organization during early embryogenesis in the preimplantation mouse embryo. *J. Cell Biol.* 74, 153–167. <https://doi.org/10.1083/jcb.74.1.153>
- Dumortier, J.G., Le Verge-Serandour, M., Tortorelli, A.F., Mielke, A., de Plater, L., Turlier, H., Maître, J.-L., 2019. Hydraulic fracturing and active coarsening position the lumen of the mouse blastocyst. *Science* 365, 465–468. <https://doi.org/10.1126/science.aaw7709>
- Dumortier, J.G., Maître, J.-L., 2017. Early embryos kept in check. *Nature* 552, 178–179. <https://doi.org/10.1038/d41586-017-07436-w>
- Ebnet, K. (Ed.), 2015. *Cell Polarity 1: Biological Role and Basic Mechanisms*. Springer

- International Publishing, Cham. <https://doi.org/10.1007/978-3-319-14463-4>
- Eddy, R.J., Weidmann, M.D., Sharma, V.P., Condeelis, J.S., 2017. Tumor Cell Invadopodia: Invasive Protrusions that Orchestrate Metastasis. *Trends Cell Biol.* 27, 595–607. <https://doi.org/10.1016/j.tcb.2017.03.003>
- Ehrlich, J.S., Hansen, M.D.H., Nelson, W.J., 2002. Spatio-Temporal Regulation of Rac1 Localization and Lamellipodia Dynamics during Epithelial Cell-Cell Adhesion. *Dev. Cell* 3, 259–270. [https://doi.org/10.1016/S1534-5807\(02\)00216-2](https://doi.org/10.1016/S1534-5807(02)00216-2)
- Elbediwy, A., Zihni, C., Terry, S.J., Clark, P., Matter, K., Balda, M.S., 2012. Epithelial junction formation requires confinement of Cdc42 activity by a novel SH3BP1 complex. *J. Cell Biol.* 198, 677–693. <https://doi.org/10.1083/jcb.201202094>
- Elosegui-Artola, A., Oria, R., Chen, Y., Kosmalska, A., Pérez-González, C., Castro, N., Zhu, C., Trepac, X., Roca-Cusachs, P., 2016. Mechanical regulation of a molecular clutch defines force transmission and transduction in response to matrix rigidity. *Nat. Cell Biol.* 18, 540–548. <https://doi.org/10.1038/ncb3336>
- Emsley, J., Knight, C.G., Farndale, R.W., Barnes, M.J., Liddington, R.C., 2000. Structural Basis of Collagen Recognition by Integrin $\alpha 2 \beta 1$. *Cell* 101, 47–56. [https://doi.org/10.1016/S0092-8674\(00\)80622-4](https://doi.org/10.1016/S0092-8674(00)80622-4)
- Etienne-Manneville, S., Hall, A., 2002. Rho GTPases in cell biology. *Nature* 420, 629–635. <https://doi.org/10.1038/nature01148>
- Eva, R., Dassie, E., Caswell, P.T., Dick, G., French-Constant, C., Norman, J.C., Fawcett, J.W., 2010. Rab11 and Its Effector Rab Coupling Protein Contribute to the Trafficking of $\alpha 2 \beta 1$ Integrins during Axon Growth in Adult Dorsal Root Ganglion Neurons and PC12 Cells. *J. Neurosci.* 30, 11654–11669. <https://doi.org/10.1523/JNEUROSCI.2425-10.2010>
- Ezraty, E.J., Bertaux, C., Marcantonio, E.E., Gundersen, G.G., 2009. Clathrin mediates integrin endocytosis for focal adhesion disassembly in migrating cells. *J. Cell Biol.* 187, 733–747. <https://doi.org/10.1083/jcb.200904054>
- Ezraty, E.J., Partridge, M.A., Gundersen, G.G., 2005. Microtubule-induced focal adhesion disassembly is mediated by dynamin and focal adhesion kinase. *Nat. Cell Biol.* 7, 581–590. <https://doi.org/10.1038/ncb1262>
- Fabbri, M., Di Meglio, S., Gagliani, M.C., Consonni, E., Molteni, R., Bender, J.R., Tacchetti, C., Pardi, R., 2005. Dynamic Partitioning into Lipid Rafts Controls the Endo-Exocytic Cycle of the $\alpha L \beta 2$ Integrin, LFA-1, during Leukocyte Chemotaxis. *Mol. Biol. Cell* 16, 5793–5803. <https://doi.org/10.1091/mbc.e05-05-0413>
- Fang, Z., Takizawa, N., Wilson, K.A., Smith, T.C., Delprato, A., Davidson, M.W., Lambright, D.G., Luna, E.J., 2010. The Membrane-Associated Protein, Supervillin, Accelerates F-Actin-Dependent Rapid Integrin Recycling and Cell Motility. *Traffic* 11, 782–799. <https://doi.org/10.1111/j.1600-0854.2010.01062.x>
- Fehon, R.G., McClatchey, A.L., Bretscher, A., 2010. Organizing the cell cortex: the role of ERM proteins. *Nat. Rev. Mol. Cell Biol.* 11, 276–287. <https://doi.org/10.1038/nrm2866>
- Fernandez-Garcia, B., Eiró, N., Marín, L., González-Reyes, S., González, L.O., Lamelas, M.L., Vizoso, F.J., 2014. Expression and prognostic significance of fibronectin and matrix metalloproteases in breast cancer metastasis. *Histopathology* 64, 512–522. <https://doi.org/10.1111/his.12300>
- Fessler, E., Medema, J.P., 2016. Colorectal Cancer Subtypes: Developmental Origin and Microenvironmental Regulation. *Trends Cancer* 2, 505–518. <https://doi.org/10.1016/j.trecan.2016.07.008>
- Flier, L.G. van der, Clevers, H., 2009. Stem Cells, Self-Renewal, and Differentiation in the Intestinal Epithelium. *Annu. Rev. Physiol.* 71, 241–260. <https://doi.org/10.1146/annurev.physiol.010908.163145>
- Fortin, S., Le Mercier, M., Camby, I., Spiegl-Kreinecker, S., Berger, W., Lefranc, F., Kiss, R., 2010. Galectin-1 Is Implicated in the Protein Kinase C μ /Vimentin-Controlled Trafficking of Integrin- $\alpha 2 \beta 1$ in Glioblastoma Cells. *Brain Pathol.* 20, 39–49. <https://doi.org/10.1111/j.1750-3639.2008.00227.x>
- Friedland, J.C., Lee, M.H., Boettiger, D., 2009. Mechanically Activated Integrin Switch

- Controls $\pm 5^2$ 1 Function. *Science* 323, 642–644. <https://doi.org/10.1126/science.1168441>
- Fu, R., Zhang, Y.-W., Li, H.-M., Lv, W.-C., Zhao, L., Guo, Q.-L., Lu, T., Weiss, S.J., Li, Z.-Y., Wu, Z.-Q., 2018. LW106, a novel indoleamine 2,3-dioxygenase 1 inhibitor, suppresses tumour progression by limiting stroma-immune crosstalk and cancer stem cell enrichment in tumour micro-environment. *Br. J. Pharmacol.* 175, 3034–3049. <https://doi.org/10.1111/bph.14351>
- Fukuyama, T., Ogita, H., Kawakatsu, T., Inagaki, M., Takai, Y., 2006. Activation of Rac by cadherin through the c-Src–Rap1–phosphatidylinositol 3-kinase–Vav2 pathway. *Oncogene* 25, 8–19. <https://doi.org/10.1038/sj.onc.1209010>
- Furtak, V., Hatcher, F., Ochieng, J., 2001. Galectin-3 Mediates the Endocytosis of α -1 Integrins by Breast Carcinoma Cells. *Biochem. Biophys. Res. Commun.* 289, 845–850. <https://doi.org/10.1006/bbrc.2001.6064>
- Gahmberg, C.G., Fagerholm, S.C., Nurmi, S.M., Chavakis, T., Marchesan, S., Grönholm, M., 2009. Regulation of integrin activity and signalling. *Biochim. Biophys. Acta BBA - Gen. Subj.* 1790, 431–444. <https://doi.org/10.1016/j.bbagen.2009.03.007>
- Gan, Y., McGraw, T.E., Rodriguez-Boulant, E., 2002. The epithelial-specific adaptor AP1B mediates post-endocytic recycling to the basolateral membrane. *Nat. Cell Biol.* 4, 605–609. <https://doi.org/10.1038/ncb827>
- Gao, J., Bao, Y., Ge, S., Sun, P., Sun, J., Liu, J., Chen, F., Han, L., Cao, Z., Qin, J., White, G.C., Xu, Z., Ma, Y.-Q., 2019. Sharpin suppresses α 1-integrin activation by complexing with the α 1 tail and kindlin-1. *Cell Commun. Signal.* CCS 17, 101. <https://doi.org/10.1186/s12964-019-0407-6>
- Gassama-Diagne, A., Yu, W., ter Beest, M., Martin-Belmonte, F., Kierbel, A., Engel, J., Mostov, K., 2006. Phosphatidylinositol-3,4,5-trisphosphate regulates the formation of the basolateral plasma membrane in epithelial cells. *Nat. Cell Biol.* 8, 963–970. <https://doi.org/10.1038/ncb1461>
- Georgiadou, M., Lilja, J., Jacquemet, G., Guzmán, C., Rafeva, M., Alibert, C., Yan, Y., Sahgal, P., Lerche, M., Manneville, J.-B., Mäkelä, T.P., Ivaska, J., 2017. AMPK negatively regulates tensin-dependent integrin activity. *J. Cell Biol.* 216, 1107–1121. <https://doi.org/10.1083/jcb.201609066>
- Gerke, V., Creutz, C.E., Moss, S.E., 2005. Annexins: linking Ca²⁺ signalling to membrane dynamics. *Nat. Rev. Mol. Cell Biol.* 6, 449–461. <https://doi.org/10.1038/nrm1661>
- Gerri, C., Menchero, S., Mahadevaiah, S.K., Turner, J.M.A., Niakan, K.K., 2020. Human Embryogenesis: A Comparative Perspective. *Annu. Rev. Cell Dev. Biol.* 36, 411–440. <https://doi.org/10.1146/annurev-cellbio-022020-024900>
- Gingras, A.R., Ziegler, W.H., Bobkov, A.A., Joyce, M.G., Fasci, D., Himmel, M., Rothemund, S., Ritter, A., Grossmann, J.G., Patel, B., Bate, N., Goult, B.T., Emsley, J., Barsukov, I.L., Roberts, G.C.K., Liddington, R.C., Ginsberg, M.H., Critchley, D.R., 2009. Structural Determinants of Integrin Binding to the Talin Rod *. *J. Biol. Chem.* 284, 8866–8876. <https://doi.org/10.1074/jbc.M805937200>
- Gomez, G.A., McLachlan, R.W., Yap, A.S., 2011. Productive tension: force-sensing and homeostasis of cell–cell junctions. *Trends Cell Biol.* 21, 499–505. <https://doi.org/10.1016/j.tcb.2011.05.006>
- Gribble, F.M., Reimann, F., 2016. Enteroendocrine Cells: Chemosensors in the Intestinal Epithelium. *Annu. Rev. Physiol.* 78, 277–299. <https://doi.org/10.1146/annurev-physiol-021115-105439>
- Grillet, F., Bayet, E., Villeronce, O., Zappia, L., Lagerqvist, E.L., Lunke, S., Charafe-Jauffret, E., Pham, K., Molck, C., Rolland, N., Bourgaux, J.F., Prudhomme, M., Philippe, C., Bravo, S., Boyer, J.C., Canterel-Thouennon, L., Taylor, G.R., Hsu, A., Pascussi, J.M., Hollande, F., Pannequin, J., 2017. Circulating tumour cells from patients with colorectal cancer have cancer stem cell hallmarks in ex vivo culture. *Gut* 66, 1802–1810. <https://doi.org/10.1136/gutjnl-2016-311447>
- Guo, X., Fan, Y., Lang, R., Gu, F., Chen, L., Cui, L., Pringle, G.A., Zhang, X., Fu, L., 2008. Tumor infiltrating lymphocytes differ in invasive micropapillary carcinoma and medullary carcinoma of breast. *Mod. Pathol.* 21, 1101–1107. <https://doi.org/10.1038/modpathol.2008.72>
- Guzmán, C., Bagga, M., Kaur, A., Westermarck, J., Abankwa, D., 2014. ColonyArea: An ImageJ Plugin to Automatically Quantify Colony Formation in Clonogenic Assays. *PLOS ONE* 9, e92444. <https://doi.org/10.1371/journal.pone.0092444>
- Hamidi, H., Ivaska, J., 2018. Every step of the way: integrins in cancer progression and

- metastasis. *Nat. Rev. Cancer* 18, 533–548. <https://doi.org/10.1038/s41568-018-0038-z>
- Han, S.J., Azarova, E.V., Whitewood, A.J., Bachir, A., Gutierrez, E., Groisman, A., Horwitz, A.R., Goult, B.T., Dean, K.M., Danuser, G., 2021. Pre-complexation of talin and vinculin without tension is required for efficient nascent adhesion maturation. *eLife* 10, e66151. <https://doi.org/10.7554/eLife.66151>
- Han, S.J., Oak, Y., Groisman, A., Danuser, G., 2015. Traction microscopy to identify force modulation in subresolution adhesions. *Nat. Methods* 12, 653–656. <https://doi.org/10.1038/nmeth.3430>
- Hang, Q., Isaji, T., Hou, S., Wang, Y., Fukuda, T., Gu, J., 2017. A Key Regulator of Cell Adhesion: Identification and Characterization of Important N-Glycosylation Sites on Integrin $\alpha 5$ for Cell Migration. *Mol. Cell. Biol.* 37, e00558-16. <https://doi.org/10.1128/MCB.00558-16>
- Harburger, D.S., Bouaouina, M., Calderwood, D.A., 2009. Kindlin-1 and -2 Directly Bind the C-terminal Region of $\beta 2$ Integrin Cytoplasmic Tails and Exert Integrin-specific Activation Effects*. *J. Biol. Chem.* 284, 11485–11497. <https://doi.org/10.1074/jbc.M809233200>
- Hassani, S.-N., Moradi, S., Taleahmad, S., Braun, T., Baharvand, H., 2019. Transition of inner cell mass to embryonic stem cells: mechanisms, facts, and hypotheses. *Cell. Mol. Life Sci.* 76, 873–892. <https://doi.org/10.1007/s00018-018-2965-y>
- Hershberg, R.M., Cho, D.H., Youakim, A., Bradley, M.B., Lee, J.S., Framson, P.E., Nepom, G.T., 1998. Highly polarized HLA class II antigen processing and presentation by human intestinal epithelial cells. *J. Clin. Invest.* 102, 792–803. <https://doi.org/10.1172/JCI3201>
- Himmel, M., Ritter, A., Rothmund, S., Pauling, B.V., Rottner, K., Gingras, A.R., Ziegler, W.H., 2009. Control of High Affinity Interactions in the Talin C Terminus: HOW TALIN DOMAINS COORDINATE PROTEIN DYNAMICS IN CELL ADHESIONS*. *J. Biol. Chem.* 284, 13832–13842. <https://doi.org/10.1074/jbc.M900266200>
- Hirakawa, T., Goto, M., Takahashi, K., Iwasawa, T., Fujishima, A., Makino, K., Shirasawa, H., Sato, W., Sato, T., Kumazawa, Y., Terada, Y., 2022. Na⁺/K⁺ ATPase $\alpha 1$ and $\alpha 3$ subunits are localized to the basolateral membrane of trophoblast cells in human blastocysts. *Hum. Reprod.* 37, 1423–1430. <https://doi.org/10.1093/humrep/deac124>
- Hirate, Y., Hirahara, S., Inoue, K., Suzuki, A., Alarcon, V.B., Akimoto, K., Hirai, T., Hara, T., Adachi, M., Chida, K., Ohno, S., Marikawa, Y., Nakao, K., Shimono, A., Sasaki, H., 2013. Polarity-Dependent Distribution of Angiomotin Localizes Hippo Signaling in Preimplantation Embryos. *Curr. Biol.* 23, 1181–1194. <https://doi.org/10.1016/j.cub.2013.05.014>
- Höfer, D., Püschel, B., Drenckhahn, D., 1996. Taste receptor-like cells in the rat gut identified by expression of alpha-gustducin. *Proc. Natl. Acad. Sci.* 93, 6631–6634. <https://doi.org/10.1073/pnas.93.13.6631>
- Hordijk, P.L., ten Klooster, J.P., van der Kammen, R.A., Michiels, F., Oomen, L.C.J.M., Collard, J.G., 1997. Inhibition of Invasion of Epithelial Cells by Tiam1-Rac Signaling. *Science* 278, 1464–1466. <https://doi.org/10.1126/science.278.5342.1464>
- Horton, E.R., Byron, A., Askari, J.A., Ng, D.H.J., Millon-Frémillon, A., Robertson, J., Koper, E.J., Paul, N.R., Warwood, S., Knight, D., Humphries, J.D., Humphries, M.J., 2015. Definition of a consensus integrin adhesome and its dynamics during adhesion complex assembly and disassembly. *Nat. Cell Biol.* 17, 1577–1587. <https://doi.org/10.1038/ncb3257>
- Horton, E.R., Humphries, J.D., James, J., Jones, M.C., Askari, J.A., Humphries, M.J., 2016. The integrin adhesome network at a glance. *J. Cell Sci.* jcs.192054. <https://doi.org/10.1242/jcs.192054>
- Hugen, N., Brown, G., Glynne-Jones, R., de Wilt, J.H.W., Nagtegaal, I.D., 2016. Advances in the care of patients with mucinous colorectal cancer. *Nat. Rev. Clin. Oncol.* 13, 361–369. <https://doi.org/10.1038/nrclinonc.2015.140>
- Hugen, N., Verhoeven, R.H., Lemmens, V.E., van Aart, C.J., Elferink, M.A., Radema, S.A., Nagtegaal, I.D., de Wilt, J.H., 2015. Colorectal signet-ring cell carcinoma: benefit from adjuvant chemotherapy but a poor prognostic factor. *Int. J. Cancer* 136, 333–339. <https://doi.org/10.1002/ijc.28981>
- Humphries, J.D., Byron, A., Bass, M.D., Craig, S.E., Pinney, J.W., Knight, D., Humphries, M.J., 2009. Proteomic Analysis of Integrin-Associated Complexes Identifies RCC2 as a Dual Regulator of Rac1 and Arp6. *Sci. Signal.* 2. <https://doi.org/10.1126/scisignal.2000396>
- Humphries, J.D., Byron, A., Humphries, M.J., 2006. Integrin ligands at a glance. *J. Cell Sci.*

- 119, 3901–3903. <https://doi.org/10.1242/jcs.03098>
- Humphries, J.D., Chastney, M.R., Askari, J.A., Humphries, M.J., 2019. Signal transduction via integrin adhesion complexes. *Curr. Opin. Cell Biol., Cell Architecture* 56, 14–21. <https://doi.org/10.1016/j.ceb.2018.08.004>
- Humphries, M., 2000. *Integrin Structure. *Biochem. Soc. Trans.* 28, 311–39. <https://doi.org/10.1042/0300-5127:0280311>
- Hurd, T.W., Gao, L., Roh, M.H., Macara, I.G., Margolis, B., 2003. Direct interaction of two polarity complexes implicated in epithelial tight junction assembly. *Nat. Cell Biol.* 5, 137–142. <https://doi.org/10.1038/ncb923>
- Hynes, R.O., 2002. Integrins: Bidirectional, Allosteric Signaling Machines. *Cell* 110, 673–687. [https://doi.org/10.1016/S0092-8674\(02\)00971-6](https://doi.org/10.1016/S0092-8674(02)00971-6)
- Hynes, R.O., 1987. Integrins: A family of cell surface receptors. *Cell* 48, 549–554. [https://doi.org/10.1016/0092-8674\(87\)90233-9](https://doi.org/10.1016/0092-8674(87)90233-9)
- Idelevich, A., Vilella, F., 2020. Mother and Embryo Cross-Communication. *Genes* 11, 376. <https://doi.org/10.3390/genes11040376>
- Isaji, T., Gu, J., Nishiuchi, R., Zhao, Y., Takahashi, M., Miyoshi, E., Honke, K., Sekiguchi, K., Taniguchi, N., 2004. Introduction of Bisecting GlcNAc into Integrin $\alpha 5 \beta 1$ Reduces Ligand Binding and Down-regulates Cell Adhesion and Cell Migration *. *J. Biol. Chem.* 279, 19747–19754. <https://doi.org/10.1074/jbc.M311627200>
- Isaji, T., Sato, Y., Fukuda, T., Gu, J., 2009. N-Glycosylation of the I-like Domain of $\alpha 5 \beta 1$ Integrin Is Essential for $\alpha 5 \beta 1$ Integrin Expression and Biological Function. *J. Biol. Chem.* 284, 12207–12216. <https://doi.org/10.1074/jbc.M807920200>
- Ishihara, A., Yoshida, T., Tamaki, H., Sakakura, T., 1995. Tenascin expression in cancer cells and stroma of human breast cancer and its prognostic significance. *Clin. Cancer Res.* 1, 1035–1041.
- Islami, F., Goding Sauer, A., Miller, K.D., Siegel, R.L., Fedewa, S.A., Jacobs, E.J., McCullough, M.L., Patel, A.V., Ma, J., Soerjomataram, I., Flanders, W.D., Brawley, O.W., Gapstur, S.M., Jemal, A., 2018. Proportion and number of cancer cases and deaths attributable to potentially modifiable risk factors in the United States. *CA. Cancer J. Clin.* 68, 31–54. <https://doi.org/10.3322/caac.21440>
- Isomursu, A., Park, K.-Y., Hou, J., Cheng, B., Mathieu, M., Shamsan, G., Fuller, B., Kasim, J., Mohsen Mahmoodi, M., Lu, T.J., Genin, G.M., Xu, F., Lin, M., Distefano, M., Ivaska, J., Odde, D.J., 2022. Negative durotaxis: cell movement toward softer environments. *Nat. Mater.* 21, 1081–1090. <https://doi.org/10.1038/s41563-022-01294-2>
- Itoh, M., Sasaki, H., Furuse, M., Ozaki, H., Kita, T., Tsukita, S., 2001. Junctional adhesion molecule (JAM) binds to PAR-3: a possible mechanism for the recruitment of PAR-3 to tight junctions. *J. Cell Biol.* 154, 491–498. <https://doi.org/10.1083/jcb.200103047>
- Izumi, G., Sakisaka, T., Baba, T., Tanaka, S., Morimoto, K., Takai, Y., 2004. Endocytosis of E-cadherin regulated by Rac and Cdc42 small G proteins through IQGAP1 and actin filaments. *J. Cell Biol.* 166, 237–248. <https://doi.org/10.1083/jcb.200401078>
- Jacquemet, G., Morgan, M.R., Byron, A., Humphries, J.D., Choi, C.K., Chen, C.S., Caswell, P.T., Humphries, M.J., 2013. Rac1 is deactivated at integrin activation sites via an IQGAP1/filamin-A/RacGAP1 pathway. *J. Cell Sci.* jcs.121988. <https://doi.org/10.1242/jcs.121988>
- Jacquemet, G., Stubb, A., Saup, R., Miihkinen, M., Kremneva, E., Hamidi, H., Ivaska, J., 2019. Filopodome Mapping Identifies p130Cas as a Mechanosensitive Regulator of Filopodia Stability. *Curr. Biol.* 29, 202–216.e7. <https://doi.org/10.1016/j.cub.2018.11.053>
- Jaffe, A.B., Kaji, N., Durgan, J., Hall, A., 2008. Cdc42 controls spindle orientation to position the apical surface during epithelial morphogenesis. *J. Cell Biol.* 183, 625–633. <https://doi.org/10.1083/jcb.200807121>
- Janik, M.E., Lityńska, A., Vereecken, P., 2010. Cell migration—The role of integrin glycosylation. *Biochim. Biophys. Acta BBA - Gen. Subj.* 1800, 545–555. <https://doi.org/10.1016/j.bbagen.2010.03.013>
- Jäntti, N.Z., Moreno-Layseca, P., Chastney, M.R., Dibus, M., Conway, J.R.W., Leppänen, V.-M., Hamidi, H., Eylmann, K., Oliveira-Ferrer, L., Veltel, S., Ivaska, J., 2024. EPLIN± controls integrin recycling from Rab21 endosomes to drive breast cancer cell migration.

<https://doi.org/10.1101/2024.06.27.600789>

Jarray, R., Allain, B., Borriello, L., Biard, D., Loukaci, A., Larghero, J., Hadj-Slimane, R., Garbay, C., Lepelletier, Y., Raynaud, F., 2011. Depletion of the novel protein PHACTR-1 from human endothelial cells abolishes tube formation and induces cell death receptor apoptosis. *Biochimie* 93, 1668–1675. <https://doi.org/10.1016/j.biochi.2011.07.010>

Jensen, J., Pedersen, E.E., Galante, P., Hald, J., Heller, R.S., Ishibashi, M., Kageyama, R., Guillemot, F., Serup, P., Madsen, O.D., 2000. Control of endodermal endocrine development by HES-1. *Nat. Genet.* 24, 36–44. <https://doi.org/10.1038/71657>

Jin, H., Tang, Y., Yang, L., Peng, X., Li, B., Fan, Q., Wei, S., Yang, S., Li, X., Wu, B., Huang, M., Tang, S., Liu, J., Li, H., 2021. Rab GTPases: Central Coordinators of Membrane Trafficking in Cancer. *Front. Cell Dev. Biol.* 9. <https://doi.org/10.3389/fcell.2021.648384>

Joberty, G., Petersen, C., Gao, L., Macara, I.G., 2000. The cell-polarity protein Par6 links Par3 and atypical protein kinase C to Cdc42. *Nat. Cell Biol.* 2, 531–539. <https://doi.org/10.1038/35019573>

Jones, J.C.R., Kam, C.Y., Harmon, R.M., Woychek, A.V., Hopkinson, S.B., Green, K.J., 2017. Intermediate Filaments and the Plasma Membrane. *Cold Spring Harb. Perspect. Biol.* 9, a025866. <https://doi.org/10.1101/cshperspect.a025866>

Jones, M.C., Caswell, P.T., Norman, J.C., 2006. Endocytic recycling pathways: emerging regulators of cell migration. *Curr. Opin. Cell Biol.*, Cell-to-cell contact and extracellular matrix 18, 549–557. <https://doi.org/10.1016/j.ceb.2006.08.003>

Julien, S., Merino-Trigo, A., Lacroix, L., Pocard, M., Goéré, D., Mariani, P., Landron, S., Bigot, L., Nemati, F., Dartigues, P., Weiswald, L.-B., Lantuas, D., Morgand, L., Pham, E., Gonin, P., Dangles-Marie, V., Job, B., Dessen, P., Bruno, A., Pierré, A., De Thé, H., Soliman, H., Nunes, M., Lardier, G., Calvet, L., Demers, B., Prévost, G., Vrignaud, P., Roman-Roman, S., Duchamp, O., Berthet, C., 2012. Characterization of a Large Panel of Patient-Derived Tumor Xenografts Representing the Clinical Heterogeneity of Human Colorectal Cancer. *Clin. Cancer Res.* 18, 5314–5328. <https://doi.org/10.1158/1078-0432.CCR-12-0372>

Kanchanawong, P., Shtengel, G., Pasapera, A.M., Ramko, E.B., Davidson, M.W., Hess, H.F., Waterman, C.M., 2010. Nanoscale architecture of integrin-based cell adhesions. *Nature* 468, 580–584. <https://doi.org/10.1038/nature09621>

Karaköse, E., Schiller, H.B., Fässler, R., 2010. The kindlins at a glance. *J. Cell Sci.* 123, 2353–2356. <https://doi.org/10.1242/jcs.064600>

Katara, G.K., Kulshrestha, A., Mao, L., Wang, X., Sahoo, M., Ibrahim, S., Pamarthy, S., Suzue, K., Shekhawat, G.S., Gilman-Sachs, A., Beaman, K.D., 2018. Mammary epithelium-specific inactivation of V-ATPase reduces stiffness of extracellular matrix and enhances metastasis of breast cancer. *Mol. Oncol.* 12, 208–223. <https://doi.org/10.1002/1878-0261.12159>

Kechagia, J.Z., Ivaska, J., Roca-Cusachs, P., 2019. Integrins as biomechanical sensors of the microenvironment. *Nat. Rev. Mol. Cell Biol.* 20, 457–473. <https://doi.org/10.1038/s41580-019-0134-2>

Kempthues, K.J., Priess, J.R., Morton, D.G., Cheng, N., 1988. Identification of genes required for cytoplasmic localization in early *C. elegans* embryos. *Cell* 52, 311–320. [https://doi.org/10.1016/S0092-8674\(88\)80024-2](https://doi.org/10.1016/S0092-8674(88)80024-2)

Kierbel, A., Gassama-Diagne, A., Rocha, C., Radoshevich, L., Olson, J., Mostov, K., Engel, J., 2007. *Pseudomonas aeruginosa* exploits a PIP3-dependent pathway to transform apical into basolateral membrane. *J. Cell Biol.* 177, 21–27. <https://doi.org/10.1083/jcb.200605142>

Klinger, S.C., Glerup, S., Raarup, M.K., Mari, M.C., Nyegaard, M., Koster, G., Prabakaran, T., Nilsson, S.K., Kjaergaard, M.M., Bakke, O., Nykjær, A., Olivecrona, G., Petersen, C.M., Nielsen, M.S., 2011. SorLA regulates the activity of lipoprotein lipase by intracellular trafficking. *J. Cell Sci.* 124, 1095–1105. <https://doi.org/10.1242/jcs.072538>

Krasna, M.J., Flancbaum, L., Cody, R.P., Shneibaum, S., Ari, G.B., 1988. Vascular and neural invasion in colorectal carcinoma. Incidence and prognostic significance. *Cancer* 61, 1018–1023. [https://doi.org/10.1002/1097-0142\(19880301\)61:5<1018::AID-CNCR2820610527>3.0.CO;2-H](https://doi.org/10.1002/1097-0142(19880301)61:5<1018::AID-CNCR2820610527>3.0.CO;2-H)

Kumari, R., Ven, K., Chastney, M., Kokate, S.B., Peränen, J., Aaron, J., Kogan, K., Almeida-Souza, L., Kremneva, E., Poincloux, R., Chew, T.-L., Gunning, P.W., Ivaska, J., Lappalainen, P., 2024. Focal adhesions contain three specialized actin nanoscale layers. *Nat. Commun.* 15, 2547.

<https://doi.org/10.1038/s41467-024-46868-7>

Kuroda, H., Sakamoto, G., Ohnisi, K., Itoyama, S., 2004. Clinical and pathologic features of invasive micropapillary carcinoma. *Breast Cancer* 11, 169–174. <https://doi.org/10.1007/BF02968297>

Labernadie, A., Kato, T., Brugués, A., Serra-Picamal, X., Derzsi, S., Arwert, E., Weston, A., González-Tarragó, V., Elosegui-Artola, A., Albertazzi, L., Alcaraz, J., Roca-Cusachs, P., Sahai, E., Trepac, X., 2017. A mechanically active heterotypic E-cadherin/N-cadherin adhesion enables fibroblasts to drive cancer cell invasion. *Nat. Cell Biol.* 19, 224–237. <https://doi.org/10.1038/ncb3478>

Laiho, P., Kokko, A., Vanharanta, S., Salovaara, R., Sammalkorpi, H., Järvinen, H., Mecklin, J.-P., Karttunen, T.J., Tuppurainen, K., Davalos, V., Schwartz, S., Arango, D., Mäkinen, M.J., Aaltonen, L.A., 2007. Serrated carcinomas form a subclass of colorectal cancer with distinct molecular basis. *Oncogene* 26, 312–320. <https://doi.org/10.1038/sj.onc.1209778>

Lakshminarayan, R., Wunder, C., Becken, U., Howes, M.T., Benzing, C., Arumugam, S., Sales, S., Ariotti, N., Chambon, V., Lamaze, C., Loew, D., Shevchenko, A., Gaus, K., Parton, R.G., Johannes, L., 2014. Galectin-3 drives glycosphingolipid-dependent biogenesis of clathrin-independent carriers. *Nat. Cell Biol.* 16, 592–603. <https://doi.org/10.1038/ncb2970>

Laprise, P., Viel, A., Rivard, N., 2004. Human Homolog of Disc-large Is Required for Adherens Junction Assembly and Differentiation of Human Intestinal Epithelial Cells *. *J. Biol. Chem.* 279, 10157–10166. <https://doi.org/10.1074/jbc.M309843200>

Larocque, G., Royle, S.J., 2022. Integrating intracellular nanovesicles into integrin trafficking pathways and beyond. *Cell. Mol. Life Sci.* 79, 335. <https://doi.org/10.1007/s00018-022-04371-6>

Latorre, R., Sternini, C., De Giorgio, R., Greenwood-Van Meerveld, B., 2016. Enteroendocrine cells: a review of their role in brain–gut communication. *Neurogastroenterol. Motil.* 28, 620–630. <https://doi.org/10.1111/nmo.12754>

Law, D.A., DeGuzman, F.R., Heiser, P., Ministri-Madrid, K., Killeen, N., Phillips, D.R., 1999. Integrin cytoplasmic tyrosine motif is required for outside-in α IIb β 3 signalling and platelet function 401.

Lawson et al., 2014. The on-off relationship of Rho and Rac during integrin-mediated adhesion and cell migration [WWW Document]. <https://doi.org/10.4161/sgtp.27958>

Lee, J.-O., Bankston, L.A., Robert C Liddington, M.A.A.A., 1995. Two conformations of the integrin A-domain (I-domain): a pathway for activation? *Structure* 3, 1333–1340. [https://doi.org/10.1016/S0969-2126\(01\)00271-4](https://doi.org/10.1016/S0969-2126(01)00271-4)

Lee, M., Vasioukhin, V., 2008. Cell polarity and cancer – cell and tissue polarity as a non-canonical tumor suppressor. *J. Cell Sci.* 121, 1141–1150. <https://doi.org/10.1242/jcs.016634>

Lehtonen, E., Badley, R.A., 1980. Localization of cytoskeletal proteins in preimplantation mouse embryos. *Development* 55, 211–225. <https://doi.org/10.1242/dev.55.1.211>

Lemmers, C., Michel, D., Lane-Guermonprez, L., Delgrossi, M.-H., Médina, E., Arsanto, J.-P., Le Bivic, A., 2004. CRB3 Binds Directly to Par6 and Regulates the Morphogenesis of the Tight Junctions in Mammalian Epithelial Cells. *Mol. Biol. Cell* 15, 1324–1333. <https://doi.org/10.1091/mbc.e03-04-0235>

Lemoine, L., Sugarbaker, P., Van der Speeten, K., 2016. Pathophysiology of colorectal peritoneal carcinomatosis: Role of the peritoneum. *World J. Gastroenterol.* 22, 7692–7707. <https://doi.org/10.3748/wjg.v22.i34.7692>

Lerche, M., Elosegui-Artola, A., Kechagia, J.Z., Guzmán, C., Georgiadou, M., Andreu, I., Gullberg, D., Roca-Cusachs, P., Peuhu, E., Ivaska, J., 2020. Integrin Binding Dynamics Modulate Ligand-Specific Mechanosensing in Mammary Gland Fibroblasts. *iScience* 23. <https://doi.org/10.1016/j.isci.2020.100907>

Li, C., Zheng, H., Jia, H., Huang, D., Gu, W., Cai, S., Zhu, J., 2019. Prognosis of three histological subtypes of colorectal adenocarcinoma: A retrospective analysis of 8005 Chinese patients. *Cancer Med.* 8, 3411–3419. <https://doi.org/10.1002/cam4.2234>

Li, H., Findlay, I.A., Sheppard, D.N., 2004. The relationship between cell proliferation, Cl-secretion, and renal cyst growth: A study using CFTR inhibitors. *Kidney Int.* 66, 1926–1938. <https://doi.org/10.1111/j.1523-1755.2004.00967.x>

Li, J., Jo, M.H., Yan, J., Hall, T., Lee, J., López-Sánchez, U., Yan, S., Ha, T., Springer, T.A., 2024. Ligand binding initiates single-molecule integrin conformational activation. *Cell* 0.

<https://doi.org/10.1016/j.cell.2024.04.049>

Li, S.R., Gulieva, R.E., Helms, L., Cruz, N.M., Vincent, T., Fu, H., Himmelfarb, J., Freedman, B.S., 2022. Glucose absorption drives cystogenesis in a human organoid-on-chip model of polycystic kidney disease. *Nat. Commun.* 13, 7918. <https://doi.org/10.1038/s41467-022-35537-2>

Liao, H.-Y., Da, C.-M., Liao, B., Zhang, H.-H., 2021. Roles of matrix metalloproteinase-7 (MMP-7) in cancer. *Clin. Biochem.* 92, 9–18. <https://doi.org/10.1016/j.clinbiochem.2021.03.003>

Libanje, F., Raingeaud, J., Luan, R., Thomas, Z., Zajac, O., Veiga, J., Marisa, L., Adam, J., Boige, V., Malka, D., Goéré, D., Hall, A., Soazec, J.-Y., Prall, F., Gelli, M., Dartigues, P., Jaulin, F., 2019. ROCK2 inhibition triggers the collective invasion of colorectal adenocarcinomas. *EMBO J.* 38, e99299. <https://doi.org/10.15252/embj.201899299>

Liebig, C., Ayala, G., Wilks, J., Verstovsek, G., Liu, H., Agarwal, N., Berger, D.H., Albo, D., 2009. Perineural Invasion Is an Independent Predictor of Outcome in Colorectal Cancer. *J. Clin. Oncol.* 27, 5131–5137. <https://doi.org/10.1200/JCO.2009.22.4949>

Lin, D., Edwards, A.S., Fawcett, J.P., Mbamalu, G., Scott, J.D., Pawson, T., 2000. A mammalian PAR-3–PAR-6 complex implicated in Cdc42/Rac1 and aPKC signalling and cell polarity. *Nat. Cell Biol.* 2, 540–547. <https://doi.org/10.1038/35019582>

Liu, J., Wang, Y., Goh, W.L., Goh, H., Baird, M.A., Ruehland, S., Teo, S., Bate, N., Critchley, D.R., Davidson, M.W., Kanchanawong, P., 2015. Talin determines the nanoscale architecture of focal adhesions. *Proc. Natl. Acad. Sci.* 112. <https://doi.org/10.1073/pnas.1512025112>

Liu, X., Ouyang, J.F., Rossello, F.J., Tan, J.P., Davidson, K.C., Valdes, D.S., Schröder, J., Sun, Y.B.Y., Chen, J., Knaupp, A.S., Sun, G., Chy, H.S., Huang, Z., Pflueger, J., Firas, J., Tano, V., Buckberry, S., Paynter, J.M., Larcombe, M.R., Poppe, D., Choo, X.Y., O'Brien, C.M., Pastor, W.A., Chen, D., Leichter, A.L., Naeem, H., Tripathi, P., Das, P.P., Grubman, A., Powell, D.R., Laslett, A.L., David, L., Nilsson, S.K., Clark, A.T., Lister, R., Nefzger, C.M., Martelotto, L.G., Rackham, O.J.L., Polo, J.M., 2020. Reprogramming roadmap reveals route to human induced trophoblast stem cells. *Nature* 586, 101–107. <https://doi.org/10.1038/s41586-020-2734-6>

Lopez, J.-B.R., 2022. Mécanismes moléculaires et cellulaires de la formation des TSIP: médiateurs de la dissémination des cancers colorectaux (phdthesis). Université Paris-Saclay.

Luciano, L., Reale, E., 1990. Brush cells of the mouse gallbladder. *Cell Tissue Res.* 262, 339–349. <https://doi.org/10.1007/BF00309889>

Luna-Moré, S., Gonzalez, B., Acedo, C., Rodrigo, I., Luna, C., 1994. Invasive micropapillary carcinoma of the breast*. *Pathol. - Res. Pract.* 190, 668–674. [https://doi.org/10.1016/S0344-0338\(11\)80745-4](https://doi.org/10.1016/S0344-0338(11)80745-4)

Lynch, H.T., Lynch, J.F., Lynch, P.M., Attard, T., 2008. Hereditary colorectal cancer syndromes: molecular genetics, genetic counseling, diagnosis and management. *Fam. Cancer* 7, 27–39. <https://doi.org/10.1007/s10689-007-9165-5>

Macara, I.G., McCaffrey, L., 2013. Cell polarity in morphogenesis and metastasis. *Philos. Trans. R. Soc. B Biol. Sci.* 368, 20130012. <https://doi.org/10.1098/rstb.2013.0012>

Macedo, J.K.A., Fox, J.W., Castro, M. de S., n.d. Disintegrins from Snake Venoms and their Applications in Cancer Research and Therapy. *Curr. Protein Pept. Sci.* 16, 532–548. <https://doi.org/10.2174/1389203716666150515125002>

Machesky, L.M., 2019. Rab11FIP proteins link endocytic recycling vesicles for cytoskeletal transport and tethering. *Biosci. Rep.* 39, BSR20182219. <https://doi.org/10.1042/BSR20182219>

Mack, N.A., Georgiou, M., 2014. The interdependence of the Rho GTPases and apicobasal cell polarity. *Small GTPases* 5, e973768. <https://doi.org/10.4161/21541248.2014.973768>

Maître, J.-L., 2017. Mechanics of blastocyst morphogenesis. *Biol. Cell* 109, 323–338. <https://doi.org/10.1111/boc.201700029>

Maître, J.-L., Turlier, H., Illukkumbura, R., Eismann, B., Niwayama, R., Nédélec, F., Hiiragi, T., 2016. Asymmetric division of contractile domains couples cell positioning and fate specification. *Nature* 536, 344–348.

Malliri, A., Es, S. van, Huveneers, S., Collard, J.G., 2004. The Rac Exchange Factor Tiam1 Is Required for the Establishment and Maintenance of Cadherin-based Adhesions *. *J. Biol. Chem.* 279, 30092–30098. <https://doi.org/10.1074/jbc.M401192200>

Mao, J.-R., Bristow, J., 2001. The Ehlers-Danlos syndrome: on beyond collagens. *J. Clin.*

- Invest. 107, 1063–1069. <https://doi.org/10.1172/JCI12881>
- Maqbool, A., 2013. Colon: Structure, Function, and Disorders, in: *Encyclopedia of Human Nutrition*. Elsevier, pp. 378–396. <https://doi.org/10.1016/B978-0-12-375083-9.00059-3>
- Margadant, C., Monsuur, H.N., Norman, J.C., Sonnenberg, A., 2011. Mechanisms of integrin activation and trafficking. *Curr. Opin. Cell Biol.* 23, 607–614. <https://doi.org/10.1016/j.ccb.2011.08.005>
- Martel, V., Vignoud, L., Dupé, S., Frachet, P., Block, M.R., Albigès-Rizo, C., 2000. Talin controls the exit of the integrin $\alpha 5 \beta 1$ from an early compartment of the secretory pathway. *J. Cell Sci.* 113, 1951–1961. <https://doi.org/10.1242/jcs.113.11.1951>
- Martin, V., Landi, L., Molinari, F., Fountzilias, G., Geva, R., Riva, A., Saletti, P., De Dosso, S., Spitale, A., Tejpar, S., Kalogeras, K.T., Mazzucchelli, L., Frattini, M., Cappuzzo, F., 2013. HER2 gene copy number status may influence clinical efficacy to anti-EGFR monoclonal antibodies in metastatic colorectal cancer patients. *Br. J. Cancer* 108, 668–675. <https://doi.org/10.1038/bjc.2013.4>
- Martin-Belmonte, F., Gassama, A., Datta, A., Yu, W., Rescher, U., Gerke, V., Mostov, K., 2007. PTEN-Mediated Apical Segregation of Phosphoinositides Controls Epithelial Morphogenesis through Cdc42. *Cell* 128, 383–397. <https://doi.org/10.1016/j.cell.2006.11.051>
- Martin-Belmonte, F., Mostov, K., 2007. Phosphoinositides Control Epithelial Development. *Cell Cycle* 6, 1957–1961. <https://doi.org/10.4161/cc.6.16.4583>
- Matsumine, A., Ogai, A., Senda, T., Okumura, N., Satoh, K., Baeg, G.-H., Kawahara, T., Kobayashi, S., Okada, M., Toyoshima, K., Akiyama, T., 1996. Binding of APC to the Human Homolog of the *Drosophila* Discs Large Tumor Suppressor Protein. *Science* 272, 1020–1023. <https://doi.org/10.1126/science.272.5264.1020>
- Maury, J., Nicoletti, C., Guzzo-Chambraud, L., Maroux, S., 1995. The Filamentous Brush Border Glycocalyx, a Mucin-like Marker of Enterocyte Hyper-Polarization. *Eur. J. Biochem.* 228, 323–331. <https://doi.org/10.1111/j.1432-1033.1995.0323n.x>
- Mekenkamp, L.J.M., Heesterbeek, K.J., Koopman, M., Tol, J., Teerenstra, S., Venderbosch, S., Punt, C.J.A., Nagtegaal, I.D., 2012. Mucinous adenocarcinomas: Poor prognosis in metastatic colorectal cancer. *Eur. J. Cancer* 48, 501–509. <https://doi.org/10.1016/j.ejca.2011.12.004>
- Menezes, L.F., Germino, G.G., 2019. The pathobiology of polycystic kidney disease from a metabolic viewpoint. *Nat. Rev. Nephrol.* 15, 735–749. <https://doi.org/10.1038/s41581-019-0183-y>
- Messmer, T., Meyenn, F. von, Savino, A., Santos, F., Mohammed, H., Lun, A.T.L., Marioni, J.C., Reik, W., 2019. Transcriptional Heterogeneity in Naive and Primed Human Pluripotent Stem Cells at Single-Cell Resolution. *Cell Rep.* 26, 815–824.e4. <https://doi.org/10.1016/j.celrep.2018.12.099>
- Michel, D., Arsanto, J.-P., Massey-Harroche, D., Béclin, C., Wijnholds, J., Le Bivic, A., 2005. PATJ connects and stabilizes apical and lateral components of tight junctions in human intestinal cells. *J. Cell Sci.* 118, 4049–4057. <https://doi.org/10.1242/jcs.02528>
- Mizuno, K., Suzuki, A., Hirose, T., Kitamura, K., Kutsuzawa, K., Futaki, M., Amano, Y., Ohno, S., 2003. Self-association of PAR-3-mediated by the Conserved N-terminal Domain Contributes to the Development of Epithelial Tight Junctions *. *J. Biol. Chem.* 278, 31240–31250. <https://doi.org/10.1074/jbc.M303593200>
- Mohammed, S.I., Torres-Luquis, O., Walls, E., Lloyd, F., 2019. Lymph-circulating tumor cells show distinct properties to blood-circulating tumor cells and are efficient metastatic precursors. *Mol. Oncol.* 13, 1400–1418. <https://doi.org/10.1002/1878-0261.12494>
- Mohrmann, Karin, Sluijs, P. van der, 1999. Regulation of membrane transport through the endocytic pathway by rabGTPases. *Mol. Membr. Biol.* 16, 81–87. <https://doi.org/10.1080/096876899294797>
- Molè, M.A., Coorens, T.H.H., Shahbazi, M.N., Weberling, A., Weatherbee, B.A.T., Gantner, C.W., Sancho-Serra, C., Richardson, L., Drinkwater, A., Syed, N., Engley, S., Snell, P., Christie, L., Elder, K., Campbell, A., Fishel, S., Behjati, S., Vento-Tormo, R., Zernicka-Goetz, M., 2021. A single cell characterisation of human embryogenesis identifies pluripotency transitions and putative anterior hypoblast centre. *Nat. Commun.* 12, 3679. <https://doi.org/10.1038/s41467-021-23758-w>
- Moreno-Layseca, P., Icha, J., Hamidi, H., Ivaska, J., 2019. Integrin trafficking in cells and tissues. *Nat. Cell Biol.* 21, 122–132. <https://doi.org/10.1038/s41556-018-0223-z>
- Moser, M., Nieswandt, B., Ussar, S., Pozgajova, M., Fässler, R., 2008. Kindlin-3 is essential

for integrin activation and platelet aggregation. *Nat. Med.* 14, 325–330. <https://doi.org/10.1038/nm1722>

Mu-sch, A., Cohen, D., Yeaman, C., Nelson, W.J., Rodriguez-Boulan, E., Brennwald, P.J., 2002. Mammalian Homolog of Drosophila Tumor Suppressor Lethal (2) Giant Larvae Interacts with Basolateral Exocytic Machinery in Madin-Darby Canine Kidney Cells. *Mol. Biol. Cell* 13, 158–168. <https://doi.org/10.1091/mbc.01-10-0496>

Muller, P.A.J., Caswell, P.T., Doyle, B., Iwanicki, M.P., Tan, E.H., Karim, S., Lukashchuk, N., Gillespie, D.A., Ludwig, R.L., Gosselin, P., Cromer, A., Brugge, J.S., Sansom, O.J., Norman, J.C., Vousden, K.H., 2009. Mutant p53 Drives Invasion by Promoting Integrin Recycling. *Cell* 139, 1327–1341. <https://doi.org/10.1016/j.cell.2009.11.026>

Nacke, M., Sandilands, E., Nikolatou, K., Román-Fernández, Á., Mason, S., Patel, R., Lilla, S., Yelland, T., Galbraith, L.C.A., Freckmann, E.C., McGarry, L., Morton, J.P., Shanks, E., Leung, H.Y., Markert, E., Ismail, S., Zanivan, S., Blyth, K., Bryant, D.M., 2021. An ARF GTPase module promoting invasion and metastasis through regulating phosphoinositide metabolism. *Nat. Commun.* 12, 1623. <https://doi.org/10.1038/s41467-021-21847-4>

Nader, G.P.F., Ezratty, E.J., Gundersen, G.G., 2016. FAK, talin and PIPKI³ regulate endocytosed integrin activation to polarize focal adhesion assembly. *Nat. Cell Biol.* 18, 491–503. <https://doi.org/10.1038/ncb3333>

Nagano, T., Yoneda, T., Hatanaka, Y., Kubota, C., Murakami, F., Sato, M., 2002. Filamin A-interacting protein (FILIP) regulates cortical cell migration out of the ventricular zone. *Nat. Cell Biol.* 4, 495–501. <https://doi.org/10.1038/ncb808>

Nagtegaal, I.D., Hugen, N., 2015. The Increasing Relevance of Tumour Histology in Determining Oncological Outcomes in Colorectal Cancer. *Curr. Colorectal Cancer Rep.* 11, 259–266. <https://doi.org/10.1007/s11888-015-0280-7>

Nagtegaal, I.D., Odze, R.D., Klimstra, D., Paradis, V., Rugge, M., Schirmacher, P., Washington, K.M., Carneiro, F., Cree, I.A., 2020. The 2019 WHO classification of tumours of the digestive system. *Histopathology* 76, 182–188. <https://doi.org/10.1111/his.13975>

Najafi, M., Farhood, B., Mortezaee, K., 2019. Extracellular matrix (ECM) stiffness and degradation as cancer drivers. *J. Cell. Biochem.* 120, 2782–2790. <https://doi.org/10.1002/jcb.27681>

Nardone, G., Oliver-De La Cruz, J., Vrbsky, J., Martini, C., Pribyl, J., Skládál, P., Pešl, M., Caluori, G., Pagliari, S., Martino, F., Maceckova, Z., Hajduch, M., Sanz-Garcia, A., Pugno, N.M., Stokin, G.B., Forte, G., 2017. YAP regulates cell mechanics by controlling focal adhesion assembly. *Nat. Commun.* 8, 15321. <https://doi.org/10.1038/ncomms15321>

Närvä, E., Stubb, A., Guzmán, C., Blomqvist, M., Balboa, D., Lerche, M., Saari, M., Otonkoski, T., Ivaska, J., 2017. A Strong Contractile Actin Fence and Large Adhesions Direct Human Pluripotent Colony Morphology and Adhesion. *Stem Cell Rep.* 9, 67–76. <https://doi.org/10.1016/j.stemcr.2017.05.021>

Nassar, H., Pansare, V., Zhang, H., Che, M., Sakr, W., Ali-Fehmi, R., Grignon, D., Sarkar, F., Cheng, J., Adsay, V., 2004. Pathogenesis of invasive micropapillary carcinoma: role of MUC1 glycoprotein. *Mod. Pathol.* 17, 1045–1050. <https://doi.org/10.1038/modpathol.3800166>

Nelson, W.J., 2003. Adaptation of core mechanisms to generate cell polarity. *Nature* 422, 766–774. <https://doi.org/10.1038/nature01602>

Ngok, S.P., Lin, W.-H., Anastasiadis, P.Z., 2014. Establishment of epithelial polarity – GEF who’s minding the GAP? *J. Cell Sci.* 127, 3205–3215. <https://doi.org/10.1242/jcs.153197>

Nikas, G., Ao, A., Winston, R.M.L., Handyside, A.H., 1996. Compaction and Surface Polarity in the Human Embryo in Vitro. *Biol. Reprod.* 55, 32–37. <https://doi.org/10.1095/biolreprod55.1.32>

Nikolatou, K., Sandilands, E., Román Fernández, A., Cumming, E.M., Freckmann, E., Lilla, S., Buetow, L., McGarry, L., Neilson, M., Shaw, R., Strachan, D., Miller, C., Huang, D.T., McNeish, I.A., Norman, J.C., Zanivan, S., Bryant, D.M., 2023. PTEN deficiency exposes a requirement for an ARF GTPase module for integrin dependent invasion in ovarian cancer. *EMBO J.* 42, e113987. <https://doi.org/10.15252/embj.2023113987>

Nobis, M., McGhee, E.J., Morton, J.P., Schwarz, J.P., Karim, S.A., Quinn, J., Edward, M., Campbell, A.D., McGarry, L.C., Evans, T.R.J., Brunton, V.G., Frame, M.C., Carragher, N.O., Wang,

- Y., Sansom, O.J., Timpson, P., Anderson, K.I., 2013. Intravital FLIM-FRET Imaging Reveals Dasatinib-Induced Spatial Control of Src in Pancreatic Cancer. *Cancer Res.* 73, 4674–4686. <https://doi.org/10.1158/0008-5472.CAN-12-4545>
- Nowak, J.A., 2020. HER2 in Colorectal Carcinoma. *Surg. Pathol. Clin.* 13, 485–502. <https://doi.org/10.1016/j.path.2020.05.007>
- O'Brien, L.E., Jou, T.-S., Pollack, A.L., Zhang, Q., Hansen, S.H., Yurchenco, P., Mostov, K.E., 2001. Rac1 orientates epithelial apical polarity through effects on basolateral laminin assembly. *Nat. Cell Biol.* 3, 831–838. <https://doi.org/10.1038/ncb0901-831>
- Ohta, Y., Hartwig, J.H., Stossel, T.P., 2006. FilGAP, a Rho- and ROCK-regulated GAP for Rac binds filamin A to control actin remodelling. *Nat. Cell Biol.* 8, 803–814. <https://doi.org/10.1038/ncb1437>
- Okuyama, H., Kondo, J., Sato, Y., Endo, H., Nakajima, A., Piulats, J.M., Tomita, Y., Fujiwara, T., Itoh, Y., Mizoguchi, A., Ohue, M., Inoue, M., 2016. Dynamic Change of Polarity in Primary Cultured Spheroids of Human Colorectal Adenocarcinoma and Its Role in Metastasis. *Am. J. Pathol.* 186, 899–911. <https://doi.org/10.1016/j.ajpath.2015.12.011>
- Onuma, K., Inoue, M., 2022. Abnormality of apico-basal polarity in adenocarcinoma. *Cancer Sci.* 113, 3657–3663. <https://doi.org/10.1111/cas.15549>
- Onuma, K., Sato, Y., Okuyama, H., Uematsu, H., Homma, K., Ohue, M., Kondo, J., Inoue, M., 2021. Aberrant activation of Rho/ROCK signaling in impaired polarity switching of colorectal micropapillary carcinoma. *J. Pathol.* 255, 84–94. <https://doi.org/10.1002/path.5748>
- Pagès, D.-L., Dornier, E., de Seze, J., Gontran, E., Maitra, A., Maciejewski, A., Wang, L., Luan, R., Cartry, J., Canet-Jourdan, C., Raingeaud, J., Lemahieu, G., Lebel, M., Ducreux, M., Gelli, M., Scoazec, J.-Y., Coppey, M., Voituriez, R., Piel, M., Jaulin, F., 2022. Cell clusters adopt a collective amoeboid mode of migration in confined nonadhesive environments. *Sci. Adv.* 8, eabp8416. <https://doi.org/10.1126/sciadv.abp8416>
- Pagliari, S., Vinarsky, V., Martino, F., Perestrelo, A.R., Oliver De La Cruz, J., Caluori, G., Vrbsky, J., Mozetic, P., Pompeiano, A., Zancla, A., Ranjani, S.G., Skladal, P., Kytyr, D., Zdráhal, Z., Grassi, G., Sampaolesi, M., Rainer, A., Forte, G., 2021. YAP-TEAD1 control of cytoskeleton dynamics and intracellular tension guides human pluripotent stem cell mesoderm specification. *Cell Death Differ.* 28, 1193–1207. <https://doi.org/10.1038/s41418-020-00643-5>
- Palangi, F., Samuel, S.M., Thompson, I.R., Triggler, C.R., Emara, M.M., 2017. Effects of oxidative and thermal stresses on stress granule formation in human induced pluripotent stem cells. *PLOS ONE* 12, e0182059. <https://doi.org/10.1371/journal.pone.0182059>
- Pappenheimer, J.R., 2001. Intestinal Absorption of Hexoses and Amino Acids: From Apical Cytosol to Villus Capillaries 184, 233–239. <https://doi.org/10.1007/s00232-001-0094-1>
- Parsons, M., Keppler, M.D., Kline, A., Messent, A., Humphries, M.J., Gilchrist, R., Hart, I.R., Quittau-Prevostel, C., Hughes, W.E., Parker, P.J., Ng, T., 2002. Site-Directed Perturbation of Protein Kinase C- Integrin Interaction Blocks Carcinoma Cell Chemotaxis. *Mol. Cell. Biol.* 22, 5897–5911. <https://doi.org/10.1128/MCB.22.16.5897-5911.2002>
- Pasquier, N., Jaulin, F., Peglion, F., 2024. Inverted apicobasal polarity in health and disease. *J. Cell Sci.* 137, jcs261659. <https://doi.org/10.1242/jcs.261659>
- Passaniti, A., Hart, G.W., 1988. Cell surface sialylation and tumor metastasis. Metastatic potential of B16 melanoma variants correlates with their relative numbers of specific penultimate oligosaccharide structures. *J. Biol. Chem.* 263, 7591–7603. [https://doi.org/10.1016/S0021-9258\(18\)68540-0](https://doi.org/10.1016/S0021-9258(18)68540-0)
- Paszek, M.J., Boettiger, D., Weaver, V.M., Hammer, D.A., 2009. Integrin Clustering Is Driven by Mechanical Resistance from the Glycocalyx and the Substrate. *PLoS Comput. Biol.* 5, e1000604. <https://doi.org/10.1371/journal.pcbi.1000604>
- Paszek, M.J., DuFort, C.C., Rossier, O., Bainer, R., Mouw, J.K., Godula, K., Hudak, J.E., Lakins, J.N., Wijekoon, A.C., Cassereau, L., Rubashkin, M.G., Magbanua, M.J., Thorn, K.S., Davidson, M.W., Rugo, H.S., Park, J.W., Hammer, D.A., Giannone, G., Bertozzi, C.R., Weaver, V.M., 2014. The cancer glycocalyx mechanically primes integrin-mediated growth and survival. *Nature* 511, 319–325. <https://doi.org/10.1038/nature13535>
- Paul, N.R., Jacquemet, G., Caswell, P.T., 2015. Endocytic Trafficking of Integrins in Cell

- Migration. *Curr. Biol.* 25, R1092–R1105. <https://doi.org/10.1016/j.cub.2015.09.049>
- Peglion, F., Etienne-Manneville, S., 2023. Cell polarity changes in cancer initiation and progression. *J. Cell Biol.* 223, e202308069. <https://doi.org/10.1083/jcb.202308069>
- Pellinen, T., Arjonen, A., Vuoriluoto, K., Kallio, K., Fransén, J.A.M., Ivaska, J., 2006. Small GTPase Rab21 regulates cell adhesion and controls endosomal traffic of $\alpha 2$ 1-integrins. *J. Cell Biol.* 173, 767–780. <https://doi.org/10.1083/jcb.200509019>
- Pellinen, T., Ivaska, J., 2006. Integrin traffic. *J. Cell Sci.* 119, 3723–3731. <https://doi.org/10.1242/jcs.03216>
- Pietilä, M., Sahgal, P., Peuhu, E., Jääntti, N.Z., Paatero, I., Närvä, E., Al-Akhrass, H., Lilja, J., Georgiadou, M., Andersen, O.M., Padzik, A., Sihto, H., Joensuu, H., Blomqvist, M., Saarinen, I., Boström, P.J., Taimen, P., Ivaska, J., 2019. SORLA regulates endosomal trafficking and oncogenic fitness of HER2. *Nat. Commun.* 10, 2340. <https://doi.org/10.1038/s41467-019-10275-0>
- Plow, E.F., Haas, T.A., Zhang, L., Loftus, J., Smith, J.W., 2000. Ligand Binding to Integrins. *J. Biol. Chem.* 275, 21785–21788. <https://doi.org/10.1074/jbc.R000003200>
- Plusa, B., Frankenberg, S., Chalmers, A., Hadjantonakis, A.-K., Moore, C.A., Papalopulu, N., Papaioannou, V.E., Glover, D.M., Zernicka-Goetz, M., 2005. Downregulation of Par3 and aPKC function directs cells towards the ICM in the preimplantation mouse embryo. *J. Cell Sci.* 118, 505–515. <https://doi.org/10.1242/jcs.01666>
- Pluskota, E., Dowling, J.J., Gordon, N., Golden, J.A., Szpak, D., West, X.Z., Nestor, C., Ma, Y.-Q., Bialkowska, K., Byzova, T., Plow, E.F., 2011. The integrin coactivator Kindlin-2 plays a critical role in angiogenesis in mice and zebrafish. *Blood* 117, 4978–4987. <https://doi.org/10.1182/blood-2010-11-321182>
- Pocard, T., Le Bivic, A., Galli, T., Zurzolo, C., 2007. Distinct v-SNAREs regulate direct and indirect apical delivery in polarized epithelial cells. *J. Cell Sci.* 120, 3309–3320. <https://doi.org/10.1242/jcs.007948>
- Powelka, A.M., Sun, J., Li, J., Gao, M., Shaw, L.M., Sonnenberg, A., Hsu, V.W., 2004. Stimulation-Dependent Recycling of Integrin $\alpha 2$ 1 Regulated by ARF6 and Rab11. *Traffic* 5, 20–36. <https://doi.org/10.1111/j.1600-0854.2004.00150.x>
- Pretzsch, E., Bösch, F., Neumann, J., Ganschow, P., Bazhin, A., Guba, M., Werner, J., Angele, M., 2019. Mechanisms of Metastasis in Colorectal Cancer and Metastatic Organotropism: Hematogenous versus Peritoneal Spread. *J. Oncol.* 2019, 7407190. <https://doi.org/10.1155/2019/7407190>
- Puthenveedu, M.A., Lauffer, B., Temkin, P., Vistein, R., Carlton, P., Thorn, K., Taunton, J., Weiner, O.D., Parton, R.G., Zastrow, M. von, 2010. Sequence-Dependent Sorting of Recycling Proteins by Actin-Stabilized Endosomal Microdomains. *Cell* 143, 761–773. <https://doi.org/10.1016/j.cell.2010.10.003>
- Quinn, K.E., Matson, B.C., Wetendorf, M., Caron, K.M., 2020. Pinopodes: Recent advancements, current perspectives, and future directions. *Mol. Cell. Endocrinol.* 501, 110644. <https://doi.org/10.1016/j.mce.2019.110644>
- Rainero, E., Caswell, P.T., Muller, P.A.J., Grindlay, J., McCaffrey, M.W., Zhang, Q., Wakelam, M.J.O., Voudsen, K.H., Graziani, A., Norman, J.C., 2012. Diacylglycerol kinase \pm controls RCP-dependent integrin trafficking to promote invasive migration. *J. Cell Biol.* 196, 277–295. <https://doi.org/10.1083/jcb.201109112>
- Rainero, E., Howe, J.D., Caswell, P.T., Jamieson, N.B., Anderson, K., Critchley, D.R., Machesky, L., Norman, J.C., 2015. Ligand-Occupied Integrin Internalization Links Nutrient Signaling to Invasive Migration. *Cell Rep.* 10, 398–413. <https://doi.org/10.1016/j.celrep.2014.12.037>
- Ramovs, V., Te Molder, L., Sonnenberg, A., 2017. The opposing roles of laminin-binding integrins in cancer. *Matrix Biol. J. Int. Soc. Matrix Biol.* 57–58, 213–243. <https://doi.org/10.1016/j.matbio.2016.08.007>
- Ramsay, A.G., Keppler, M.D., Jazayeri, M., Thomas, G.J., Parsons, M., Violette, S., Weinreb, P., Hart, I.R., Marshall, J.F., 2007. HSI-Associated Protein X-1 Regulates Carcinoma Cell Migration and Invasion via Clathrin-Mediated Endocytosis of Integrin $\alpha v \beta 6$. *Cancer Res.* 67, 5275–5284. <https://doi.org/10.1158/0008-5472.CAN-07-0318>
- Ratheesh, A., Gomez, G.A., Priya, R., Verma, S., Kovacs, E.M., Jiang, K., Brown, N.H.,

- Akhmanova, A., Stehbens, S.J., Yap, A.S., 2012. Centralspindlin and \pm -catenin regulate Rho signalling at the epithelial zonula adherens. *Nat. Cell Biol.* 14, 818–828. <https://doi.org/10.1038/ncb2532>
- Reddy, B.V.V.G., Kalraiya, R.D., 2006. Sialylated ²1,6 branched N-oligosaccharides modulate adhesion, chemotaxis and motility of melanoma cells: Effect on invasion and spontaneous metastasis properties. *Biochim. Biophys. Acta BBA - Gen. Subj.* 1760, 1393–1402. <https://doi.org/10.1016/j.bbagen.2006.05.003>
- Reeve, W.J.D., Ziomek, C.A., 1981. Distribution of microvilli on dissociated blastomeres from mouse embryos: evidence for surface polarization at compaction. *Development* 62, 339–350. <https://doi.org/10.1242/dev.62.1.339>
- Reglero-Real, N., Álvarez-Varela, A., Cernuda-Morollón, E., Feito, J., Marcos-Ramiro, B., Fernández-Martín, L., Gómez-Lechón, M.J., Muntané, J., Sandoval, P., Majano, P.L., Correas, I., Alonso, M.A., Millán, J., 2014. Apicobasal Polarity Controls Lymphocyte Adhesion to Hepatic Epithelial Cells. *Cell Rep.* 8, 1879–1893. <https://doi.org/10.1016/j.celrep.2014.08.007>
- Ridley, A.J., Hall, A., 1992. Distinct Patterns of Actin Organization Regulated by the Small GTP-binding Proteins Rac and Rho. *Cold Spring Harb. Symp. Quant. Biol.* 57, 661–671. <https://doi.org/10.1101/SQB.1992.057.01.072>
- Ritch, S.J., Telleria, C.M., 2022. The Transcoelomic Ecosystem and Epithelial Ovarian Cancer Dissemination. *Front. Endocrinol.* 13. <https://doi.org/10.3389/fendo.2022.886533>
- Rizzo, G., Bertotti, A., Leto, S.M., Vetrano, S., 2021. Patient-derived tumor models: a more suitable tool for pre-clinical studies in colorectal cancer. *J. Exp. Clin. Cancer Res.* 40, 178. <https://doi.org/10.1186/s13046-021-01970-2>
- Roberts, M., Barry, S., Woods, A., Norman, J., n.d. PDGF-regulated rab4-dependent recycling of α v β 3 integrin from early endosomes is necessary for cell adhesion and spreading.
- Robertson, J., Jacquemet, G., Byron, A., Jones, M.C., Warwood, S., Selley, J.N., Knight, D., Humphries, J.D., Humphries, M.J., 2015. Defining the phospho-adesome through the phosphoproteomic analysis of integrin signalling. *Nat. Commun.* 6, 6265. <https://doi.org/10.1038/ncomms7265>
- Roca-Cusachs, P., del Rio, A., Puklin-Faucher, E., Gauthier, N.C., Biais, N., Sheetz, M.P., 2013. Integrin-dependent force transmission to the extracellular matrix by \pm -actinin triggers adhesion maturation. *Proc. Natl. Acad. Sci.* 110, E1361–E1370. <https://doi.org/10.1073/pnas.1220723110>
- Rodriguez-Boulan, E., Macara, I.G., 2014. Organization and execution of the epithelial polarity programme. *Nat. Rev. Mol. Cell Biol.* 15, 225–242. <https://doi.org/10.1038/nrm3775>
- Roh, M.H., Margolis, B., 2003. Composition and function of PDZ protein complexes during cell polarization. *Am. J. Physiol.-Ren. Physiol.* 285, F377–F387. <https://doi.org/10.1152/ajprenal.00086.2003>
- Rossier, O., Octeau, V., Sibarita, J.-B., Leduc, C., Tessier, B., Nair, D., Gatterdam, V., Destaing, O., Albigès-Rizo, C., Tampé, R., Cognet, L., Choquet, D., Lounis, B., Giannone, G., 2012. Integrins ²1 and ²3 exhibit distinct dynamic nanoscale organizations inside focal adhesions. *Nat. Cell Biol.* 14, 1057–1067. <https://doi.org/10.1038/ncb2588>
- Rostovskaya, M., Stirparo, G.G., Smith, A., 2019. Capacitation of human naïve pluripotent stem cells for multi-lineage differentiation. *Development* 146, dev172916. <https://doi.org/10.1242/dev.172916>
- Rubashkin, M.G., Cassereau, L., Bainer, R., DuFort, C.C., Yui, Y., Ou, G., Paszek, M.J., Davidson, M.W., Chen, Y.-Y., Weaver, V.M., 2014. Force engages vinculin and promotes tumor progression by enhancing PI3K activation of phosphatidylinositol (3,4,5)-triphosphate. *Cancer Res.* 74, 4597–4611. <https://doi.org/10.1158/0008-5472.CAN-13-3698>
- Sahgal, P., Alanko, J., Icha, J., Paatero, I., Hamidi, H., Arjonen, A., Pietilä, M., Rokka, A., Ivaska, J., 2019. GGA2 and RAB13 promote activity-dependent ²1-integrin recycling. *J. Cell Sci.* 132, jcs233387. <https://doi.org/10.1242/jcs.233387>
- Salat-Canela, C., Pérez, P., Ayté, J., Hidalgo, E., 2023. Stress-induced cell depolarization through the MAP kinase–Cdc42 axis. *Trends Cell Biol.* 33, 124–137. <https://doi.org/10.1016/j.tcb.2022.06.004>
- Saotome, I., Curto, M., McClatchey, A.I., 2004. Ezrin Is Essential for Epithelial Organization and Villus Morphogenesis in the Developing Intestine. *Dev. Cell* 6, 855–864.

<https://doi.org/10.1016/j.devcel.2004.05.007>

Sasaki, A.T., Chun, C., Takeda, K., Firtel, R.A., 2004. Localized Ras signaling at the leading edge regulates PI3K, cell polarity, and directional cell movement. *J. Cell Biol.* 167, 505–518. <https://doi.org/10.1083/jcb.200406177>

Schiller, H.B., Hermann, M.-R., Polleux, J., Vignaud, T., Zanivan, S., Friedel, C.C., Sun, Z., Raducanu, A., Gottschalk, K.-E., Théry, M., Mann, M., Fässler, R., 2013. α 1- and α v-class integrins cooperate to regulate myosin II during rigidity sensing of fibronectin-based microenvironments. *Nat. Cell Biol.* 15, 625–636. <https://doi.org/10.1038/ncb2747>

Schlüter, M.A., Pfarr, C.S., Pieczynski, J., Whiteman, E.L., Hurd, T.W., Fan, S., Liu, C.-J., Margolis, B., 2009. Trafficking of Crumbs3 during Cytokinesis Is Crucial for Lumen Formation. *Mol. Biol. Cell* 20, 4652–4663. <https://doi.org/10.1091/mbc.e09-02-0137>

Schmidt, V., Schulz, N., Yan, X., Schürmann, A., Kempa, S., Kern, M., Blüher, M., Poy, M.N., Olivecrona, G., Willnow, T.E., 2016. SORLA facilitates insulin receptor signaling in adipocytes and exacerbates obesity. *J. Clin. Invest.* 126, 2706–2720. <https://doi.org/10.1172/JCI84708>

Schneeberger, K., Vogel, G.F., Teunissen, H., van Ommen, D.D., Begthel, H., El Bouazzaoui, L., van Vugt, A.H.M., Beekman, J.M., Klumperman, J., Müller, T., Janecke, A., Gerner, P., Huber, L.A., Hess, M.W., Clevers, H., van Es, J.H., Nieuwenhuis, E.E.S., Middendorp, S., 2015. An inducible mouse model for microvillus inclusion disease reveals a role for myosin Vb in apical and basolateral trafficking. *Proc. Natl. Acad. Sci.* 112, 12408–12413. <https://doi.org/10.1073/pnas.1516672112>

Schuck, S., Simons, K., 2004. Polarized sorting in epithelial cells: raft clustering and the biogenesis of the apical membrane. *J. Cell Sci.* 117, 5955–5964. <https://doi.org/10.1242/jcs.01596>

Semel, A.C., Seales, E.C., Singhal, A., Eklund, E.A., Colley, K.J., Bellis, S.L., 2002. Hyposialylation of Integrins Stimulates the Activity of Myeloid Fibronectin Receptors*. *J. Biol. Chem.* 277, 32830–32836. <https://doi.org/10.1074/jbc.M202493200>

Shafaq-Zadah, M., Dransart, E., Wunder, C., Chambon, V., Valades-Cruz, C.A., Leconte, L., Sarangi, N.K., Robinson, J., Bai, S.-K., Regmi, R., Cicco, A.D., Hovasse, A., Bartels, R., Nilsson, U.J., Cianférani-Sangler, S., Leffler, H., Keyes, T.E., Lévy, D., Raunser, S., Roderer, D., Johannes, L., 2023. Spatial N-glycan rearrangement on α 5 β 1 integrin nucleates galectin-3 oligomers to determine endocytic fate. <https://doi.org/10.1101/2023.10.27.564026>

Shafaq-Zadah, M., Gomes-Santos, C.S., Bardin, S., Maiuri, P., Maurin, M., Iranzo, J., Gautreau, A., Lamaze, C., Caswell, P., Goud, B., Johannes, L., 2016. Persistent cell migration and adhesion rely on retrograde transport of α 1 integrin. *Nat. Cell Biol.* 18, 54–64. <https://doi.org/10.1038/ncb3287>

Shin, H.-W., Hayashi, M., Christoforidis, S., Lacas-Gervais, S., Hoepfner, S., Wenk, M.R., Modregger, J., Uttenweiler-Joseph, S., Wilm, M., Nystuen, A., Frankel, W.N., Solimena, M., De Camilli, P., Zerial, M., 2005. An enzymatic cascade of Rab5 effectors regulates phosphoinositide turnover in the endocytic pathway. *J. Cell Biol.* 170, 607–618. <https://doi.org/10.1083/jcb.200505128>

Shin, K., Straight, S., Margolis, B., 2005. PATJ regulates tight junction formation and polarity in mammalian epithelial cells. *J. Cell Biol.* 168, 705–711. <https://doi.org/10.1083/jcb.200408064>

Shroyer, N.F., Wallis, D., Venken, K.J.T., Bellen, H.J., Zoghbi, H.Y., 2005. Gfi1 functions downstream of Math1 to control intestinal secretory cell subtype allocation and differentiation. *Genes Dev.* 19, 2412–2417. <https://doi.org/10.1101/gad.1353905>

Siegel, R.L., Wagle, N.S., Cercek, A., Smith, R.A., Jemal, A., 2023. Colorectal cancer statistics, 2023. *CA. Cancer J. Clin.* 73, 233–254. <https://doi.org/10.3322/caac.21772>

Simpson, J.C., Jones, A.T., 2005. Early endocytic Rabs: functional prediction to functional characterization. *Biochem. Soc. Symp.* 72, 99–108. <https://doi.org/10.1042/bss0720099>

Siriaunkgul, S., Tavassoli, F.A., 1993. Invasive micropapillary carcinoma of the breast. *Mod. Pathol.* 6, 660–662.

Slováková, J., Sikora, M., Arslan, F.N., Caballero-Mancebo, S., Krens, S.F.G., Kaufmann, W.A., Merrin, J., Heisenberg, C.-P., 2022. Tension-dependent stabilization of E-cadherin limits cell–cell contact expansion in zebrafish germ-layer progenitor cells. *Proc. Natl. Acad. Sci.* 119, e2122030119. <https://doi.org/10.1073/pnas.2122030119>

Speiser, D.E., Chijioke, O., Schaeuble, K., Münz, C., 2023. CD4⁺ T cells in cancer. *Nat. Cancer* 4, 317–329. <https://doi.org/10.1038/s43018-023-00521-2>

- Spoelgen, R., Adams, K.W., Koker, M., Thomas, A.V., Andersen, O.M., Hallett, P.J., Bercury, K.K., Joyner, D.F., Deng, M., Stoothoff, W.H., Strickland, D.K., Willnow, T.E., Hyman, B.T., 2009. Interaction of the apolipoprotein E receptors low density lipoprotein receptor-related protein and sorLA/LR11. *Neuroscience* 158, 1460–1468. <https://doi.org/10.1016/j.neuroscience.2008.10.061>
- Stachowiak, J.C., Schmid, E.M., Ryan, C.J., Ann, H.S., Sasaki, D.Y., Sherman, M.B., Geissler, P.L., Fletcher, D.A., Hayden, C.C., 2012. Membrane bending by protein–protein crowding. *Nat. Cell Biol.* 14, 944–949. <https://doi.org/10.1038/ncb2561>
- Stanifer, M.L., Muench, M., Muenchau, S., Pervolaraki, K., Kanaya, T., Albrecht, D., Odendall, C., Hielscher, T., Hauke, V., Kagan, J.C., Bartfeld, S., Ohno, H., Boulant, S., 2020. Asymmetric distribution of TLR3 leads to a polarized immune response in human intestinal epithelial cells. *Nat. Microbiol.* 5, 181–191. <https://doi.org/10.1038/s41564-019-0594-3>
- Steinberg, F., Heesom, K.J., Bass, M.D., Cullen, P.J., 2012. SNX17 protects integrins from degradation by sorting between lysosomal and recycling pathways. *J. Cell Biol.* 197, 219–230. <https://doi.org/10.1083/jcb.20111121>
- Stewart, C.J.R., Koay, M.H.E., Leslie, C., Acott, N., Leung, Y.C., 2018. Cervical carcinomas with a micropapillary component: a clinicopathological study of eight cases. *Histopathology* 72, 626–633. <https://doi.org/10.1111/his.13419>
- Straight, S.W., Shin, K., Fogg, V.C., Fan, S., Liu, C.-J., Roh, M., Margolis, B., 2004. Loss of PALS1 Expression Leads to Tight Junction and Polarity Defects. *Mol. Biol. Cell* 15, 1981–1990. <https://doi.org/10.1091/mbc.e03-08-0620>
- Stubb, A., Guzmán, C., Närvä, E., Aaron, J., Chew, T.-L., Saari, M., Miihkinen, M., Jacquemet, G., Ivaska, J., 2019. Superresolution architecture of cornerstone focal adhesions in human pluripotent stem cells. *Nat. Commun.* 10, 4756. <https://doi.org/10.1038/s41467-019-12611-w>
- Su, Y., Xia, W., Li, J., Walz, T., Humphries, M.J., Vestweber, D., Cabañas, C., Lu, C., Springer, T.A., 2016. Relating conformation to function in integrin $\alpha 5 \beta 1$. *Proc. Natl. Acad. Sci.* 113, E3872–E3881. <https://doi.org/10.1073/pnas.1605074113>
- Suardet, L., Gaide, A.-C., Calmès, J.-M., Sordat, B., Givel, J.-C., Eliason, J.F., Odartchenko, N., 1992. Responsiveness of Three Newly Established Human Colorectal Cancer Cell Lines to Transforming Growth Factors 2^1 and 2^2 . *Cancer Res.* 52, 3705–3712.
- Sun, P., Zhong, Z., Lu, Q., Li, M., Chao, X., Chen, D., Hu, W., Luo, R., He, J., 2020. Mucinous carcinoma with micropapillary features is morphologically, clinically and genetically distinct from pure mucinous carcinoma of breast. *Mod. Pathol.* 33, 1945–1960. <https://doi.org/10.1038/s41379-020-0554-8>
- Sutherland, A.E., Calarco, P.G., Damsky, C.H., 1993. Developmental regulation of integrin expression at the time of implantation in the mouse embryo. *Development* 119, 1175–1186. <https://doi.org/10.1242/dev.119.4.1175>
- Suwidka, A., Czołowska, R., Ojdowski, W., Tarkowski, A.K., 2008. Blastomeres of the mouse embryo lose totipotency after the fifth cleavage division: Expression of *Cdx2* and *Oct4* and developmental potential of inner and outer blastomeres of 16- and 32-cell embryos. *Dev. Biol.* 322, 133–144. <https://doi.org/10.1016/j.ydbio.2008.07.019>
- Suzuki, A., Yamanaka, T., Hirose, T., Manabe, N., Mizuno, K., Shimizu, M., Akimoto, K., Izumi, Y., Ohnishi, T., Ohno, S., 2001. Atypical Protein Kinase C Is Involved in the Evolutionarily Conserved Par Protein Complex and Plays a Critical Role in Establishing Epithelia-Specific Junctional Structures. *J. Cell Biol.* 152, 1183–1196. <https://doi.org/10.1083/jcb.152.6.1183>
- Sveen, A., Bruun, J., Eide, P.W., Eilertsen, I.A., Ramirez, L., Murumägi, A., Arjama, M., Danielsen, S.A., Kryeziu, K., Elez, E., Taberero, J., Guinney, J., Palmer, H.G., Nesbakken, A., Kallioniemi, O., Dienstmann, R., Lothe, R.A., 2018. Colorectal Cancer Consensus Molecular Subtypes Translated to Preclinical Models Uncover Potentially Targetable Cancer Cell Dependencies. *Clin. Cancer Res.* 24, 794–806. <https://doi.org/10.1158/1078-0432.CCR-17-1234>
- Swain, S.M., Baselga, J., Kim, S.-B., Ro, J., Semiglazov, V., Campone, M., Ciruelos, E., Ferrero, J.-M., Schneeweiss, A., Heeson, S., Clark, E., Ross, G., Benyunes, M.C., Cortés, J., 2015. Pertuzumab, Trastuzumab, and Docetaxel in HER2-Positive Metastatic Breast Cancer. *N. Engl. J. Med.* 372, 724–734. <https://doi.org/10.1056/NEJMoa1413513>
- Taei, A., Rasooli, P., Braun, T., Hassani, S.-N., Baharvand, H., 2020. Signal regulators of

- human naïve pluripotency. *Exp. Cell Res.* 389, 111924. <https://doi.org/10.1016/j.yexcr.2020.111924>
- Takada, Y., Ye, X., Simon, S., 2007. The integrins. *Genome Biol.* 8, 215. <https://doi.org/10.1186/gb-2007-8-5-215>
- Takahashi, K., Tanabe, K., Ohnuki, M., Narita, M., Ichisaka, T., Tomoda, K., Yamanaka, S., 2007. Induction of Pluripotent Stem Cells from Adult Human Fibroblasts by Defined Factors. *Cell* 131, 861–872. <https://doi.org/10.1016/j.cell.2007.11.019>
- Takahashi, K., Yamanaka, S., 2006. Induction of Pluripotent Stem Cells from Mouse Embryonic and Adult Fibroblast Cultures by Defined Factors. *Cell* 126, 663–676. <https://doi.org/10.1016/j.cell.2006.07.024>
- Tepass, U., Theres, C., Knust, E., 1990. crumbs encodes an EGF-like protein expressed on apical membranes of *Drosophila* epithelial cells and required for organization of epithelia. *Cell* 61, 787–799. [https://doi.org/10.1016/0092-8674\(90\)90189-L](https://doi.org/10.1016/0092-8674(90)90189-L)
- Tiger, C.-F., Fougereuse, F., Grundström, G., Velling, T., Gullberg, D., 2001. $\alpha 11^2 1$ Integrin Is a Receptor for Interstitial Collagens Involved in Cell Migration and Collagen Reorganization on Mesenchymal Nonmuscle Cells. *Dev. Biol.* 237, 116–129. <https://doi.org/10.1006/dbio.2001.0363>
- Tiwari, S., Askari, J.A., Humphries, M.J., Bulleid, N.J., 2011. Divalent cations regulate the folding and activation status of integrins during their intracellular trafficking. *J. Cell Sci.* 124, 1672–1680. <https://doi.org/10.1242/jcs.084483>
- Toolan, H.W., 1953. Growth of Human Tumors in Cortisone-treated Laboratory Animals: The Possibility of Obtaining Permanently Transplantable Human Tumors*. *Cancer Res.* 13, 389–394.
- Tran, C.S., Eran, Y., Ruch, T.R., Bryant, D.M., Datta, A., Brakeman, P., Kierbel, A., Wittmann, T., Metzger, R.J., Mostov, K.E., Engel, J.N., 2014. Host Cell Polarity Proteins Participate in Innate Immunity to *Pseudomonas aeruginosa* Infection. *Cell Host Microbe* 15, 636–643. <https://doi.org/10.1016/j.chom.2014.04.007>
- Tsunoyama, T.A., Watanabe, Y., Goto, J., Naito, K., Kasai, R.S., Suzuki, K.G.N., Fujiwara, T.K., Kusumi, A., 2018. Super-long single-molecule tracking reveals dynamic-anchorage-induced integrin function 14, 497–506. <https://doi.org/10.1038/s41589-018-0032-5>
- Tulla, M., Pentikäinen, O.T., Viitasalo, T., Käpylä, J., Impola, U., Nykvist, P., Nissinen, L., Johnson, M.S., Heino, J., 2001. Selective Binding of Collagen Subtypes by Integrin $\alpha 11$, $\alpha 21$, and $\alpha 101$ Domains *. *J. Biol. Chem.* 276, 48206–48212. <https://doi.org/10.1074/jbc.M104058200>
- U Kroneld, R.J., 1998. Expression of the mucosal lymphocyte integrin $\alpha E\beta 7$ and its ligand E-cadherin in salivary glands of patients with Sjögren's syndrome. *Scand. J. Rheumatol.* <https://doi.org/10.1080/030097498440831>
- Veillat, V., Spuul, P., Daubon, T., Egaña, I., Kramer, Ij., Génot, E., 2015. Podosomes: Multipurpose organelles? *Int. J. Biochem. Cell Biol.* 65, 52–60. <https://doi.org/10.1016/j.biocel.2015.05.020>
- Verdú, M., Román, R., Calvo, M., Rodón, N., García, B., González, M., Vidal, A., Puig, X., 2011. Clinicopathological and molecular characterization of colorectal micropapillary carcinoma. *Mod. Pathol.* 24, 729–738. <https://doi.org/10.1038/modpathol.2011.1>
- Verras, G.-I., Tchabashvili, L., Mulita, F., Grypari, I.M., Sourouni, S., Panagodimou, E., Argentou, M.-I., 2023. Micropapillary Breast Carcinoma: From Molecular Pathogenesis to Prognosis. *Breast Cancer Targets Ther.* 14, 41–61. <https://doi.org/10.2147/BCTT.S346301>
- Wang, Q., Chen, X.-W., Margolis, B., 2007. PALS1 Regulates E-Cadherin Trafficking in Mammalian Epithelial Cells. *Mol. Biol. Cell* 18, 874–885. <https://doi.org/10.1091/mbc.e06-07-0651>
- Wang, W., Huang, J., Chen, J., 2011. Angiotensin-like Proteins Associate with and Negatively Regulate YAP1 *. *J. Biol. Chem.* 286, 4364–4370. <https://doi.org/10.1074/jbc.C110.205401>
- Wang, X., Xiang, Y., Yu, Y., Wang, R., Zhang, Y., Xu, Q., Sun, H., Zhao, Z.-A., Jiang, X., Wang, Xiaoqing, Lu, X., Qin, D., Quan, Y., Zhang, J., Shyh-Chang, N., Wang, H., Jing, N., Xie, W., Li, L., 2021. Formative pluripotent stem cells show features of epiblast cells poised for gastrulation. *Cell Res.* 31, 526–541. <https://doi.org/10.1038/s41422-021-00477-x>
- Wang, Y., Arjonen, A., Pouwels, J., Ta, H., Pausch, P., Bange, G., Engel, U., Pan, X., Fackler, O.T., Ivaska, J., Grosse, R., 2015. Formin-like 2 Promotes $\alpha 1$ -Integrin Trafficking and Invasive Motility Downstream of PKC \pm . *Dev. Cell* 34, 475–483. <https://doi.org/10.1016/j.devcel.2015.06.015>

- Wang, Y., Zhang, C., Yang, W., Shao, S., Xu, X., Sun, Y., Li, P., Liang, L., Wu, C., 2021. LIMD1 phase separation contributes to cellular mechanics and durotaxis by regulating focal adhesion dynamics in response to force. *Dev. Cell* 56, 1313-1325.e7. <https://doi.org/10.1016/j.devcel.2021.04.002>
- Watanabe, N., Bodin, L., Pandey, M., Krause, M., Coughlin, S., Boussiotis, V.A., Ginsberg, M.H., Shattil, S.J., 2008. Mechanisms and consequences of agonist-induced talin recruitment to platelet integrin α IIb β 3. *J. Cell Biol.* 181, 1211–1222. <https://doi.org/10.1083/jcb.200803094>
- Wegener, K.L., Partridge, A.W., Han, J., Pickford, A.R., Liddington, R.C., Ginsberg, M.H., Campbell, I.D., 2007. Structural Basis of Integrin Activation by Talin. *Cell* 128, 171–182. <https://doi.org/10.1016/j.cell.2006.10.048>
- Whitby, S., Zhou, W., Dimitriadis, E., 2020. Alterations in Epithelial Cell Polarity During Endometrial Receptivity: A Systematic Review. *Front. Endocrinol.* 11. <https://doi.org/10.3389/fendo.2020.596324>
- Whittaker, C.A., Hynes, R.O., 2002. Distribution and Evolution of von Willebrand/Integrin A Domains: Widely Dispersed Domains with Roles in Cell Adhesion and Elsewhere. *Mol. Biol. Cell* 13, 3369–3387. <https://doi.org/10.1091/mbc.E02-05-0259>
- Whittle, A.J., Jiang, M., Peirce, V., Relat, J., Virtue, S., Ebinuma, H., Fukamachi, I., Yamaguchi, T., Takahashi, M., Murano, T., Tatsuno, I., Takeuchi, M., Nakaseko, C., Jin, W., Jin, Z., Campbell, M., Schneider, W.J., Vidal-Puig, A., Bujo, H., 2015. Soluble LR11/SorLA represses thermogenesis in adipose tissue and correlates with BMI in humans. *Nat. Commun.* 6, 8951. <https://doi.org/10.1038/ncomms9951>
- Wick, M.R., Vitsky, J.L., Ritter, J.H., Swanson, P.E., Mills, S.E., 2005. Sporadic Medullary Carcinoma of the Colon: A Clinicopathologic Comparison With Nonhereditary Poorly Differentiated Enteric-Type Adenocarcinoma and Neuroendocrine Colorectal Carcinoma. *Am. J. Clin. Pathol.* 123, 56–65. <https://doi.org/10.1309/1VFJ1C3LP52A4FP8>
- Wiezlak, M., Diring, J., Abella, J., Moulleron, S., Way, M., McDonald, N.Q., Treisman, R., 2012. G-actin regulates the shuttling and PP1 binding of the RPEL protein Phactr1 to control actomyosin assembly. *J. Cell Sci.* 125, 5860–5872. <https://doi.org/10.1242/jcs.112078>
- Wilhelmsen, K., Litjens, S.H.M., Kuikman, I., Margadant, C., van Rheenen, J., Sonnenberg, A., 2007. Serine Phosphorylation of the Integrin α 4 Subunit Is Necessary for Epidermal Growth Factor Receptor–induced Hemidesmosome Disruption. *Mol. Biol. Cell* 18, 3512–3522. <https://doi.org/10.1091/mbc.e07-04-0306>
- Wilson Patricia D., 2004. Polycystic Kidney Disease. *N. Engl. J. Med.* 350, 151–164. <https://doi.org/10.1056/NEJMra022161>
- Winklbauer, R., 2015. Cell adhesion strength from cortical tension – an integration of concepts. *J. Cell Sci.* 128, 3687–3693. <https://doi.org/10.1242/jcs.174623>
- Winograd-Katz, S.E., Fässler, R., Geiger, B., Legate, K.R., 2014. The integrin adhesome: from genes and proteins to human disease. *Nat. Rev. Mol. Cell Biol.* 15, 273–288. <https://doi.org/10.1038/nrm3769>
- Wishart, A.L., Conner, S.J., Guarin, J.R., Fatherree, J.P., Peng, Y., McGinn, R.A., Crews, R., Naber, S.P., Hunter, M., Greenberg, A.S., Oudin, M.J., 2020. Decellularized extracellular matrix scaffolds identify full-length collagen VI as a driver of breast cancer cell invasion in obesity and metastasis. *Sci. Adv.* 6, eabc3175. <https://doi.org/10.1126/sciadv.abc3175>
- Wodarz, A., Näthke, I., 2007. Cell polarity in development and cancer. *Nat. Cell Biol.* 9, 1016–1024. <https://doi.org/10.1038/ncb433>
- Woods, A.J., White, D.P., Caswell, P.T., Norman, J.C., 2004. PKD1/PKC μ promotes α v β 3 integrin recycling and delivery to nascent focal adhesions. *EMBO J.* 23, 2531–2543. <https://doi.org/10.1038/sj.emboj.7600267>
- Wosen, J.E., Mukhopadhyay, D., Macaubas, C., Mellins, E.D., 2018. Epithelial MHC Class II Expression and Its Role in Antigen Presentation in the Gastrointestinal and Respiratory Tracts. *Front. Immunol.* 9. <https://doi.org/10.3389/fimmu.2018.02144>
- Xia, S., Yim, E.K.F., Kanchanawong, P., 2019. Molecular Organization of Integrin-Based Adhesion Complexes in Mouse Embryonic Stem Cells. *ACS Biomater. Sci. Eng.* 5, 3828–3842. <https://doi.org/10.1021/acsbiomaterials.8b01124>

- Yamada, S., Nelson, W.J., 2007. Localized zones of Rho and Rac activities drive initiation and expansion of epithelial cell–cell adhesion. *J. Cell Biol.* 178, 517–527. <https://doi.org/10.1083/jcb.200701058>
- Yamazaki, D., Oikawa, T., Takenawa, T., 2007. Rac-WAVE-mediated actin reorganization is required for organization and maintenance of cell-cell adhesion. *J. Cell Sci.* 120, 86–100. <https://doi.org/10.1242/jcs.03311>
- Yang, S., Yu, M., 2021. Role of Goblet Cells in Intestinal Barrier and Mucosal Immunity. *J. Inflamm. Res.* 14, 3171–3183. <https://doi.org/10.2147/JIR.S318327>
- Ye, P., Wang, Y., Li, R., Chen, W., Wan, L., Cai, P., 2022. The HER family as therapeutic targets in colorectal cancer. *Crit. Rev. Oncol. Hematol.* 174, 103681. <https://doi.org/10.1016/j.critrevonc.2022.103681>
- Yilmaz, A., Benvenisty, N., 2019. Defining Human Pluripotency. *Cell Stem Cell* 25, 9–22. <https://doi.org/10.1016/j.stem.2019.06.010>
- Yin, H.L., Janmey, P.A., 2003. Phosphoinositide Regulation of the Actin Cytoskeleton. *Annu. Rev. Physiol.* 65, 761–789. <https://doi.org/10.1146/annurev.physiol.65.092101.142517>
- Yonesaka, K., Zejnullahu, K., Okamoto, I., Satoh, T., Cappuzzo, F., Souglakos, J., Ercan, D., Rogers, A., Roncalli, M., Takeda, M., Fujisaka, Y., Philips, J., Shimizu, T., Maenishi, O., Cho, Y., Sun, J., Destro, A., Taira, K., Takeda, K., Okabe, T., Swanson, J., Itoh, H., Takada, M., Lifshits, E., Okuno, K., Engelman, J.A., Shivdasani, R.A., Nishio, K., Fukuoka, M., Varella-Garcia, M., Nakagawa, K., Jänne, P.A., 2011. Activation of ERBB2 Signaling Causes Resistance to the EGFR-Directed Therapeutic Antibody Cetuximab. *Sci. Transl. Med.* 3, 99ra86-99ra86. <https://doi.org/10.1126/scitranslmed.3002442>
- Yu, W., Datta, A., Leroy, P., O'Brien, L.E., Mak, G., Jou, T.-S., Matlin, K.S., Mostov, K.E., Zegers, M.M.P., 2004. α 1-Integrin Orients Epithelial Polarity via Rac1 and Laminin. *Mol. Biol. Cell* 16, 433–445. <https://doi.org/10.1091/mbc.e04-05-0435>
- Yu, W., Shewan, A.M., Brakeman, P., Eastburn, D.J., Datta, A., Bryant, D.M., Fan, Q., Weiss, W.A., Zegers, M.M.P., Mostov, K.E., 2008. Involvement of RhoA, ROCK I and myosin II in inverted orientation of epithelial polarity. *EMBO Rep.* 9, 923–929. <https://doi.org/10.1038/embor.2008.135>
- Zaidel-Bar, R., Ballestrem, C., Kam, Z., Geiger, B., 2003. Early molecular events in the assembly of matrix adhesions at the leading edge of migrating cells. *J. Cell Sci.* 116, 4605–4613. <https://doi.org/10.1242/jcs.00792>
- Zaidel-Bar, R., Cohen, M., Addadi, L., Geiger, B., 2004. Hierarchical assembly of cell–matrix adhesion complexes. *Biochem. Soc. Trans.* 32, 416–420. <https://doi.org/10.1042/bst0320416>
- Zaidel-Bar, R., Milo, R., Kam, Z., Geiger, B., 2007. A paxillin tyrosine phosphorylation switch regulates the assembly and form of cell-matrix adhesions. *J. Cell Sci.* 120, 137–148. <https://doi.org/10.1242/jcs.03314>
- Zajac, O., Raingeaud, J., Libanje, F., Lefebvre, C., Sabino, D., Martins, I., Roy, P., Benatar, C., Canet-Jourdan, C., Azorin, P., Polrot, M., Gonin, P., Benbarche, S., Souquere, S., Pierron, G., Nowak, D., Bigot, L., Ducreux, M., Malka, D., Lobry, C., Scoazec, J.-Y., Eveno, C., Pocard, M., Perfettini, J.-L., Elias, D., Dartigues, P., Goéré, D., Jaulin, F., 2018. Tumour spheres with inverted polarity drive the formation of peritoneal metastases in patients with hypermethylated colorectal carcinomas. *Nat. Cell Biol.* 20, 296–306. <https://doi.org/10.1038/s41556-017-0027-6>
- Zerial, M., McBride, H., 2001. Rab proteins as membrane organizers. *Nat. Rev. Mol. Cell Biol.* 2, 107–117. <https://doi.org/10.1038/35052055>
- Zhang, K., Chen, J., 2012. The regulation of integrin function by divalent cations. *Cell Adhes. Migr.* 6, 20–29. <https://doi.org/10.4161/cam.18702>
- Zhang, N., Zhang, H., Khan, L.A., Jafari, G., Eun, Y., Membreno, E., Gobel, V., 2023. The biosynthetic-secretory pathway, supplemented by recycling routes, determines epithelial membrane polarity. *Sci. Adv.* 9, eade4620. <https://doi.org/10.1126/sciadv.ade4620>
- Zhao, B., Li, L., Lu, Q., Wang, L.H., Liu, C.-Y., Lei, Q., Guan, K.-L., 2011. Angiominin is a novel Hippo pathway component that inhibits YAP oncoprotein. *Genes Dev.* 25, 51–63. <https://doi.org/10.1101/gad.2000111>
- Zhao, S., Xu, J., Liu, S., Cui, K., Li, Z., Liu, N., 2019. Dppa3 in pluripotency maintenance of

ES cells and early embryogenesis. *J. Cell. Biochem.* 120, 4794–4799. <https://doi.org/10.1002/jcb.28063>
Zhao, Y., Sato, Y., Isaji, T., Fukuda, T., Matsumoto, A., Miyoshi, E., Gu, J., Taniguchi, N.,
2008. Branched N-glycans regulate the biological functions of integrins and cadherins. *FEBS J.* 275,
1939–1948. <https://doi.org/10.1111/j.1742-4658.2008.06346.x>



**TURUN
YLIOPISTO**
UNIVERSITY
OF TURKU

université
PARIS-SACLAY

ISBN 978-951-29-9869-2 (print)
ISBN 978-951-29-9870-8 (pdf)
ISSN 2736-9390 (print)
ISSN 2736-9684 (online)